NICOLE PAMELA DA SILVA NASCIMENTO

DIAGNOSTIC OF CONCRETE SAMPLES EXTRACTED FROM PILE CAPS AFFECTED BY INTERNAL SWELLING REACTIONS

Master's Thesis presented to the Graduate Program in Civil Engineering of the Catholic University of Pernambuco as a partial requirement to obtain the title of Master in Civil Engineering.

Concentration Area: Construction Engineering

Advisor: Prof. Dr. Fernando Artur Nogueira Silva

Recife

2020

CATHOLIC UNIVERSITY OF PERNAMBUCO GRADUATE PROGRAM IN CIVIL ENGINEERING

NICOLE PAMELA DA SILVA NASCIMENTO

Diagnostic of concrete samples extracted from pile caps affected by Internal Swelling Reactions

Examining Committee:

Prof. Dr. Fernando Artur Nogueira Silva
Advisor - Catholic University of Pernambuco, Brazil - UNICAP

Prof. Dr. Joaquim Teodoro Romão de Oliveira
Internal Examiner - Catholic University of Pernambuco, Brazil - UNICAP

Prof. Dr. Mahfoud Tahlaiti
Co-Advisor - Institut catholique d'arts et métiers, France - ICAM

Prof. Dr. Abdelhafid Khelidj
External Examiner - Université de Nantes, France - UN

Approved on 24 of march of 2020

CATHOLIC UNIVERSITY OF PERNAMBUCO GRADUATE PROGRAM IN CIVIL ENGINEERING

NICOLE PAMELA DA SILVA NASCIMENTO

Diagnostic of concrete samples extracted from pile caps affected by Internal Swelling Reactions

Approved by:

Prof. Dr. Fernando Artur Nogueira Silva
President of the Examining Committee - Catholic University of Pernambuco, Brazil - UNICAP

Prof. Dr. Joaquim Teodoro Romão de Oliveira
Internal Examiner - Catholic University of Pernambuco, Brazil - UNICAP

Prof. Dr. Abdelhafid Khelidj
External Examiner - Université de Nantes, France - UN

Approved on 24 of march of 2020

To my parents (Valci and Mônica),
and to the society in which I live, may
this research contribute to transforming it.

Acknowledgements

The research reported in this Master's Thesis was developed at the Graduate Program in Civil Engineering of the Catholic University of Pernambuco during the period 2017.2 to 2019.1. During 2019, part of the research was developed at the Institut catholique d'arts et métiers, Nantes, France.

The activities developed in Brazil were under the guidance of Prof. Dr. Fernando Artur Nogueira Silva and the activities developed in France were co-oriented and supervised by Prof. Dr. Mahfoud Thalaiti and Prof. Dr. Abdelhafid Khelidj, respectively. I thank in this opportunity the dedication and interest that both of them gave to this research.

To my advisor, Prof. Fernando, for all confidence, encouragement, support wherever I was, guidance and friendship throughout my studies, for inspiring me as a person and professional. Thank you very much, for everything!

To Unicap, who since my graduation has contributed to my human and professional formation.

To Capes, for the monetary incentive of this Masters research for two years.

To ICAM, who welcomed me during the six months I was in France, for the space, tests, analyses, opportunity and experiences acquired, and to GeM Laboratory, of the University of Nantes, for the tests and analyses carried out.

To the companies that contributed and supported our research, especially to Construtora Habitar, GMG Engenharia e Consultoria LTDA, Lafarge Holcim, Supermix, Areiasil and Gravel Pit Itamatamirim.

To the people who believed in this Project, and contributed in various ways to its development, through the "Amor num Gesto", my most heartfelt thanks for the generosity and encouragement, I will be eternally grateful.

To the friends and colleagues that the Exchange brought me, Guy de Solminihac, Elenilson, Olivier, Geneviève, Christiane, Gaëlle, Khaterine, Lara, Fátima, Meriem, Joseph, Hakima, Fádime and Ana, for the exchange of experiences during these six months away and for so many memories.

To the friends I've made over the years through Unicap, among employees, teachers and students, Profª Marta, Profº Joaquim, Profª Ana, Profº Sérgio, Washington, Gleizer, Elias, Mariano, Pammello, Mônica, Jéssica, Isaque, Manoella, Klayne and Roberto, I thank them for their friendship and contribution in the development of this research.

To all my friends, especially those of the Community of Saint Theresa of the Child Jesus and the Holy Face, who were like a balm to my soul, for each encounter, conversation, sharing, gesture, smile, prayer and shared life, I take you all in my heart, you make life lighter.

To my dear friends, Priest Francisco Sales and Sister Loreto (in memory), who during this journey have been strong instruments of God in my life, contributing to the relationship of my soul with God and the understanding of myself.

To my fiancé Guilherme and his family, for his fidelity, respect, love, understanding, patience and friendship in all this journey that we have lived and learned together.

To all my family, especially my sister Monique and Hiago, for their unconditional love, understanding for the moments when I was not present and for the joy in each encounter.

To my parents, Valci and Mônica, for a lifetime dedicated to me and my sister, for the support and understanding during all this time that I developed this research.

To God, the beginning and the end of everything, for the gift of life, for granting me the vocation of an Engineer and for giving me all the aids to live it, all my gratitude and love.

"Know all the theories, master all the techniques, but in touching a human soul be just another human soul."
Carl Gustav Jung

ABSTRACT

NASCIMENTO, N. P. S. **Diagnostic of concrete samples extracted from pile caps affected by Internal Swelling Reactions**. 2020. 112p. Engineering Master's Thesis in Civil Engineering Graduate School, Catholic University of Pernambuco, Recife, Brazil.

Due to the early deterioration of pile cap foundations in residential buildings and bridges in the Metropolitan Region of Recife, several studies have been conducted over the past decade to diagnose the problem and to discover the reasons for this process and to stabilize measures implemented that can provide an acceptable level of performance of such elements. In this master's research, samples taken from a pile cap block of a residential building built about ten years ago were studied. Laboratory tests were performed to evaluate the mechanical and transport properties of concrete samples, as well as their physical and chemical composition using advanced analyses. The tests performed were: compressive strength, static and dynamic modulus of concrete elasticity, apparent porosity, gas permeability, scanning electron microscopy, X-ray diffraction and raman spectroscopy. Visually it was possible to identify some evidences, such as: cracks in map in the foundation surface, white stains in the aggregates, silico-alkaline gel edges, cracks in the aggregate, leaching, stains around the aggregates, white material deposited in the voids and pores completely filled with ettringite crystals. The problem of the extensive cracking in the pile cap foundation had its origin in the delayed ettringite formation, possibly coming from a high heat of hydration coming from the concreting of the large volume of concrete. The mechanisms that caused damage to the investigated pile cap blocks were the internal expansion reactions, mainly the alkali-aggregate reaction and the delayed ettringite formation. The presence of crystalline products of the alkali-aggregate reaction was proven through physical-chemical analyses, such as Raman spectroscopy and EDS. As well as the ettringite crystals found in XRD standards, SEM images and the chemical composition of EDS. The values of the mechanical properties of concrete were influenced in different ways by the reactions, namely: the compressive strength of the concrete was not affected by the reactions. On the other hand, the values of the static and dynamic modulus of elasticity of the concrete tend to decrease, about 74% and 53%, respectively. The porosity showed a high value (between 9 and 10%), as well as the concrete permeability (10^{-16} and 10^{-15}), determining the negative influence of ISR on the transport properties. Therefore, the methods used have proven to be effective in understanding the problem encountered and have the potential to be used in the design and execution of pile cap blocks.

Keywords: Internal swelling reactions, Alkali-Aggregate reaction, Delayed Ettringite Formation, Diagnostic of Pathologies on Concrete, Characterization and Analysis of Concrete Specimens.

RESUMO

NASCIMENTO, N. P. S. **Diagnóstico de amostras de concreto extraídas de blocos sobre estacas afetadas por Reações de Expansão Interna**. 2020. 112f. Dissertação (mestrado em engenharia) Programa de Pós Graduação em Engenharia Civil, Universidade Católica de Pernambuco, Recife, Brasil.

Devido à deterioração precoce dos blocos de fundação em edifícios residenciais e pontes na Região Metropolitana do Recife, vários estudos têm sido realizados na última década para diagnosticar o problema e descobrir as razões para este processo e para estabilizar medidas aplicadas que possam proporcionar um nível de desempenho aceitável de tais elementos. Nesta pesquisa de mestrado, foram estudadas amostras extraídas de um bloco de fundação de um edifício residencial construído há cerca de dez anos. Foram realizados ensaios laboratoriais para avaliar as propriedades mecânicas e de transporte das amostras de concreto, bem como sua composição físico-química utilizando análises avançadas. Os ensaios realizados foram os seguintes: resistência à compressão, módulo estático e dinâmico de elasticidade do concreto, porosidade aparente, permeabilidade a gases, microscopia eletrônica de varredura, difração de raios X e espectroscopia raman. Visualmente foi possível identificar algumas evidências, tais como: fissura em mapa na superfície da fundação, manchas brancas nos agregados, bordas de gel sílico-alcalino, fissura no agregado, lixiviação, manchas ao redor dos agregados, material branco depositado nos vazios e poros completamente preenchidos com cristais de etringita. O problema do extenso quadro de fissuração nas fundações teve sua origem na formação de etringita tardia, proveniente possivelmente de um elevado calor de hidratação oriundo da concretagem do grande volume de concreto. Os mecanismos que causaram danos aos blocos de fundações investigados foram as reações de expansão interna, principalmente a reação álcalis agregado e a formação de etringita tardia. Ficou comprovada a presença de produtos cristalinos da reação álcali-agregado através das análises físico-químicas, como espectroscopia Raman e EDS. Assim como os cristais de etringita encontrados nos padrões XRD, nas imagens do SEM e na composição química do EDS. Os valores das propriedades mecânicas do concreto foram influenciados de maneiras diferentes pelas reações, a saber: a resistência à compressão do concreto não foi prejudicada pelas reações. Já os valores do módulo estático e dinâmico de elasticidade do concreto tendem a diminuir, cerca de 74% e 53%, respectivamente. A porosidade apresentou valor elevado (entre 9 e 10%), assim como a permeabilidade do concreto (10^{-16} e 10^{-15}), determinando a influência negativa das ISR nas propriedades de transporte. Portanto, os métodos utilizados provaram ser eficazes na compreensão do problema encontrado e têm potencial para serem utilizados no projeto e execução de blocos de fundações.

Palavras-Chave: Reações internas de expansão, Reação Álcali-Agregado, Formação de Etringita Tardia, Diagnóstico das Patologias do Concreto, Caracterização e Análise das Amostras de Testemunhos de Concreto.

RÉSUMÉ

NASCIMENTO, N. P. S. **Diagnostic d'échantillons de béton extraits de foundations affectés par des réactions de tuméfaction interne**. 2020. 112p. Thèse de maîtrise en génie civil, Université catholique de Pernambuco, Recife, Brésil.

En raison de la détérioration précoce des fondations sur pieux dans les bâtiments résidentiels et les ponts de la région métropolitaine de Recife, plusieurs études ont été menées au cours de la dernière décennie pour diagnostiquer le problème et découvrir les raisons de ce processus et pour stabiliser les mesures mises en œuvre qui peuvent fournir un niveau acceptable de performance de ces éléments. Dans le cadre de cette recherche de master, des échantillons prélevés sur un bloc de pieux d'un immeuble résidentiel construit il y a une dizaine d'années ont été étudiés. Des tests en laboratoire ont été effectués pour évaluer les propriétés mécaniques et de transport des échantillons de béton, ainsi que leur composition physique et chimique à l'aide d'analyses avancées. Les tests effectués étaient les suivants : résistance à la compression, module d'élasticité statique et dynamique du béton, porosité apparente, perméabilité aux gaz, microscopie électronique à balayage, diffraction des rayons X et spectroscopie Raman. Visuellement, il a été possible d'identifier certaines preuves, telles que : des fissures dans la carte à la surface des fondations, des taches blanches dans les agrégats, des bords de gel silico-alcalin, des fissures dans les agrégats, des lixiviats, des taches autour des agrégats, de la matière blanche déposée dans les vides et des pores complètement remplis de cristaux d'ettringrite. Le problème des fissures étendues dans les fondations des chapeaux de pieux trouve son origine dans la formation tardive de l'ettringite, peut-être due à une forte chaleur d'hydratation provenant du bétonnage du grand volume de béton. Les mécanismes qui ont causé des dommages aux blocs de pieux étudiés sont les réactions d'expansion interne, principalement la réaction alcali-agrégats et la formation retardée d'ettringite. La présence de produits cristallins de la réaction alcali-agrégats a été prouvée par des analyses physico-chimiques, telles que la spectroscopie Raman et l'EDS. De même que les cristaux d'ettringite trouvés dans les étalons XRD, les images MEB et la composition chimique des SDE. Les valeurs des propriétés mécaniques du béton ont été influencées de différentes manières par les réactions, à savoir : la résistance à la compression du béton n'a pas été affectée par les réactions. D'autre part, les valeurs des modules d'élasticité statique et dynamique du béton ont tendance à diminuer, respectivement d'environ 74% et 53%. La porosité a montré une valeur élevée (entre 9 et 10%), ainsi que la perméabilité du béton (10^{-16} et 10^{-15}), déterminant l'influence négative de l'ISR sur les propriétés de transport. Par conséquent, les méthodes utilisées se sont avérées efficaces pour comprendre le problème rencontré et peuvent être utilisées dans la conception et l'exécution des blocs de fondation.

Mots Clés : Réactions de gonflement interne, réaction alcali-agrégats, formation retardée d'ettringite, diagnostic de pathologies sur béton, caractérisation et analyse d'échantillons de béton.

SUMMARY

FIGURE INDEX

TABLE INDEX

LIST OF ABBREVIATIONS AND ACRONYMS

AAR - Alkali-Aggregate Reaction

ABCP - Brazilian Portland Cement Association

ASR - Alkali-Silica Reaction

ASSR - Alkali-Silicate Reaction

ACR - Alkali-Carbonate Reaction

ATG or TGA - Analysis Thermogravimetric

CSH - Hydrated calcium silicate

C2S - Dicalcium silicate

C3S - Tricalcium silicate

C3A - Tricalcium aluminate

C4AF - Tetracalcium ferroaluminate

DEF - Delayed Ettringite Formation

ε (%) - Apparent Porosity

Eci - Static Modulus of Elasticity

Ed - Dynamic Modulus of Elasticity

EDS or EDX - Energy Dispersive X-Ray Spectroscopy

Fc - Compressive Strength

FT - Freezing and Thawing

ISR - Internal Swelling Reaction

ITZ - Interfacial Transition Zone

MIP - Mercury Intrusion Porosity

MRR - Metropolitan Region of Recife

SEM - Scanning electron microscopy

SP - Samples

σ-ε - Stress versus Strain Curve

XRD - X-Ray Diffraction

CHAPTER 01

1. INTRODUCTION

1.1 Research Significance

In the last decade, the occurrence of early deterioration of pile cap blocks in residential buildings and concrete bridges in the Metropolitan Region of Recife (MMR) has been reported with relative frequency. This process usually starts with the occurrence of a horizontal crack of large opening in the lateral faces of the element, located approximately 30 centimeters from the upper face of the block, and its installation is usually attributed to the expansions of concrete resulting from the alkali-aggregate reaction.

This issue is of particular local and national interest because early deterioration of the foundations of buildings and bridges many times involve a large amount of money to execute recovering works. This theme has payed, this way, the attention of technical community to adopt design and building strategies to find out solutions to overcome the difficulties associated with the favorable environment that we have in our region, such as: high alkali content of the cements used, reactive aggregates and water that arises from the underground of buildings.

No matter the origin of the cracking process is due the alkali-aggregate reactions - a point supported by some design engineers - or it arises from an inappropriate detailing of the anchorage of the vertical reinforcement, this occurrence creates preferential paths for aggressive agents to penetrate into the element causing deleterious effects.

Because of these occurrences, ultimately, civil and structural engineers should work together to assess, repair and manage the ongoing problems of internal swelling reactions that affect foundation structures. It is important that the recovery of these structures occurs with an acceptable level of safety and therefore qualified information on the effects of the reaction on the mechanical and transport properties of the concrete of such structures is required. On the other hand, owners of concrete structures demand reasonable assurance that their assets will retain their value and remains safe, functional and economic in terms of ongoing repairs costs. Therefore, the knowledge regarding the mechanisms whereby the concrete is damaged by ISR (Internal Swelling Reactions),

its effects on the behavior of concrete structures, as well as the choices of retrofitting techniques are an opened fields to research.

The pathological manifestations associated with chemical phenomena are more common all over the world in construction works containing large volumes of concrete, such as dams and pavements, but in Brazil, especially in the northeast of the country, the occurrence of alkali aggregate reaction and delayed ettringite formation in pile cap blocks and in spread footing foundations of residential buildings and bridges at early ages is very common. This fact has payed the attention of the civil construction industry and local research centers to the need to understand the mechanisms involved in this process so that mitigating or corrective measures can be adopted.

The research aims to contribute to the generation of knowledge that allows the execution of foundations of concrete buildings and bridges within a level of durability compatible with the standards of performance currently adopted in Brazil.

1.2 Research Objectives

The general objective of the master research is to perform the diagnosis of concrete samples collected from a pile cap block of a 41-storey residential building affected by internal swelling reactions using advanced laboratory tests.

The objectives of the study of this research are:

- Collect concrete samples from a pile cap block affected by internal swelling reactions in the city of Recife;

- To thoroughly characterize a solid concrete structure degraded by internal swelling reactions, through advanced tests, trying to correlate the problem in the field with the characteristics found in the laboratory tests;

- Perform the full characterization of the sample collected using advanced, destructive and non-destructive laboratory tests;

- To study the concrete transfer properties (durability indicators) using the gas permeability, apparent porosity and mercury intrusion porosity tests;

- Perform physical and chemical analysis of the concrete microstructure using scanning electron microscopy (SEM) associated with energy dispersive X-ray (EDX), X-ray diffraction (XRD) and Raman spectroscopy.

1.3 Outline of the Master Thesis

The Dissertation is organized in 6 (six) chapters. This first one presents the introduction, the statement of the research theme and its justification, the statement of the general objective and the specific objectives, the delimitations of the work and the organization of the dissertation.

Chapter 2 presents the bibliographic review on the internal swelling reactions, types and behavior. As well as a review of the concrete mechanical, transport and physical-chemical properties and characteristics.

Chapter 3 presents the description of the methodology used to develop the research in order to formulate the hypotheses to the diagnosis of the early deterioration of the concrete pile cap block from where the samples were collected.

Chapter 4 presents the results obtained through the experimental program performed as well as the complete discussion regarding the correlation of this results with the pathological manifestation observed in the pile cap block investigated.

Chapter 5 presents the conclusions drawn from the research performed as well as recommendations for future works.

After Chapter 5 there is the bibliographic of references used in the development of the research.

Finally, we find the Appendice with additional information and images about the study.

CHAPTER 02

2. STATE-OF-THE-ART

Concrete is a heterogeneous material, composed of a cement matrix, interfacial transition zone and aggregate. According to some researchers (Machovic, Kopecký, Nemecek, Kolár, Svítilová, Bittnar and Andertová), the typical thickness of interfacial transition zone (ITZ) is around 15-50 μm. It is considered the weakest phase of concrete due to the large amount of calcium hydroxide and needle-shaped of ettringite crystals in the open pores of the transition zone [64].

For a hardened concrete structure to have durability, it needs to ensure a long service life. There are several phenomena that can affect its performance. These attacks can be chemical, physical, mechanical, electrochemical or even biological, with two or more of them being able to act simultaneously. The chemical reactions that include the formation of expansive products are: external sulfate attack, delayed hydration of free calcium oxide (CaO) and free periclase (MgO), more commonly known as delayed ettringite formation (DEF), alkali-aggregate reaction (AAR) and corrosion of concrete reinforcement [39].

Cement has four main compounds - dicalcium silicate (C2S), tricalcium silicate (C3S), tricalcium aluminate (C3A) and tetracalcium ferroaluminate (C4AF). However, industrial Portland cements do not only contain the chemical composition present in silicates and aluminates. In the production of clinker, many elements and impurities, such as sulfur, magnesium, sodium and potassium are incorporated into these compounds and can be harmful if they are present in large amounts [39].

Soon after the hydration of C3A, the primary ettringite is formed, and it has no negative effect on concrete. However, secondary or “delayed ettringite” promotes expansions and cracks in the structure. The ettringite mineral or the hydrated calcium trisulfoaluminate depends on the amount of sulfate ions and the concentration of aluminate ions present in the solution [39]. Its formulation is as follows:

$$[Al(OH)_4]^- + 3[SO_4]^{2-} + 6[Ca]^{2+} + aq. \rightarrow C_6AS_3H_{32} \quad (1)$$

Sulfate expansion in concrete is generally attributed to the ettringite formation. The internal origin of sulfate ions can be from an aggregate contaminated by gypsum or from a cement that contains a very high sulfate content in its composition. With thermal cure temperatures are higher than 65°C, the ettringite is unstable, decomposing into hydrated monosulfate and it, in turn, is adsorbed by C-S-H. Subsequently there is a desorption to form of a secondary ettringite, which generates expansion and cracking [30, 39].

The expansion generated by the DEF mechanism causes cracks between the pulp and in the transition zone. Regarding the crystals, they come from the recrystallization of the ettringite in the cracks and the submicrometer crystals that are along the cement paste [39].

Some interesting hypotheses were suggested by [44] to understand the delayed ettringite formation. One of them was that the origin of the sulfate ions necessary for the phenomenon to occur comes from the release of hydration products. The presence of water inside the concrete is also of paramount importance for the migration of ions. For [44, 77, 83], whatever the origin of microcracks in concrete (ASR, arising from the manufacturing process or loading during the use of the structure) increase its permeability. The other hypothesis admits that the ettringite is deposited in the existing microcracks, and there are two ways of its propagation - expansion or by growing from the crystals.

There are three types of known Alkali-Aggregate Reactions: Alkali-Carbonate Reaction (ACR), Alkali-Silicate Reaction (ASSR) and Alkali-Silica Reaction (ASR), the latter being the most frequently one.

The concept of alkali-silicate reaction was originally introduced to differentiate AAR involving reactions with aggregates of rocks such as filites, clays and certain grauvaques (rock of sedimentary origin formed by fragments of other rocks and another type of cement, which can be of natural siliceous and, more rarely, calcareous, in which these are trapped) that contain phyllosilicates (for example, vermiculite, chlorite and mica) from reaction involving different forms of silica. In this case, the reaction occurs with silica in the combined form of phyllosilicates and not with free silica [51]. These reactions are complicated and difficult to characterize, but they are usually expansive.

The alkali-carbonate reaction does not produce a gel. Instead, coarse aggregates particles expand due to the reaction of alkaline hydroxide with small dolomite crystals in a clay matrix, resulting in a de-dolomitization reaction (i.e., the decomposition of dolomite into brucite, alkaline carbonate and calcite).

It is of great interest to the academic and technical community to better understand the alkali-silica reaction (ASR) because the damage it imposes to the concrete structures such as pile cap blocks, dams bridges, concrete walls, pavements and nuclear power plant usually demands a

large amount of money to perform retrofitting works. ASR is one of the main problems for concrete durability, which can cause several damages, like expansion and cracking that can lead to loss of strength and modulus of elasticity [26]. The damage generated by ASR also affects the serviceability of concrete infrastructures [16, 77].

ASR is a reaction that demands special conditions to develop, such as enough amount of alkali in pore solution (pH: 13,0 - 13,5) and portlandite from cement paste, certain siliceous phases in some natural and synthetic aggregates and sufficient moisture (more than 70%). These combined factors results in secondary products that can be lead to expansion [1, 16, 26, 53]. The alkali content of the cement is expressed as sodium oxide soluble in equivalent acid corresponding to Na_2O + 0,658.K_2O. The alkalis (generally sodium and potassium) in the cement usually range from 0,2 to 1,5% of Na_2O equivalent and come from the raw materials of clinker. Depending on this alkali content, the solution of the concrete pores may present a pH between 12,5 to 13,5 [39].

The chemical process of the ASR reaction begins when the silica structure is dissolved by the nucleophilic attack of hydroxide ion (OH-) which due to its highly degraded structure, it behaves like a hygroscopic silica gel. The reaction product is a gel known as Alkali Silica Gel, which is not harmful for the concrete [32, 78]. However, this gel has a tendency to swell when it absorbs moisture present in the concrete pore solution and, if confined in the matrix, can generate internal stresses. As far as absorbs more moisture, the pressures increase inducing the development of microcracks, which in extreme situations, can lead to concrete rupture [26, 32, 18, 78].

The reactions that govern the ASR damages [26] are, including: (1) dissolution of metastable silica, (2) formation of nano-colloidal silica sol, (3) gelation of the sol, and (4) swelling of the gel:

$$(SiO_2)_{solid} \xrightarrow{1} (SiO_2)_{aqueous} \xrightarrow{2} (SiO_2)_{sol} \xrightarrow{3} (SiO_2)_{gel} \xrightarrow{4} \text{swelling of gel.} \quad (2)$$

Gel expansion depends on both the dissolution of reactive or potentially reactive silica and the mass transport properties of the concrete and the availability of moisture, and there may be less damage to dry and dense concrete.

In a confined environment, concrete exhibits considerable sensitivity due to the presence of internal defects, faults and microcracks. Thus, solid concrete under triaxial compression states present localized tensions because of their heterogeneous features. In view of these aspects, their behavior becomes even more complex when damage occurs [41, 85, 86].

The pattern characteristics and extension of the cracking process provide information on the mechanism of internal expansion reactions and the magnitude of the microscopic damage to the concrete structure, explained in [41, 77].

The British Cement Association [14] proposed a scheme to show how cracks occur from different expansion phenomena caused by different types of expansion, as illustrated in Figure 1.

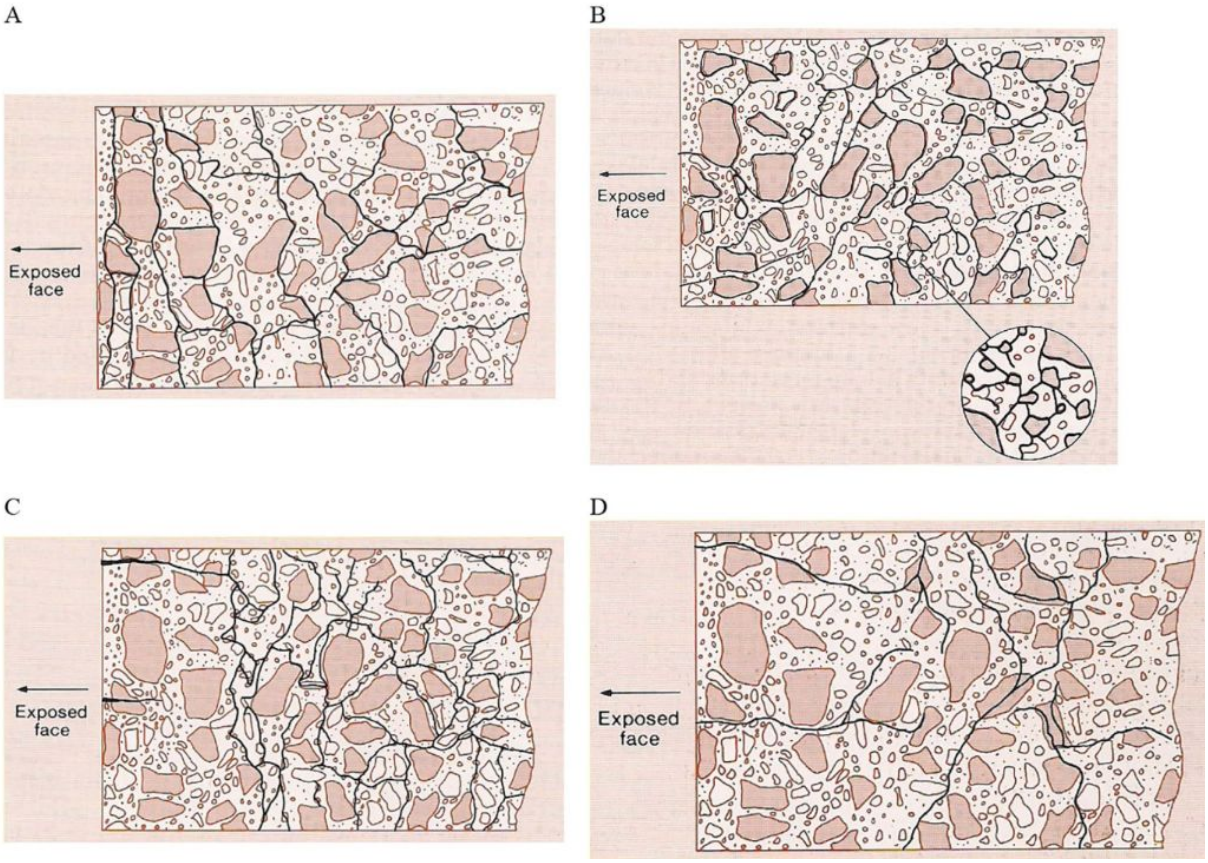

Figure 1. Representation of cracking generated by different expansion phenomena: A) Freezing and thawing; B) Delayed ettringite formation; C) Alkali-silica reaction (fine aggregate); D) Alkali-silica reaction (coarse aggregate) [14], apud [41].

The formation of cracks resulting from freezing and thawing (FT) occurs from the pores or voids of the cement paste, following to the transition zone (A). The hydrated monosulfates, resulting from the decomposition of ettringite, are distributed homogeneously in the cement paste, therefore, the expansion propagates homogeneously, generating cracks in the paste-aggregate interface (B). For the alkali-silica reaction phenomenon, cracking develops in a different way, starting in the particles of the fine (C) or coarse (D) reactives aggregates, reaching the cement paste afterward.

The alkali-silica reaction does not develop rapidly, taking many years for its propagation and, it is very destructive when alkalis are found in high concentration in the pore fluid [47]. The damages due to the reaction can be identified by some features exhibited in the concrete structure, such as, cracking, misalignment of structural elements, spalling and discoloration at the concrete surface, disintegration of the cement paste, surface pop-outs and gel exudation [16, 22, 23, 26, 46, 55, 78].

Depending on the type and composition of the aggregate (fine or coarse), they can be classified into: Non-reactive (NR) or Innocuous, Potentially Reactive (PR), or Potentially Reactive Pessimistic Effect (PRP).

The minerals considered reactive are all silicates or minerals of silica, hydrated silica (opal) and amorphous silica (obsidian and silica glass) [39]. In descending order of reactivity, the minerals considered reactive are opal, obsidian, cristobalite, tridymite, chalcedony, chert, andesite, rhyolite and tensioned or metamorphic quartz. Minerals constituents of granite, gneiss, shale, sandstone and basalt (feldspars, pyroxenes, amphiboles and micas) are minerals considered innocuous. The minerals that can produce the alkali-silica reaction found in Thomas et al. and Hasparyk [46, 48] are opal or amorphous silica, chalcedony, cristobalite, volcanic glass, tridymite natural and artificial glass, various forms of microcrystalline, cryptocrystalline and strained quartz.

There are two processes during this reaction.

The physical one, which occurs first, where the Na+, K+ and OH^- ions migrate from the interstitial liquid phase to the existing reactive silica particles in the aggregate. And the chemical, when the ions Hydroxyl (OH^-) attack the siloxane bridge (SiO - O - SiO) near the surface of the components of the reactive silica, generating the rupture of the crystalline chain. If the reactive particles of the aggregate silica have low permeability, this attack will be superficial, but when there is a high permeability, the gel can be visualized inside the aggregate, in its cleavage planes [37]. This gel produced in the reaction is essentially composed of silica, the alkali forms present in the cement or aggregate (sodium or potassium), calcium and water and has a viscous nature, whitish in color.

The gel formation through these processes can occur with two different elements, as it was shown by Figueirôa and Andrade [37]. The reaction equations are the followings:

$$2NaOH + SiO_2 + H_2O \rightarrow Na_2SiO_3 \cdot 2H_2O$$

Or

$$2KOH + SiO_2 + H_2O \rightarrow K_2SiO_3 \cdot 2H_2O$$

Many standard procedures to test reactivity of aggregate and/or cement-aggregate combinations were developed [31-32, 78] in order to evaluate the potential reactivity of these materials when combined in the concrete structure. There are several methods for classifying the potential reactivity of aggregates prior to their use in construction, many of them disseminated internationally. However, besides presenting results considered as false-cognate, they do not reproduce the reality found in the field in the structures [26, 42, 78].

Even after almost 80 years of Stanton's discovery of the alkali-silica reaction [61], many gaps [26] still exist in its properties (e. g., composition, mineralogy and surface characteristics; pH, alkalis amount; temperature and humidity) and mechanisms, as well as in the test methods to determine and effective prevention measures. There are not enough literature characterizing ASR products, so the mechanism that develops expansion in the reaction is still not well understood [3].

It is common to charge exclusively to a single factor the damage of a concrete structure, when affected by internal swelling reactions, but the interaction between several factors - AAR and DEF - is usually more frequent [49, 83, 84].

Several authors presented studies of the occurrence of alkali-aggregate reaction and the delayed ettringite formation occurring simultaneously. We can mention [64] that analyzed the concrete microstructure through scanning electron microscopy (SEM) and found the two phenomena. Another interesting case was the one presented by Shayan and Morris [08] in which visual inspection and analysis identified the AAR, mainly because in the composition of the concrete of the bridge it was found gneiss with reactive quartz. On the other hand, the heat of hydration released during concrete casting around 80°C caused the DEF.

In an advanced investigation of concrete cores carried out by Hasparyk [48], the two reactions were found, where in addition to visual inspection, several tests were performed, as well as analyses of the microstructure by means of SEM, EDX and XRD. A bridge deck damaged by AAR and DEF studied by Shayan et al. [09] showed significant reductions in the modulus of elasticity, as well as residual expansion. Another foundation structure that presented combined attack was studied by Hasparyk et al. [49], where the causes of the occurrence of these phenomena were the temperature around 80°C and the presence of reactive aggregates in concrete. A comprehensive understanding of the damage generated by the combination of DEF + ASR presented by Sanchez et al. [41, 77, 78, 85, 86] showed reductions in the mechanical properties of the concrete analyzed.

Many structures in Britain and France that had in their composition high cement consumption (between 420 and 550 kg/m³) and high equivalent alkali content (>4,0 kg/m³) presented several damages between 5 and 20 years after their construction, in the presence of moisture and in a temperature close to 80ºC, besides being concreted during the summer, which potentiated the heat release [34].

DEF manifests itself when the source of sulfate ions is internal and not external, in the presence of an aggregate contaminated by gypsum or cement with high sulfate content. In addition to these factors, the process of steam-curing the concrete at temperatures above 65ºC can cause the development of delayed ettringite, since it is not stable in these conditions [39].

In concrete submitted to a high temperature during concrete casting in place, it is possible that the primary ettringite formed during the hydration reactions is decomposed [34]. When it returns to room temperature and in the presence of humidity, this ettringite can re-crystallize inside the hardened concrete, causing expansion pressures that are capable of generating cracking, which potentiates damages to the structure.

According to Bensted [70], the causes, the physical-chemical mechanisms and the kinetics of the reaction that originates the DEF are still not fully understood. However, the combination of several factors is of utmost importance for this internal expansion reaction to begin.

Water is an essential factor to produce the reaction, whether in structures that are in contact with water, susceptible to water ingress or exposed to a high humidity level, such as foundations. Other elements described in Guide Technique [70] are the maximum temperature reached by the structure and the time duration in which this temperature is maintained. Thus, if the temperature exceeds 65°C and other key parameters are present, the probability of occurrence of DEF is high.

Ettringite is a hydrated calcium trisulfoaluminate, so the sulfate and aluminate contents are directly linked to its formation process. A necessary condition is that the cement used contains a sufficient amount of tricyclic aluminates (3CaO, Al2O3 or C3A) and sulfates (SO3). As ettringite is highly soluble in large quantities of alkalis, the use of a type of cement with a lower alkaline content would contribute to the non-occurrence of the reaction [70].

Another recommendation for the delayed ettringite formation not to occur as described in [70] is the use of mineral additions. It was observed that they contribute to a less exothermic concrete, as they reduce the amount of clinker aluminates and end up modifying the type and texture of the moisturizer. The additions indicated are those that have components with latent or pozzolanic hydraulic properties, such as blast furnace slag or fly ash, natural or artificial pozzolana).

Finally, the petrographic nature and the volumetric mass of the aggregate are elements which influence heat transfers in the reactions of concrete.

Studies have shown that an isolated factor is not sufficient for the internal expansion reactions to develop, but the presence of several parameters acting simultaneously under certain conditions.

Both expansion reactions (AAR and DEF) have similar symptoms and the two have moisture as a conditioning factor to develop expansion. According to Torres and Andrade researchers [34] what may be happening in the Metropolitan Region of Recife is the combination of AAR/DEF attack mechanisms.

One of the important challenges that researchers have to answer is to understand as fully as possible these phenomena of expansion that affect various concrete pile cap foundations in the

region at an early stage and how it is possible to correlate the level of damage generated with the change in strength and deformation properties of concrete and its durability. Furthermore, it is equally important to relate the results of laboratory tests to the situations found in the field so that possible design and construction strategies can be proposed to minimize the possibility of these expansion phenomena take place on concrete. That is why there is a need for a greater understanding of their features and mechanisms.

This study aims to provide a mechanical and transfer properties characterization and the physical-chemical analysis, using advanced techniques to analyze cores extracted from real buildings that have concrete elements affected by internal swelling reactions.

2.1 Brief Report Regarding Some Cases of Internal Swelling Reactions on Pile Cap Blocks in Recife

The city of Recife is very close to sea level, making the level of moisture in contact with pile cap foundations quite high in the region. Besides the hot tropical climate and the average annual temperature being around 26ºC, other factors such as the chemical composition of the cements used and the high temperatures released in the process of building the pile cap foundations contribute directly to the large number of cases of internal expansion reactions in Recife.

The foundations of multifamily residential buildings in the Recife City have presented over recent years an early process of deterioration.

This process is characterized, in some cases, by cracks in the form of a map, and in other cases, cracks with very well defined orientation have been observed, usually horizontal at the top of the blocks on stakes or shoes. The Figures (2, 3, 4 and 5) below illustrate the cracking process described.

Figure 2. Pile cap foundation with longitudinal cracking [11].

Figure 3. Longitudinal crack and relative horizontal displacement [25].

Figure 4. Characteristic of the cracking in the pile cap block surface [25].

Figure 5. Pile cap block with cracked upper surface, with openings in the order of 25mm [37].

These cracking processes were presented in public and residential buildings of MMR. In the Metropolitan Region of Recife (MRR) there are others several cases described in literature about the occurrence of blocks with large-aperture horizontal cracking [25, 29, 37, 58, 59, 60].

According to the adaptation of the Technical Guide [70] made in research developed by [34], it was confirmed the risk of delayed ettringite formation in pile cap foundations of the MMR. Therefore, the City of Recife presents the ideal conditions for the occurrence of internal reactions of expansion in concrete that, allied, the poor choice of materials and construction processes, create a very favourable framework for the early degradation of the foundation elements of buildings.

2.2 Mechanical Properties

2.2.1 Compressive Strength

The compressive strength can be considered the main parameter of structural concrete. Many factors interfere in its results, such as aggregate, water-cement ratio (w/c), age, molding process, curing, microcracks, porosity, among others. It is also considered when evaluating the durability of a structure. The evaluation of concrete samples extracted from real structures is used to evaluate their overall stability/safety.

This property is affected when the concrete has certain expansion mechanisms. The study carried out by [41, 77, 78, 80, 85, 86] showed how these reactions can directly affect this property, acting alone or in combination.

According to Kubo and Nakata [73] apud by Sanchez et al. [41] compressive strength is little influenced by the internal expansion reaction ASR, considering high expansion levels (0,30%).

The concrete presents loss of compressive strength around (0,29 to 0,43%) when it has DEF combined with ASR or only DEF acting solely. When the material presents only the ASR, the loss is between (20 to 35%), the two cases when the level of expansion is very high [41].

The compression strength test was conducted at the GeM Laboratory, University of Nantes, Saint Nazaire, France. The press used was the RP 3000 DC/LC, with a force of up to 2500 KN.

2.2.2 Static Modulus of Elasticity

The elastic characteristics of a certain material contribute to the definition of its stiffness, depends too on the degree of hydration or the maturity of the concrete. As the technical community already knows, concrete has a non-linear behavior, contrary to the aggregate and some cement

pastes. Thus, for being a complex composite material, its properties end up not being equivalent to the addition of the properties of its components (Figure 6) [39].

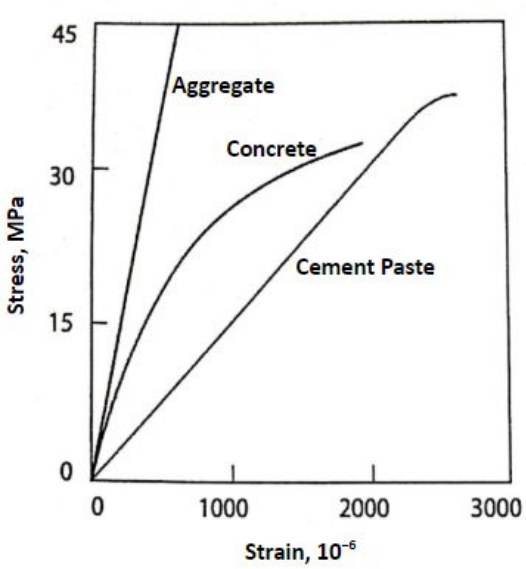

Figure 6. Stress-strain curve behavior for different types of materials, adapted from [48], apud [39].

Although the concrete has not been subjected to external loads, there may be microcracks in the aggregate paste interface. There is a stage in which the cracks in the transition zone remain stable, that is, 30% of the ultimate load. In it, the stress and strain are proportional to each other and the curve σ-ε is linear. Static modulus of elasticity, also called initial tangent modulus, is equivalent to the slope of a straight line drawn tangent to the curve σ-ε, at any point on that curve [39].

The determination of the deformation modulus of concrete can be done by means of cylindrical test specimens, by means of empirical equations used to estimate it in structural projects and by the inclination of the curve σ-ε in the elastic regime, generated in the compressive strength test.

According to Sanchez et al. and Hasparyk in [40, 41, 48, 77, 78, 80, 85, 86] the static modulus of elasticity is more sensitive to the effects of the internal expansion reactions in relation to the compressive strength.

The presence of DEF or ettringite combined with ASR in the concrete provides stiffness loss between 50 and 65%, and when it presents only ASR the decrease of the values of static elasticity modulus can reach up to 67% [41]. Reactive aggregates can also contribute to the concrete expansion process through DEF [30].

From the strength test the force versus displacement curve was obtained, so the position was divided by the length of the sample, finding the deformation. In this way a new strain graph was

generated. A tangent line to the curve (σ-ε) at the origin was designed to find the initial static tangent module of each concrete sample tested to compression. And this was done for all three samples.

2.2.3 Dynamic Modulus of Elasticity

One of the most important mechanical properties of structural concrete in situ is the modulus of elasticity, which can be evaluated by the static or dynamic method.

One of the non-destructive methods that allows evaluating the degradation of concrete and contributes to the study of its durability is the dynamic modulus of elasticity. As mentioned [39], it presents values higher than the static modulus of elasticity, about 20, 30 and 40% for high, medium and low strength concretes, respectively, and is equivalent to a very small instantaneous strain.

This test measures the velocity of propagation of ultrasonic longitudinal wave pulses in concrete in the hardened phase, in addition to allowing the detection of cracks, voids or defects, correlate the velocity of pulses with the quality and strength of concrete and measure changes in material properties over time. The standard that recommends it is BS EN 12504-4:2004 [15].

It is important to note that microcracks reduce the modulus of elasticity of concrete, even reducing the wave velocity inside the sample. The frequencies used to measure the velocity of this pulse are around 20 kHz to 150 kHz [39].

One of the ways of measuring dynamic modulus of elasticity is by means of an electro-acoustic transducer. It is kept in contact with the concrete surface, so that a pulse of longitudinal vibrations is produced, crossing a known length. Thus, this pulse is converted by a second transducer into an electrical signal, allowing the electronic timing circuits to measure the duration of pulse transit, according to standard [15]. Another way is by using the Grindosonic apparatus. This method is described by [12] and measures the frequency of a stationary acoustic wave inside a concrete cylinder by means of two vibrational modes, namely bending and twisting.

The stiffness of the concrete is a property that ends up being influenced by the level of internal cracking of the structure. The values of this property may also decrease due to internal microcracks, which was explained by Picandet et al. in [66].

The dynamic module test was performed at GeM Laboratory, University of Nantes, Saint Nazaire, France. The equipment adopted was the Grindosonic, J. W. LEMMENS (Mk5 "Industrial").

2.3 Concrete Durability Aspects - Concepts and Tests

2.3.1 Gas Permeability (K)

Permeability is a property that governs the rate of flow of a gas under pressure through the pore structure of a solid, and the permeability coefficient is given by the letter K [39]. This property is used to evaluate durability characteristics of concrete, but it is commonly estimated by measuring the gas permeability of never stressed nor damaged specimens [65, 81].

As explained by Picandet et al. in [66], the study of transfer properties in cracked concrete is of paramount importance in predicting durability, because the leaching and freezing processes depend on the flow of aggressive agents through the porous material. Mechanisms such as ASR and DEF also depend on the flow of liquids or gases in the microstructure to be generated.

The cracks produce voids in the materials, increasing porosity and modifying the pore structure, regardless of the source of this degradation, either by tensile or compressive stresses. Microcracks are connected until they generate macro cracks, and this interconnectivity allows the entry of more aggressive agents into the concrete [43, 63, 81]. In the study developed by Picandet et al. in [66], the overall gas flow controls the cracking pattern in samples that presented deterioration.

The concrete is a thin porous body, and the percolation of gas through it can be the result of two modes of flow: viscous and slipping, also called Knudsen's flow [66]. One of the most used methods to determine the non-viscous flow is by the relation proposed by Klinklenberg, where there is an intrinsic permeability coefficient K_v (m^2) relative to the viscous flow.

It is possible to associate the changes in permeability of the material studied with information obtained in microscopic analyses, such as evolution of microcracking, orientation and opening of cracks, data that may indicate the level of damage to the structure [65, 84]. Another correlation that can be made is with porosity, and these transfer properties are intrinsically related, as reported by Tahlaiti in [45].

The gas permeability test was performed at the ICAM Materials Laboratory in Nantes - France, with the device called "debitmètre massique" or mass flow meter, which will be described in section 4.3.1.

2.3.2 Mercury Intrusion Porosimetry (MIP) and Apparent Porosity (ε)

The durability of cement based materials like concrete depends on the diffuse and convective transport properties. These mechanisms should be studied taking into account the microstructure of

the material, for example, porosity and pore size. By obtaining the microstructural parameters it is possible to relate them to the physical properties and thus obtain a better characterization of the concrete [17, 81].

Porosity is an inherent property of material, and there are certain ways of measuring it. One of them is mercury intrusion porosimetry (MIP), that is of great importance to characterize the pore structure of concrete in different scales. Another method is through apparent porosity, based on the principle of Archimedes, which are play important role for understanding the durability of concrete [45, 81].

The permeability of the environment is characterized by pores, which are defined as free spaces distributed within the solid structure, which allow the fluid to flow. Figure 7 exhibits a scheme of the porous structure of the materials.

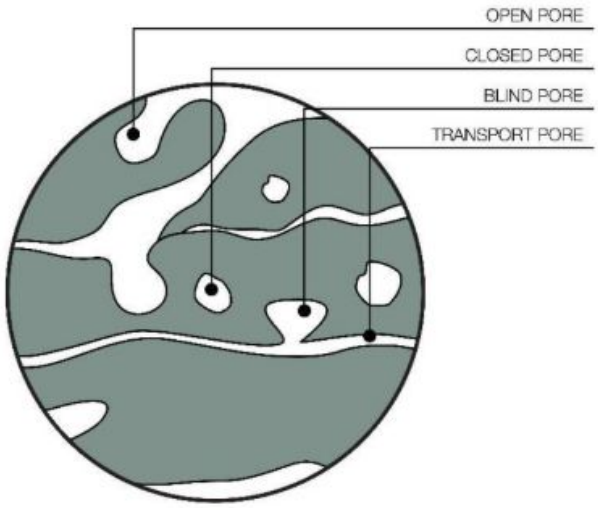

Figure 7. Material porous structure [71].

Mercury intrusion porosimetry is a technique to characterize the transport properties of concrete and investigate the porous space of its microstructure. The MIP test requires the complete removal of water from the sample by drying.

According to Diamond in [57], mercury intrusion porosimetry is a technique used to estimate the pore size distribution of porous solids. However, it was also concluded that there are limitations when applying MIP in hydrated cementitious materials, because the measurements misallocate the pore volume, providing smaller sizes than the actual ones. This comes from the difficulty of access of the pores to the mercury that is introduced in the sample.

In the study developed by Galle in [17] it was evaluated how desaturation, desorption and dehydration, associated with drying, during the MIP test can cause damage to the pore structure and

provide incoherent information. Drying in an oven-drying at 105°C overestimates the total porosity, while vacuum drying, freeze-drying and drying in an oven-drying at 60 °C, are more realistic. In relation to the pore structure, the porosity generated by the 60°C and 105°C oven-dryings may be due to capillary stress, or to micro cracks in the internal thermohydraulic stress and to the dehydration of cement hydrates.

Some negative points were found when the porosimetry test is performed through the intrusion of mercury, as a change in the results due to previous drying and the size of the internal pores are considered even smaller than they are in reality [57].

In a study conducted by Tahlaiti in [45] with different w/c ratios, it was observed that the C15 concrete (with higher w/c ratio) presented a distribution of multimodal pores, considered wide or scattered, illustrated in Figure 8.

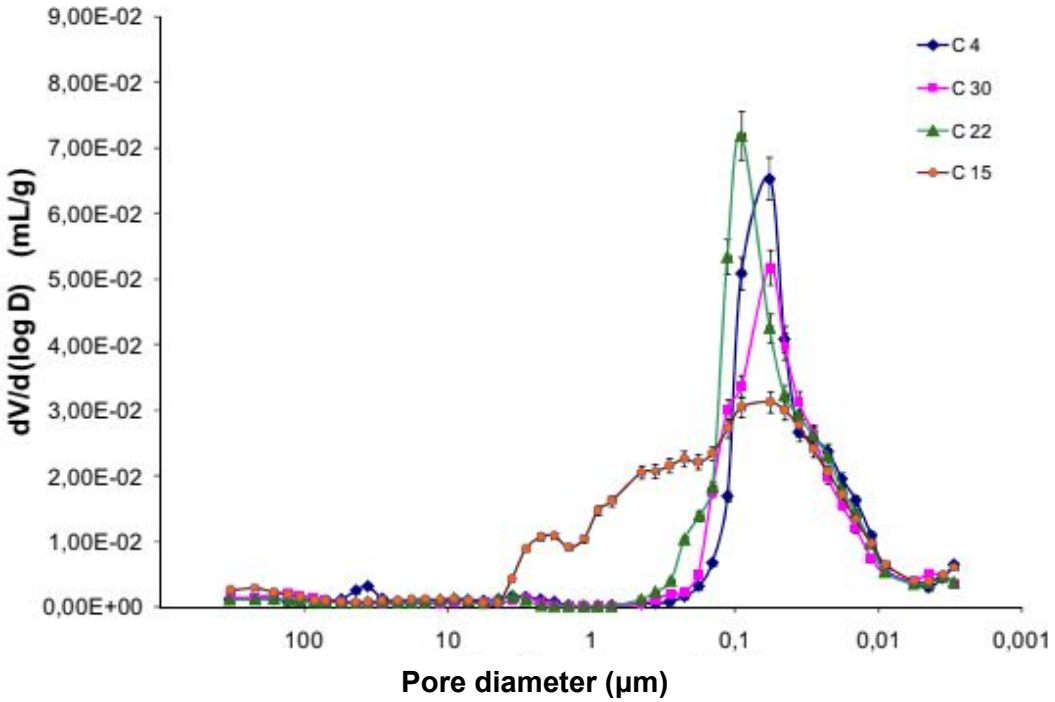

Figure 8. Porous distribution curve for C4, C15, C22 and C15 concretes [45].

The other concretes (C22, C30 and C4) resulted in a monomodal distribution, that is, with the presence of only one peak in the porosity curve. Another important aspect to be highlighted is that when the w/c ratio is higher, the porosity also presents its highest value, a factor explained by the higher number of pores when there is a higher w/c [45].

When comparing the results of two types of porosity for the same concrete [45], there are lower values for the one that was performed with mercury, an inconvenience that was highlighted by [57].

The properties of concrete as porosity and permeability are intrinsically related, as presented by Thalaiti in [45, 81]. The results obtained in this study were that as the porosity values increase, the permeability increases proportionally.

In the case of the influence of the delayed ettringite formation on the transport properties, it was observed by Glasser et al. [28], and mentioned by Taylor et al. in [30] that ettringite accumulates in freely available spaces, thus not contributing to expansion. In other words, this causes the expansion to be influenced by the amount of space available in the pores.

Another important consideration made by Taylor et al. [30] was that ettringrite can cause greater expansions in smaller pores with low connectivity than in larger pores with large connections.

The apparent porosity was performed at the ICAM Materials Laboratory in Nantes - France, and the apparatus was made with a white absorbent tissue surrounding the samples and was covered with a transparent plastic, where it was sealed from the inside with a double-face acrylic gray tape, where a vacuum pump removed all the air and then water was inserted into the system.

2.4 Physical-Chemical Analysis

2.4.1 Scanning Electron Microscopy (SEM)

The scanning electron microscopy technique is of great importance for the analysis of damaged concrete because it provides qualified information on the microstructure, such as primary and secondary mineral phases in pores or cracks, morphology, chemical composition and other data.

For the research developed by Leemann in [3], concretes of different years and types of structure were studied. The concrete of a bridge built in 1969 was given the name CS-1. That of a retaining wall built in 1980 was named CS-2.

The following is a series of SEM images from several researchers showing the possibilities of obtaining information on concrete samples.

Figure 9 shows a SEM image of a concrete analysed by Leemann in [3], where cracks can be seen in the aggregates filled with ASR products.

Some fragments of calcite incorporated to the crystalline ASR product were also found, as well as layers parallel to the crack wall, composed of silica gel, C-S-H and calcite. They are usually formed when the aggregate has dolomite (Figure 10).

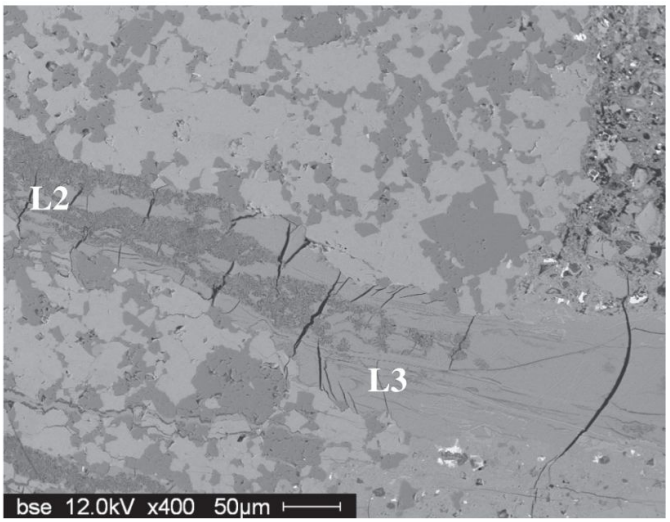

Figure 9. Vein in CS-1 concrete aggregate that has crystalline and amorphous reaction products in L2 and only amorphous in L3 [3].

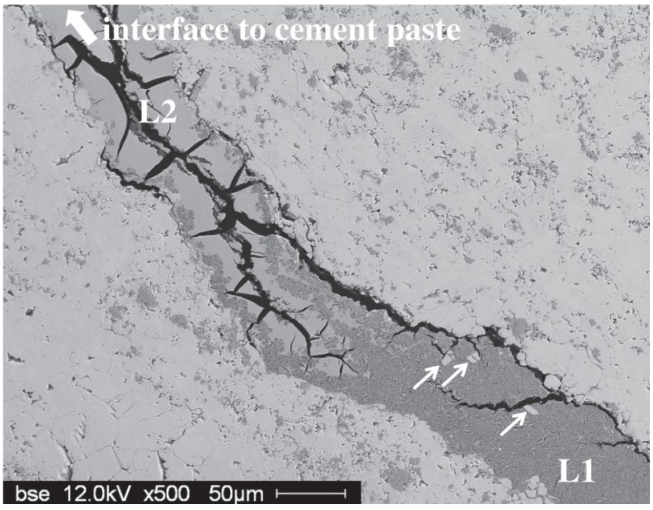

Figure 10. Vein with transition between the amorphous product (L2) and the crystalline product (L1), where the white arrows indicate calcite fragments incorporated in the product L1 (CS-2 concrete) [3].

The chemical composition of the reaction products found in the cracks inside the concrete aggregates with damage is also very similar. In another analysis performed on concrete affected by ASR, calcite, quartz and feldspar minerals were found in the veins of the aggregates that developed the reaction, illustrated in Figure 11 [53].

The crystalline structure is presented in the form of a fan or plate, and the amorphous has a constant and homogeneous shape, shown in Figure 12. The composition of the crystalline product does not present great differences when comparing different aggregates of concrete [2].

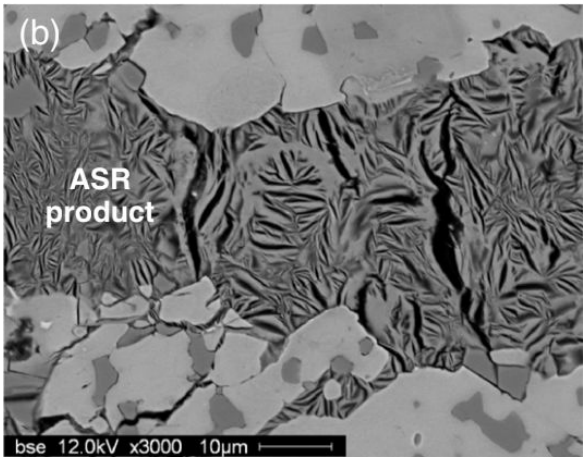

Figure 11. Aggregate with ASR products inside the crack, where the light grey color represents the calcite mineral and the dark ashes are quartz and feldspar [53].

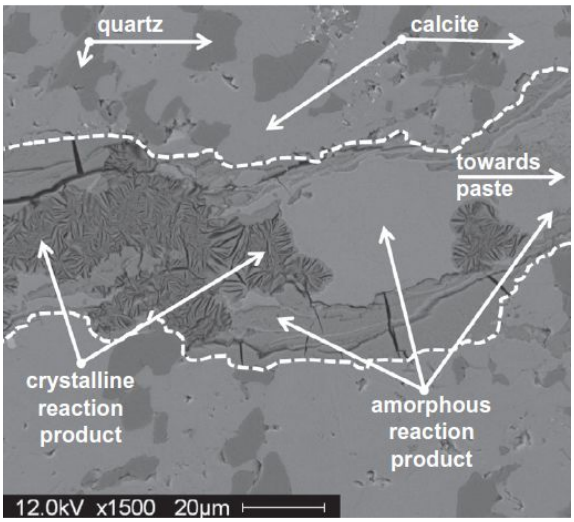

Figure 12. Aggregate cracking with calcite and quartz in its composition. On the right side it is possible to find amorphous product and on the left, crystalline product [2].

Other characteristics observed were the increase in the calcium content and the reduction in the alkali content, which goes from the product of the crystalline reaction to the amorphous, a fact also found by [2] and other researchers [3, 79]. The amorphous reaction product has a slight increase in the calcium content, and when the crack starts from the aggregate to the cement paste, the Ca/Si ratio of the ASR product increases to a value of 0,6 [6].

In a study developed by [48] about 100 concrete cores deteriorated by chemical phenomena were extracted. The analysis by scanning electron microscopy (SEM) showed several characteristics of RAA, as well as DEF acting simultaneously. For the microanalysis, the dispersive X-ray energy (EDX) technique was used.

The SEM images present the micrography of the crystallized and ettringite products dispersed in the sample, respectively (Figures 13 and 14). Figure 15 shows the spectrum where it is possible to see the crystalline product of alkaline silica calcium composition generated by the alkali-aggregate reaction.

The products observed were mostly the chemical elements silicon, calcium and potassium, and various forms, showing to be coherent with the gels formed in the reaction [48].

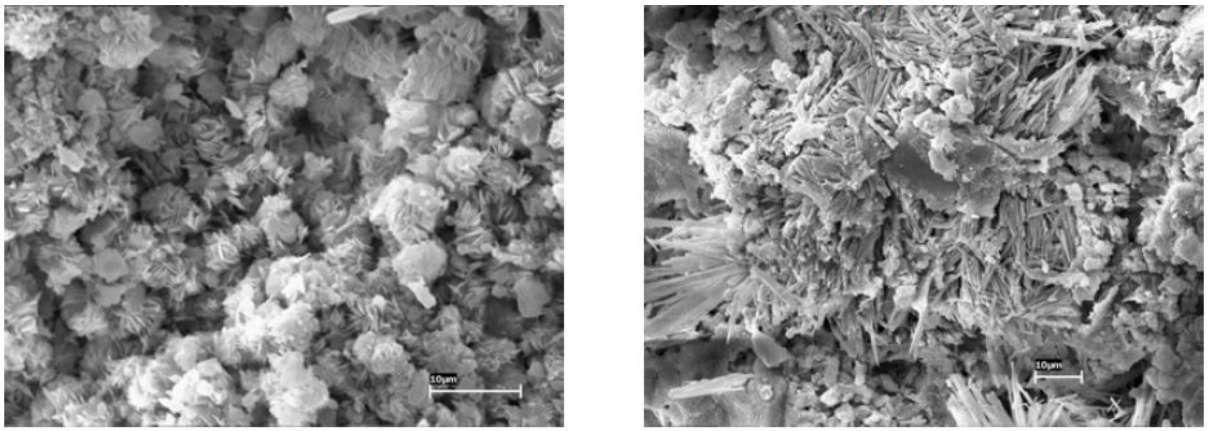

Figures 13 and 14. Crystallized products and ettringite spread in the mortar [48].

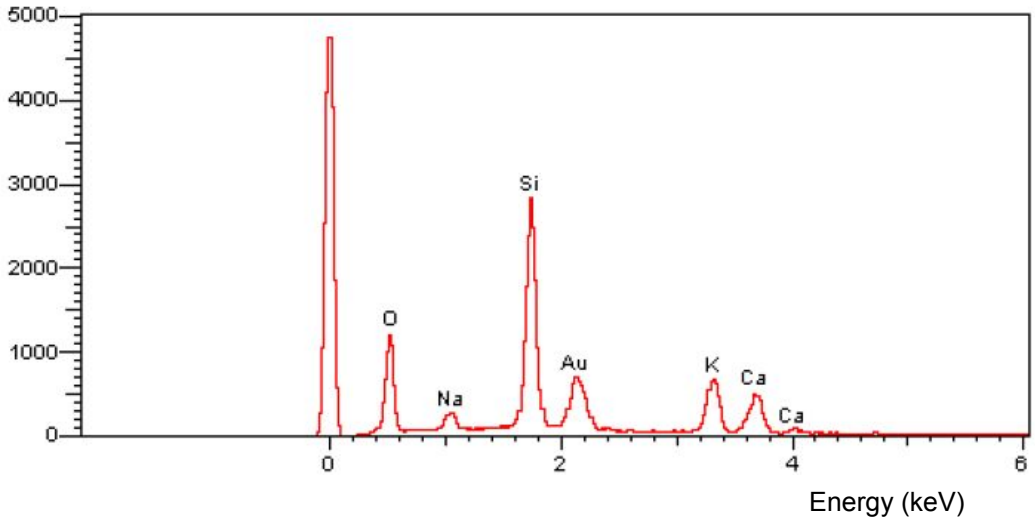

Figure 15. Characteristic spectrum of AAR products in concrete pores [48].

Crystallized products were identified in [48] on the aggregate as well as gel, the two with alkaline silica calcium composition. There was white material of the reaction in the pores and cracked gel at the edge, with vitreous characteristic. Additionally, there was ettringite dispersed in the whitish mortar and crystals deposited in some pores. The products found as indicators of this reaction were sulfur, aluminum and calcium.

The scanning electron microscopy technique provides characteristics such as the morphology of the microstructure, and although it is not quantitative, it allows a greater or lesser incidence of the components to be observed [48, 79].

SEM analyses were conducted at the GeM Laboratory of the University of Nantes in Saint Nazaire, France, and the SEM used for observations is a ZEISS ЄVO®40 equipped with a Back-scattered Electron (BSE) detector.

2.4.2 X-Ray Diffraction (XRD)

The X-ray diffraction method provides information on the atomic and molecular structure of the materials, especially crystalline materials, allowing to identify the atomic positions and the chemical composition of the samples.

The XRD standards found by Leemann et al. in [6] indicate for samples MS10 and MS10-Mk that the C-S-H was the main product of the reaction. MS10-CA also presents, but with low crystallization, showing strong signs of strätlingite, illustrated in Figure 16.

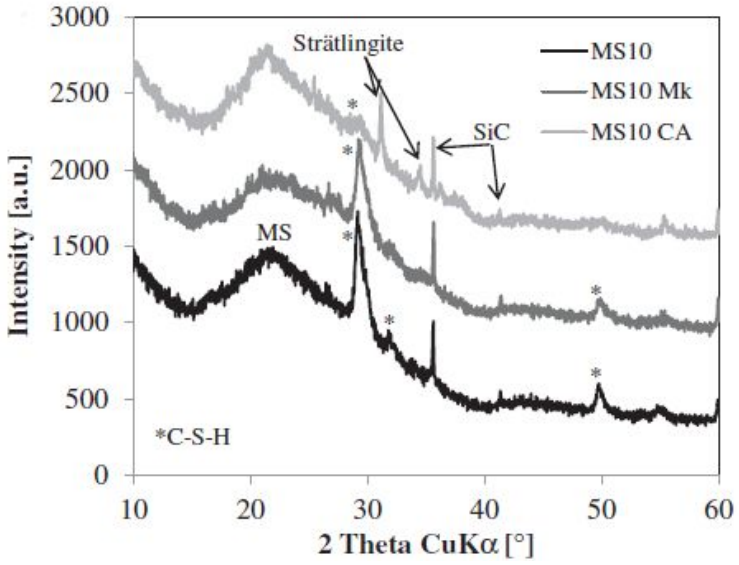

Figure 16. XRD patterns in the samples MS10, MS10 Mk and MS10 CA after 28 days [6].

Four pure gel samples from alkali aggregate reaction were analyzed by Hasparyk in [48] through X-ray diffraction. The results of the sample diffractograms were very similar. In 2 theta of 26° there was strong reflection, which normally appears between 24 and 31°, being compatible with the amorphous silicates (Figure 17).

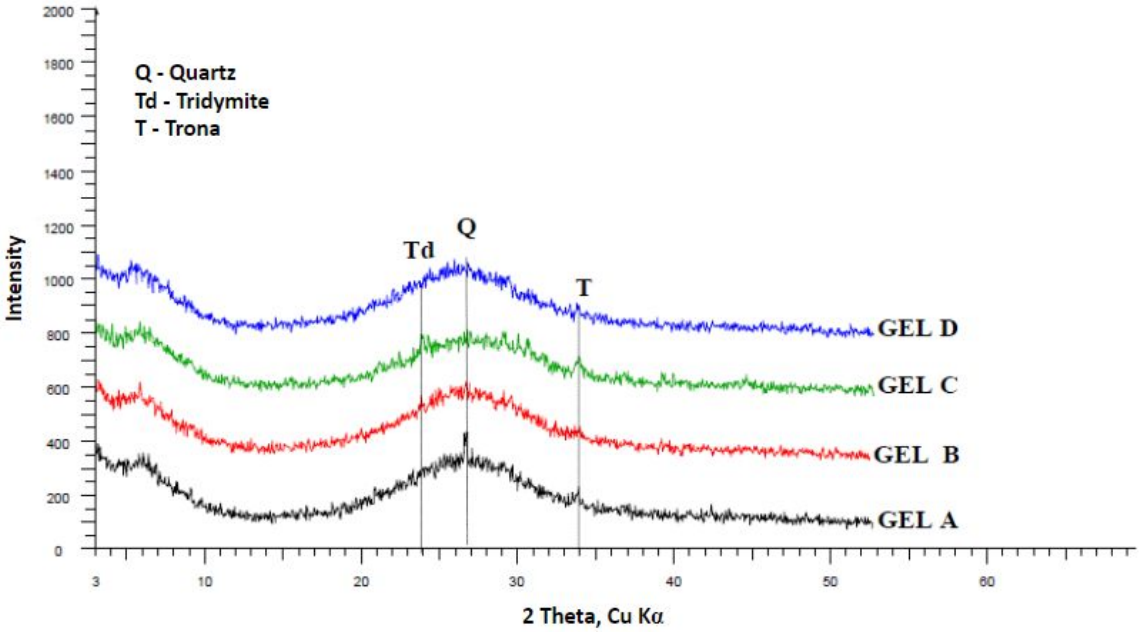

Figure 17 . XRD patterns obtained from four exudate gel samples from the alkali-aggregate reaction [48].

The detected peaks indicate crystalline phases, such as quartz, tridymite and trona, which corresponds to a hydrated sodium carbonate. Tridymite is a reactive component of aggregates and its composition contains silicon dioxide, or silica [39]. Another constituent found in the analyses made by [48] was sodium, combined in the form of trona, which is a highly crystalline product.

Another important detail observed was that in the crystalline phases there was no presence of potassium and silicon, indicating that these elements are part of the amorphous phase of the gel (reaction product) [48].

Through X-ray diffraction analysis performed by [7], it was observed that the products of the ASR reaction are formed first, followed by the delayed ettringite and soon after the cracking occurs in the transition zone. Mature concrete samples generally present in their composition hydrated calcium silicate, sodium hydroxide and hydrated monosulfate. This can be confirmed by means of XRD patterns.

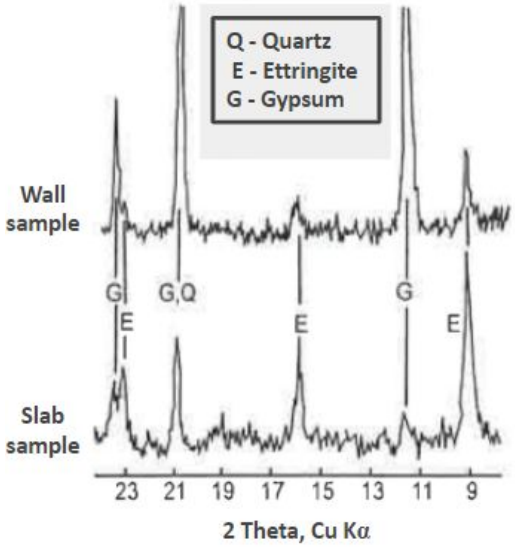

Figure 18. Concrete diffractogram of Fort Peck Dam after sulfate attack [39].

A concrete diffractogram (Figure 18) of the Fort Peck Dam that had a sulfate attack in 1971 showed higher amounts of ettringite and gispsite, contrary to the compounds that should exist and confirming the presence of the chemical effect. The quartz peaks that can be seen in Figure 18 are attributed to the contamination of the paste by the aggregate [39].

The XRD were conducted at the GeM Laboratory of the University of Nantes in Saint Nazaire, France, and XRD patterns were done by using an X-ray diffractometer SEIFERT MZ VI E with Co Ka radiation.

2.4.3 Raman Spectroscopy

Raman spectroscopy is commonly used in the chemical analysis of cement clinker and hydration products, and can also identify the distribution of minerals in a particular sample [64].

This technique can be used as a laboratory tool to identify molecules, compounds and to study the chemical bond, as well as to reveal information about the structure of ASR products. With Raman spectroscopy it is possible to analyze amorphous and crystalline materials, making it possible to review cementitious materials and concrete [16].

Raman spectroscopic analysis is based on the inelastic dispersion of monochromatic light, where light is generated by a laser and the Raman spectrum produced consists of a range of characteristics, each one associated with a vibrational mode of the analyzed material. A phase specific fingerprint is one of the results of the Raman spectrum, being unique for each material [3].

In a study developed by Leemann in [3] two concretes affected by ASR analyzed - one from a bridge and another from a retaining wall, built in 1969 and 1980, respectively. The aggregates of the CS-1 and CS-2 concretes showed cracks that were filled by the reaction products, which often had their layers parallel to the edges of the crack. They were smooth and non-textured, i.e. amorphous.

In different locations of a CS-1 concrete aggregate, Raman spectra were found almost identical to two main bands 630 and 1110 cm-1. Other bands with relative intensity between 7 and 36% were also observed in 202, 284, 341, 427, 483, 603, 688, 784 and 1016 cm-1 (Figure 19) [3].

The CS-1 concrete spectra were identical, with little variation. The band with a value of 465 cm-1 corresponds to the quartz and the additional bands, with values of 714 and 1088 cm-1, are two calcite bands. The CS-2 concrete behaved in the same way. In both concretes, the reaction products were crystalline. The transition from crystalline to amorphous product, extending from the periphery of the aggregate to the cement paste, was the place where the Raman spectra were collected in the CS-1 concrete.

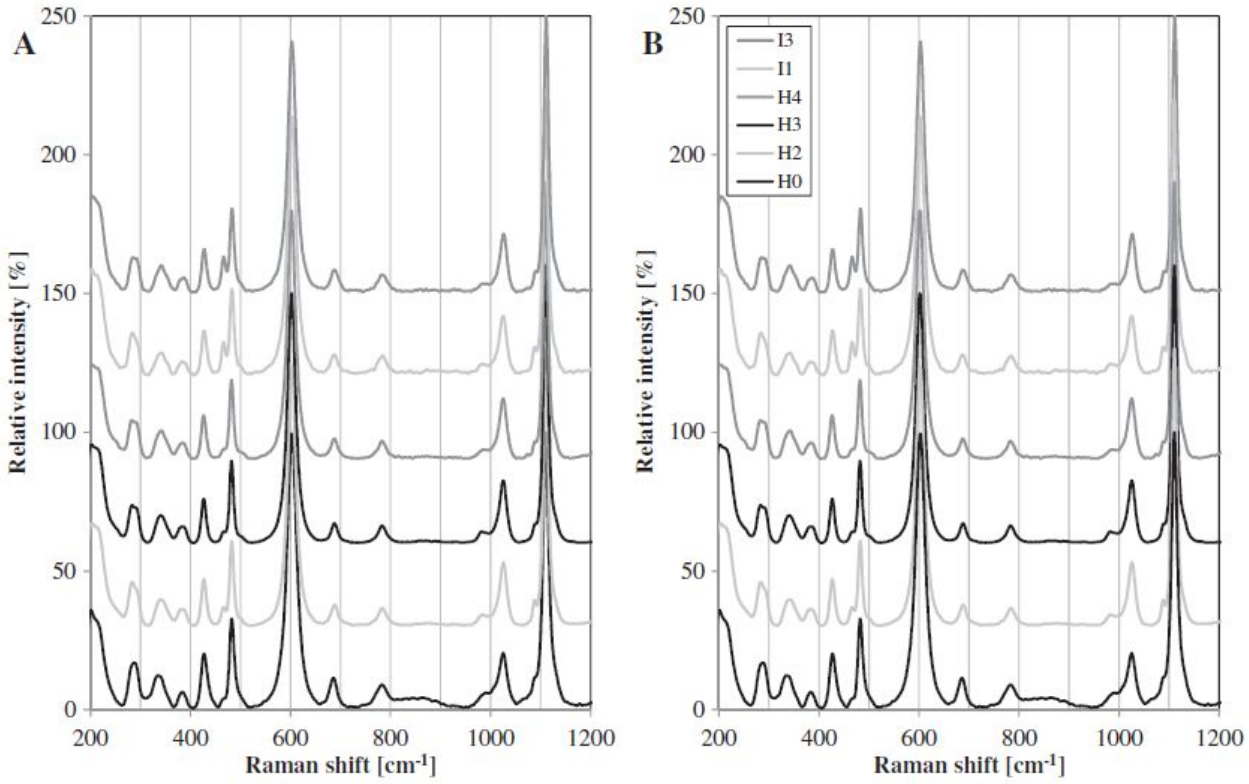

Figure 19. Raman spectra of the crystalline reaction products obtained in different places in an aggregate of the concrete CS-1 (A) and of different aggregates in the same concrete (B) [3].

At the edge of the aggregate, the bands of the ASR crystalline product disappear, and when the vein progresses to the cement paste, the spectra show an increase in noise, causing the signal of the products to be no longer recognized (Figure 20) [3].

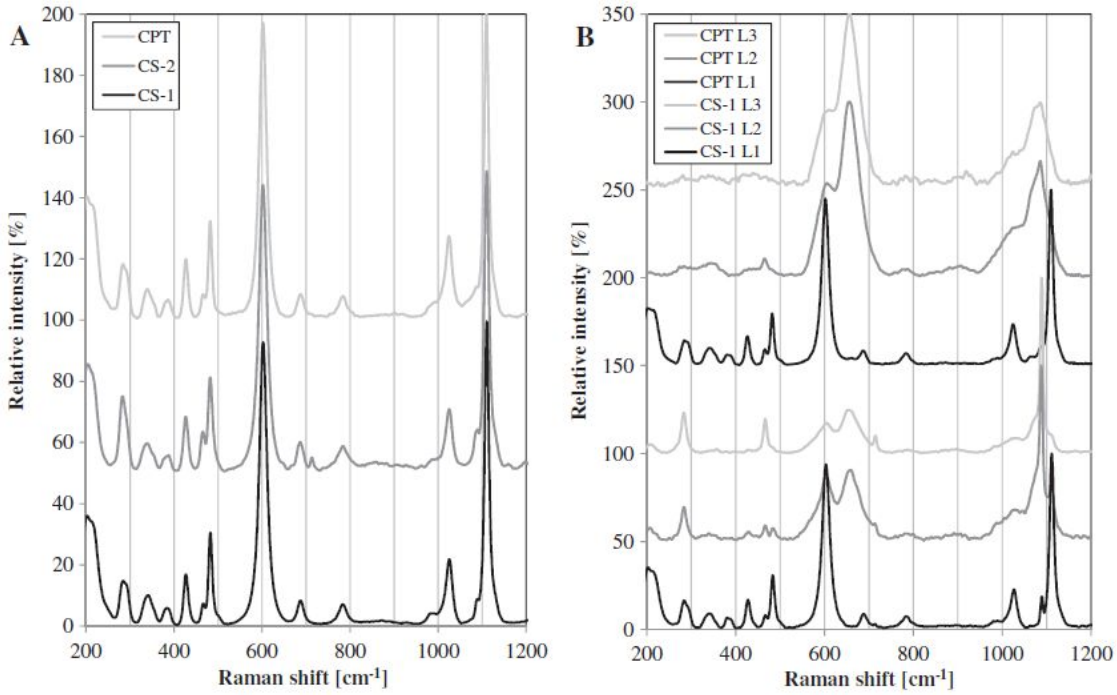

Figure 20. Mean of the Raman spectra values found in the ASR products of the CS-1 and CS-2 (A) concretes and three different locations of the same aggregate of the CS-1 and CPT concrete (B) [3].

In a study developed by Balachandran et al. in [16] Raman spectra were found in two broad bands in the range of 800 to 1200 cm-1 (high frequency region) and in the range of 400 to 700 cm-1 (low frequency region), indicating that the gel had an amorphous nature (Figure 21). It was also possible to conclude that Raman spectroscopy has great potential to study the gel structure generated by the silica alkali reaction.

The chemical analysis performed with Raman spectroscopy complements the SEM and XRD analyses, allowing a confirmation of the microstructure components of the sample. The presence of some phases found in the analysis with the diffractometer can also be confirmed through the Raman spectroscopy technique.

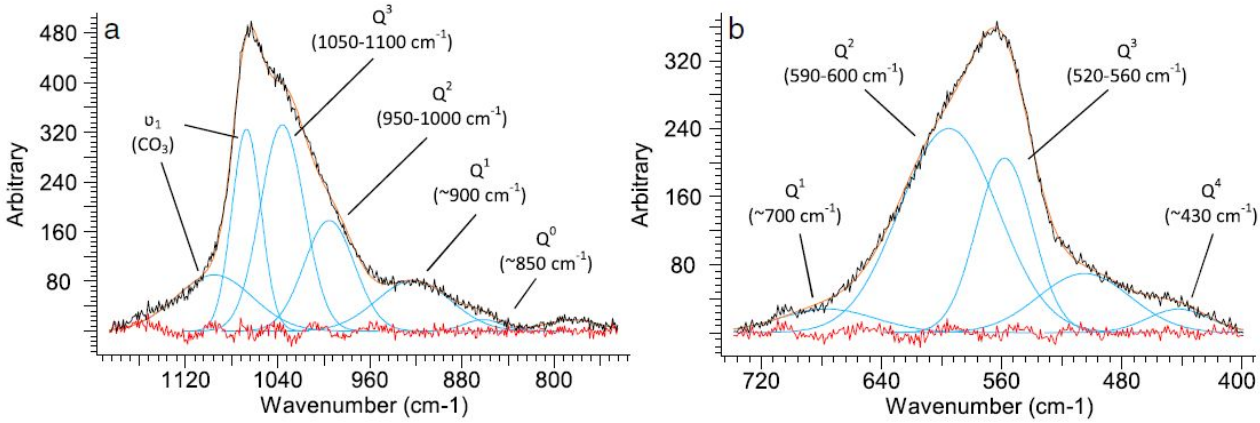

Figure 21. Representative curves of Na gel: a) High frequency region and b) Low frequency region [16].

The analyses Raman was performed at the ICAM Materials Laboratory in Nantes - France, and the Raman spectra were produced using the Confocal Raman Microscope SENTERRA II (Bruker).

2.4.4 Thermogravimetric Analysis (TGA)

The principle of TGA is to characterize the degradation occurring in a material when exposed to an environment with controlled temperature and atmosphere. It is possible to obtain the temperature at which degradation starts and ends, and at which the rate of change in the mass of the sample is maximum.

Through the thermogravimetric analysis it is possible to determine in cement pastes the evolution of the non-evaporable water content and calcium hydroxide during hydration. Thus, the degree of hydration of the cement used can be estimated [52]. In the thermogravimetric analysis the loss of mass occurs due to the decomposition of some of the phases or the loss of water [48]. Chemically bound water is the term referring to the total amount of anhydrous solids present in the sample, and can be determined by thermogravimetric analysis [5].

The DTA curves found by [6] are shown in Figure 22. The loss of mass is indicated in it. The behavior of the curves were similar, which indicates similar amounts of covering water present in hydration products.

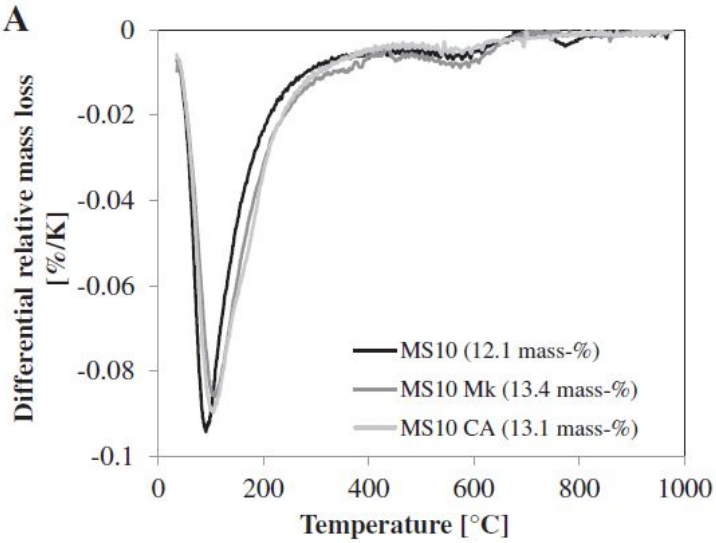

Figure 22. Ignition loss of 30-1000°C obtained by TGA analyses after a reaction time of 28 days [16].

In Figure 23 the DTA curve was used to verify endothermic or exothermic peaks, and it was possible to verify three reactions that generate loss of mass of the sample during its heating. The temperature values were: 110°C, 238°C and 463°C. In another curve, the peak found was 772,9°C, also endothermic [48].

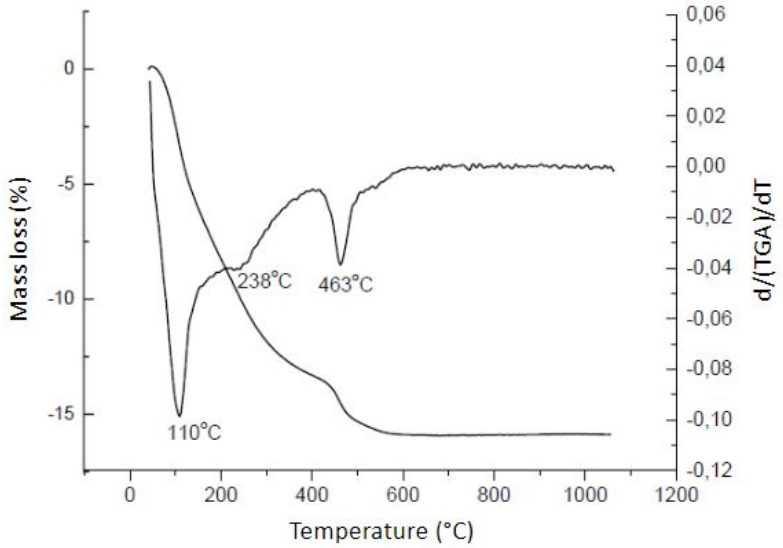

Figure 23. Thermogravimetric and thermogravimetric derivative curves of exuded gel [48].

CHAPTER 03

3. METHODOLOGY

The methodological strategy of the research contemplated four distinct phases: (a) choice of a typical multi-family residential building whose pile cap foundations had presented symptoms of the occurrence of the alkali-aggregate reaction in its concrete elements; (b) choice of a foundation element more affected by the reaction: (c) extraction of concrete samples and (d) carrying out various laboratory tests to the complete characterization of the samples.

The main characteristics of the building chosen for the study are the following:

● 41-storey residential reinforced concrete building located in Recife, Pernambuco, Brazil;

● Foundation of the main tower of the building executed with steel pile caps over concrete blocks. The average depth of the piles was 17 meters;

● Building located in the urban area of Recife about 5 km from to the sea;

● Environmental Aggressiveness Class adopted in Building Structures Design in accordance with the Brazilian NBR 6118:2014 concrete structure design standard: CAA II;

● Concrete compressive characteristic strength (fck) = 35 MPa;

● Type of cement used in foundations - It was not possible to obtain more precise information but local construction market practice suggest the possible of use CP II E or F cements;

● Approximate date of construction of the building: 2010.

Figure 24 shows an overview of the foundation of the main building tower where the location of the pile cap blocks can be observed.

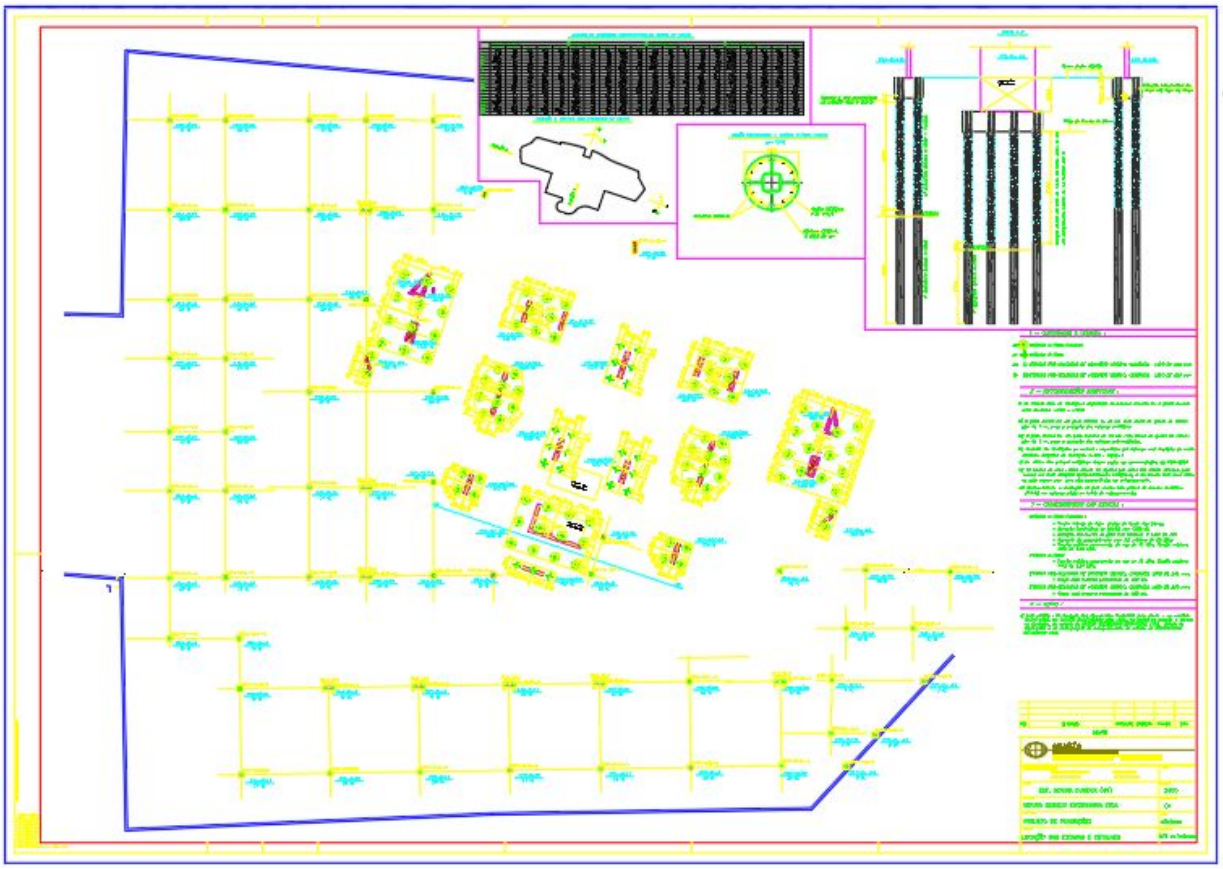

Figure 24. Plan of location of the pile caps [11].

The pile cap block chosen to extract concrete samples to deeply investigation was the one that presented a more expressive cracking process. In this block it was visible a horizontal cracking located approximately 25 cm from its upper face, corresponding to the upper end of the main reinforcements. Other pile cap blocks of the building presented the same cracking pattern with similar features with changes only in the magnitude of the crack openings.

These cracks had a wide, non-uniform opening of approximately 10 cm, and in the extension of the entire pile cap foundation, around 6,55 m. It was also observed that the connections between the piles and the lower face of the pile cap were intact.

The following figures that were executed by the author represent the typical cracking frame found in various pile cap blocks of the building (Figures 25, 26, 27, 28, 29, 30 and 31).

The map cracking in the block was not uniform over the entire block surface (Figures 25 and 26), but at some points it was quite predominant (Figure 29).

Figure 25. Horizontal and map cracking in pile cap block.

Figure 26. Horizontal and map cracking in pile cap block.

Figure 27. Cracking in pile cap and place where a sample was extracted.

Figure 28. Overview of the pile cap foundation S(P1+P8+P32).

Figure 28 contains an overview of the pile cap foundation chosen for the analysis, showing the three columns, the cracking in the pile cap surface and some of the points where the samples

were extracted. The cracks in maps were widened for the injection of epoxy in the recovery of damage to the block.

Figure 29. Cracking in map format on the surface of the pile cap foundation S(P1+P8+P32).

The cracks were larger on the front face of the pile cap block when compared to the cracks in the back part of the structure, as shown in Figure 30.

Figure 30. Longitudinal cracking with a large opening in the pile cap block S(P6+P9) [11].

Figures 31 and 32 illustrated the pathological manifestations in the pile cap block (P6+P9) on the face between the E1 and E2 piles [11].

Figure 31. Opening of cracks and depth of the crack [11].

Figure 32. Horizontal displacement and sloping cracks [11].

In the images above, the existence of a horizontal crack approximately 25 cm from the upper face, corresponding to the upper extremity of the main armors, was verified on all faces of the pile cap block. These cracks had a high opening, not uniform, of about 40 mm, as shown in Figure 31.

Besides the crack presenting a high opening, it was also observed the presence of relative horizontal displacement of about 3.5 cm on the frontal face and 3 cm on the posterior face. On the lateral side, this movement, although existing, was of lesser magnitude. Note the presence of inclined cracks, proper to the shear, on the frontal face, as shown in Figure 32.

It is a pile cap foundation with a concrete volume of approximately 64 m³, containing a total of 12 metal piles. In this pile cap block the following non-factored loads applied are indicated below. The X and Y direction are shown in Figure 33.

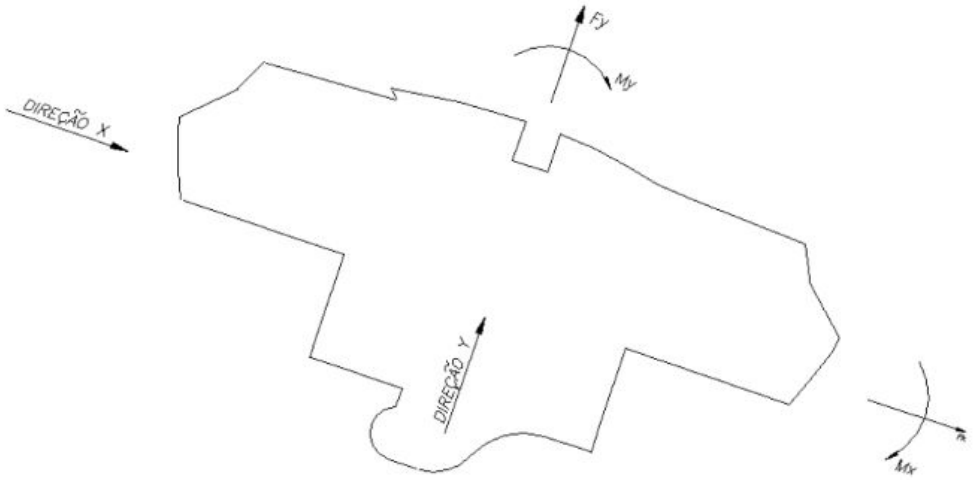

Figure 33. Direction and course of the wind's forces [11].

Pillar P1

- Normal Design Effort = 6.870 kN;
- Design Bending Moment in X Direction = 7.040 kN;
- Design Bending Moment in Y Direction = 3.140 kN;

Pillar P8

- Normal Design Effort = 13.320 kN;
- Design Bending Moment in X Direction = 1.760 kN;
- Design Bending Moment in Y Direction = 250 kN;

Pillar P32

- Normal Design Effort = 380 kN;
- Design Bending Moment in X Direction = not available;
- Design Bending Moment in Y Direction = not available;

Figure 34 represents the pile cap S(P1+P8+P32), with the extraction sites of each core, identified by the notations (SP-01, SP-02, SP-03, SP-04, SP-05 and SP-06). The another points identified by (A, B, C and D) are where were extracted the samples of smaller sizes also used for analysis and characterization. All samples were extracted in the direction parallel to the launching of

the concrete and only the SP-06 was in the direction perpendicular to the launching. The face chosen was where there was longitudinal cracking along the pile cap block.

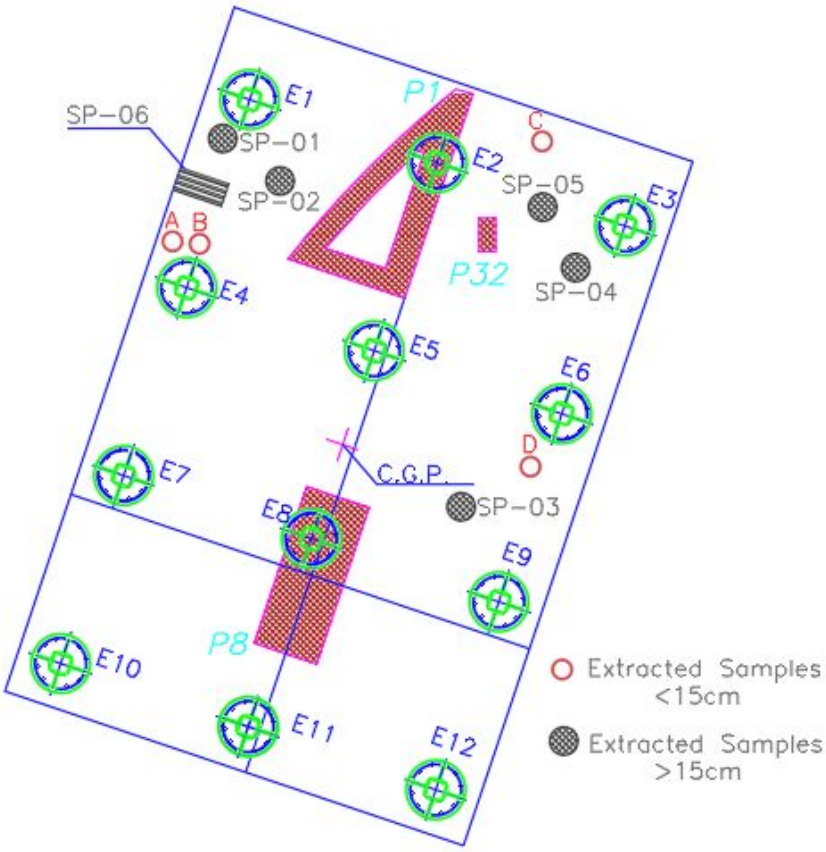

Figure 34. Place of extraction of the samples in the Pile Cap Block S(P1+P8+P32).

The concrete samples were extracted with two single-phase electric drills of such dimensions with 75 mm diameter - Model Husqvarna dm2 240 and Tyrolit dk32. The extraction procedure was executed in such a way that the sectioning of the block reinforcements was avoided as much as possible. The specimens were extracted from the upper part and from lateral faces of the pile cap block, totalling 6 (six) cylindrical concrete samples with dimension of 15 cm x 7,5 cm - height and diameter, respectively. The entire sample extraction process was performed in a single day and lasted approximately 7 hours.

In the following figures (Figures 35 and 36) one can see the six concrete samples extracted in the pile cap block investigated.

Figure 35. Samples extracted from the block (SP-01, SP-02 and SP-03).

Figure 36. Samples extracted from the block (SP-04, SP-05 and SP-06).

The laboratory tests were carried out partly in the facilities of the Institut Catholique D'Arts et Métiers and other partly in the GeM - Institut de Recherche en Génie Civil et Mécanique - UMR 8183 - CNRS - École Centrale de Nantes - Université de Nantes, both institutions located in France where the researcher worked as a visiting researcher for six months (January to June 2019).

There are several ways to study the mechanical and transfer properties of concrete, as well as perform physical-chemical analysis in its structure [82, 83, 84]. The Figue 37 shows the schema of the content of each group of tested performed.

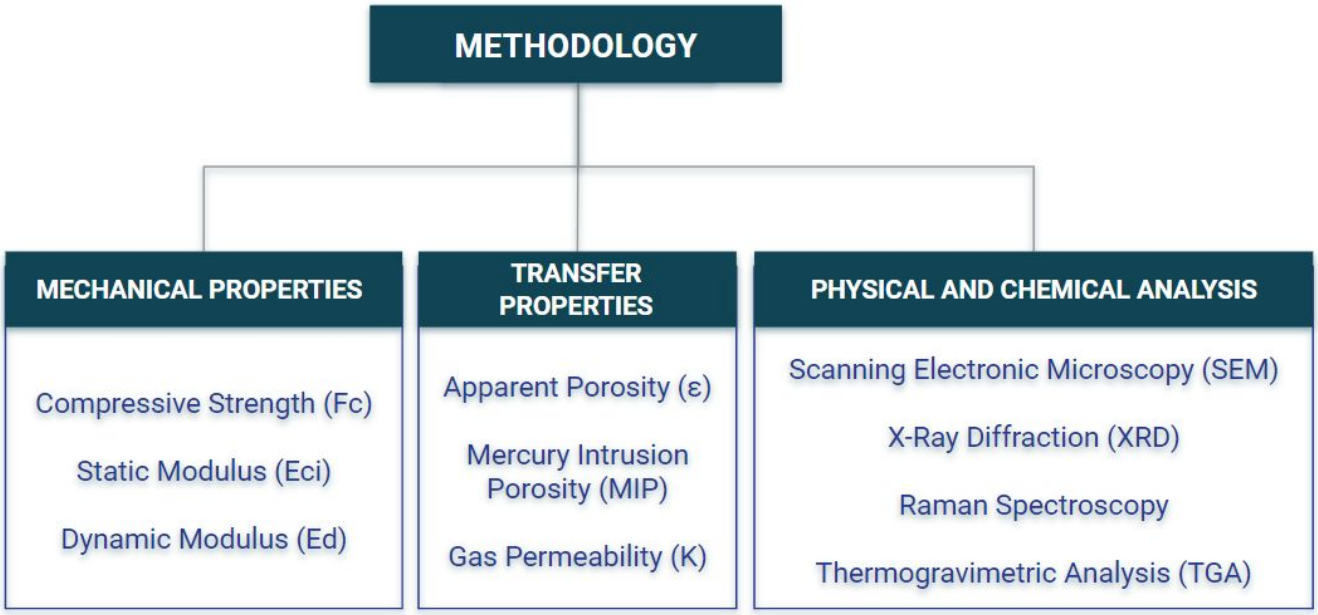

Figure 37. Schema of the content of each group of tests and analyses executed.

Table 1 provides the characteristics of each sample and the arrangement of the tests. The samples used in the Raman, SEM, EDS, XRD, MIP and ATG analyses were from fragments collected simultaneously with the core samples.

Table 1 . Distribution of the tests for each sample.

Samples	Extraction Direction	Tests
A, B, C and D	Parallel to launch	Point A - Permeability and Apparent Porosity (P-01)
SP-01	Parallel to launch	Permeability and Apparent Porosity (P-02)
SP-02	Parallel to launch	-
SP-03	Parallel to launch	Static and Dynamic Modulus; Compressive Strength (AM-02)
SP-04	Parallel to launch	-
SP-05	Parallel to launch	Static and Dynamic Modulus, Compressive Strength (AM-1A and AM-1B)
SP-06	Orthogonal to launch	-

The Technical Reports [11, 62] on the damage that occurred in the pile cap foundations affected by the internal expansion reactions in 2016 was consulted to obtain information about these structures. This report deals with the diagnosis of the causes of the pathological manifestations in the pile cap foundations, the design, tests and analyses carried out with their results and the guidelines for the recovery project of these blocks. The block studied in this research S(P1+P8+P32) presented pathological manifestations similar to those of the block investigated in the report [11, 62], as well as analogous dimensions and load.

After choosing the parameters for characterization and diagnosis of pathological manifestations in concrete, the samples were separated, identified and prepared. In the field, it is necessary that the cores are removed from the structure to be studied. Some tests required specific treatments on the samples collected. In some cases, the sample needs to be reduced to very small sizes or even pulverized.

A visual analysis was performed to identify possible characteristics of the internal expansion reactions and they were directed to the tests to be performed. Then, a characterization of the concrete samples affected by the reaction was performed with destructive tests and analyses. Each analysis or test required a type of preparation, which will be described in each section.

3.1 Mechanical Properties

These properties of strength and deformation were chosen because they are usually employed in the design of concrete structures and are used to evaluate the quality of the material used.

Of the six samples extracted, two were chosen for the compression test (SP-03 and SP-05). As SP-05 was large enough to divide into two samples, this was done. The classification given was SP-05 (AM-1A and AM-1B) and SP-03 (AM-02).

The first test to be performed was the dynamic module test and then the concrete compressive strength test. The static module was found through the stress-strain curve obtained at the time of the strength test.

3.1.1 Compressive Strength

The three samples (Figure 38) were identified and rectified to perform the test. Their dimensions were measured so that the parameters were placed in the press software. The press used was the RP 3000 DC/LC, with force up to 2500 KN (Figure 39).

Figure 38. Samples selected for the compressive test.

Figure 39. Equipment for the test of compressive strength.

3.1.2 Static Modulus of Elasticity

The modulus of elasticity of the concrete is given by the slope of the stress-strain curve submitted to a uniaxial loading.

From the strain graph obtained from the compressive test, a tangent line to the curve (σ-ε) at the origin was drawn to find the initial static tangent module of each concrete sample tested.

The formulations used to estimate the modulus values at the ages of interest were from NBR 6118:2014 [74].

3.1.3 Dynamic Modulus of Elasticity

The Grindosonic apparatus - J. W. LEMMENS (Mk5 "Industrial") - was used to measure the dynamic modulus of elasticity. In the test, the vibration probe was placed at one end of the specimen and the other received a pulse with the impactor, then the frequency was automatically generated in the apparatus, and subsequently the module was calculated, based on the standard [10].

The method covers a dynamic determination of the elastic properties of materials. The procedure comprises of firstly exciting a test object by means of a light external mechanical impulse, and secondly of the analysis of the transient natural vibration during the subsequent free relaxation. The test procedure is illustrated in Figure 40 and the equation used to obtain the dynamic modulus was the following:

$$Ed = \frac{0.001606700000\, L^3 m \left(1 + \frac{5.173483964\, D^2}{L^2} - \frac{0.4883\, D^4}{L^4} - \frac{5.28853958\, D^4}{L^4\left(1 + \frac{5.16094240\, D^2}{L^2}\right)}\right) F^2}{D^4}$$

Where m is the mass of the specimen, L the length, D the diameter and F the pulse frequency. According to ASTM C215-14, with nu=0.2 the module was obtained.

Figure 40. Grindosonic apparatus for measuring the dynamic modulus of elasticity.

3.2 Transfer Properties

3.2.1 Gas Permeability (K)

The permeability test was performed on two concrete specimens of the pile cap block. A sample (P-02) was taken from the fragments extracted from the SP-01 sample and the sample (P-01) was separated from the point A. They were rectified and left in the dimensions 5 cm x 7 cm. The specified cell size of the permeability equipment ("debitmètre massique") was 10 cm in diameter, so the samples were wrapped in black silicone resin and placed in a rigid cylindrical mold.

This resin also had the function of waterproofing the lateral surface of the samples. Figure 41 illustrates how the concrete samples were ready for the test. The concrete gas permeability measurement test is easy and quick to perform and its results are important for assessing the durability of the material. These aspects should be considered so that its use can be more widespread in the practice of concrete structure execution.

Figure 41. Samples P-01 and P-02 prepared for the gas permeability test.

To obtain the dry mass of the samples, it was chosen to dry them at a temperature of 60°C in the oven until the mass was stabilized. The dry mass of the samples is obtained when the loss of relative mass of 24 hours does not exceed 0,05%. Every day for twelve days the weight of the samples was measured until the stabilization.

The scheme of the permeability equipment was shown by [66] and demonstrates how the sample is confined in the permeability cell (Figure 42).

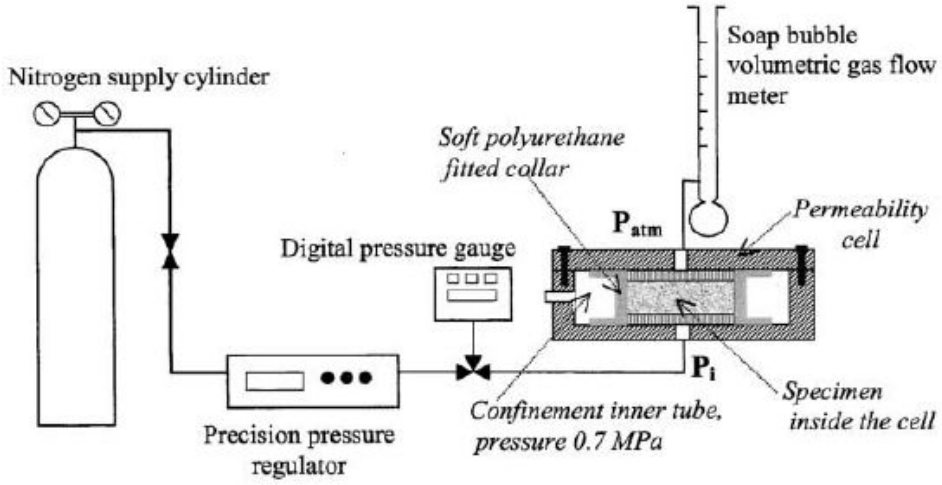

Figure 42. Layout of permeability equipment [66].

The complete apparatus of the permeability equipment ("debitmètre massique") used in the test is shown in Figure 43. Details of the equipment can be found in Appendice.

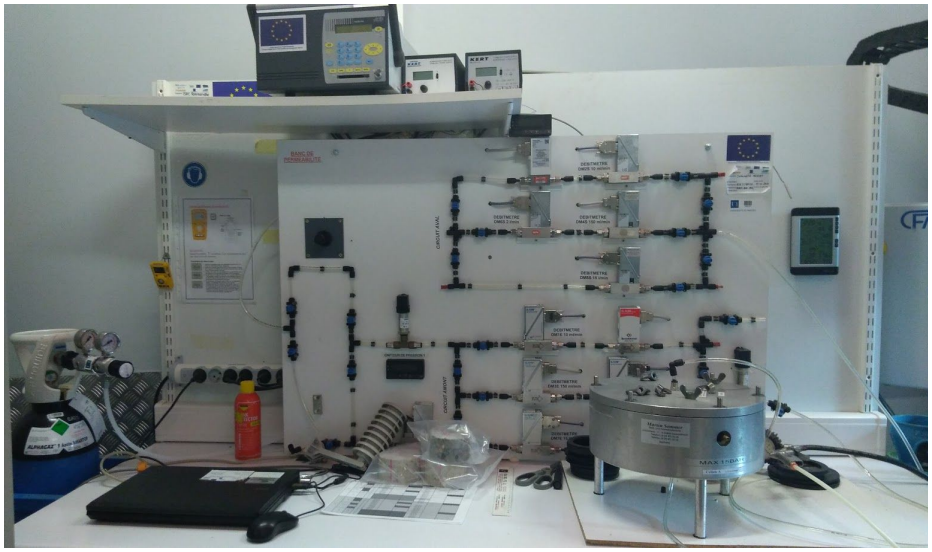

Figure 43. Flowmeter massique equipment.

The intrinsic permeability is measured through a permeameter, with nitrogen being the neutral percolating gas. A manometer reads the relative pressure (Pi-Patm) applied to the sample. Laboratory temperature and humidity are controlled (T = 17,8 ºC and RH = 76%).

3.2.2 Apparent Porosity (ε)

After the concrete gas permeability tests have been performed, all the waterproofing resin and the apparatus used were removed to put the samples back in the oven until the mass stabilization.

To obtain the dry mass of the samples, it was chosen to dry them at a temperature of 60°C in the oven until the mass was stabilized. The dry mass of the samples is obtained when the loss of relative mass of 24 hours does not exceed 0,05%. Every day for one month the weight of the samples was measured until the stabilization.

After the stabilization of the mass has occurred by drying in the oven, the samples were wrapped in a white absorbent tissue covered with a transparent plastic, from which it was possible to remove the air present in the sample and the environment with a vacuum pump. The vacuum pump was then stopped for five minutes to check if air was coming out, as the device was well sealed, suction continued for another 48 hours. After this period of time the air suction process was interrupted to introduce water into the apparatus and consequently into the samples.

Figure 44. System used for the apparent porosity test.

Figure 44 shows the devices used for porosity tests, where you can see that at one end you have the place where the vacuum pump for air suction is installed and at the other end the water inlet is located. 48 hours later, the water end was opened and it was placed the hose in a tank with water, reconnected the vacuum pump that began sucking the water until the whole system was filled.

After 72 hours the sample was taken and its weight was measured. The saturated samples are shown in Figure 45. More details about the tests and the samples treatment can be found in Apendice.

Figure 45. Saturated concrete samples.

3.2.3 Mercury Intrusion Porosimetry (MIP)

In the MIP test, several pressure levels are applied to a sample immersed in mercury. The pressure sufficient to introduce mercury into the pores of the concrete sample is inversely proportional to the size of the pores. Three cubes of 1cmx1cmx1cm were separated to perform the test. To obtain the dry mass of the samples, was chosen to dry them at a temperature of 60°C until the mass was stabilized. The dry mass of the samples is obtained when the loss of relative mass of 24 hours does not exceed 0,05%. The duration was one month in the oven.

3.3 Physical-Chemical Analysis

3.3.1 Scanning Electron Microscopy (SEM)

The SEM used for observations is a ZEISS ЄVO®40 equipped with a Back-scattered Electron (BSE) detector to determine the chemical composition. The microscopic examinations were carried out on fresh fractures sections on concrete specimens. The specimens were coated with a gold deposit for observations using the SEM in High-Vacuum (HV) mode.

The samples were analyzed by scanning electron microscopy and the spectrum obtained with EDX showed the chemical composition existing in each part analyzed. Some images showed only the morphology of the ettringite or other observed component.

3.3.2 X-Ray Diffraction (XRD)

Through the X-ray diffraction it is possible to obtain the detailed information of the atomic and molecular structure of materials.

When a material is exposed to X-rays, a specific peak pattern of the mineral is generated. The ordinate provides the diffraction angle, which corresponds to the spacing of the crystalline arrangement. In the abscissa we see the intensity of the diffracted ray, which is proportional to its quantity in a composite sample and each peak is equivalent to a type of mineral.

XRD patterns were obtained by using an X-ray diffractometer SEIFERT MZ VI E with Co Ka radiation. Measures were done on the bulk powdered samples.

3.3.3 Raman Spectroscopy

The Raman displacement band, that is, the difference in energy between the incident and the scattered, is typically described as a wave number (wavenumber). The most used unit is 1/cm, this is equivalent to joule divided by conversion factor (hc), where h is Planck constant and c is the speed of light.

The sample selection criteria for analysis by Raman spectroscopy were: fragments of the extracted concrete samples with apparent gel edges, pores filled with ettringite and white spots inside the aggregates.

An acrylic resin PRESI Powder KM-U with a liquid catalyst PRESI KM-U suitable for this type of cold resin was used in the concrete samples. The function of resin was to allow the sample to remain flat, allowing the analysis in Raman. After placing the resin in the mold with the sample, it waited 10 minutes until it warmed up and hardened, and then the sample was polished on #320 silicon carbide paper and then on #120 paper in a specific machine until the surface was polished and flat. In Figure 46 you have the five samples prepared for analysis in the Raman spectroscope. The samples were identified by the following notations: RA-01, RA-02, RA-03, RA-04 and RA-05.

The Raman spectra were produced using the Confocal Raman Microscope SENTERRA II (Bruker) with Opus Software, 532m wavelength laser, 20mW power, 50x magnification, 20s integration time with two accumulations.

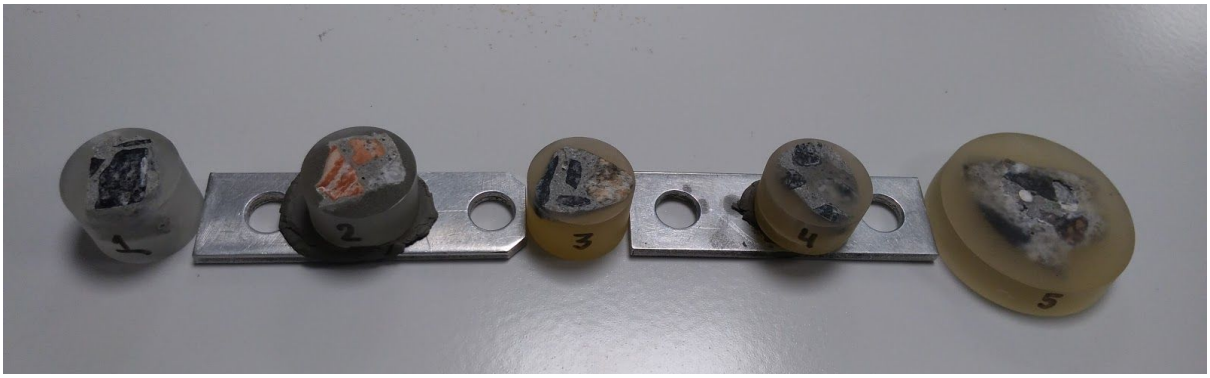

Figure 46. Samples analyzed by Raman Spectroscopy.

3.3.4 Thermogravimetric Analysis (TGA)

TGA is a destructive experiment where samples must be removed from the structure and powdered. In thermogravimetric analysis it is important to have control over the atmospheric system, because the gases present in the medium can interact with the sample, interfering directly in the mass variations. To obtain a better resolution of the transitions, the temperature sweep rate can be modified by digitizing more slowly, and instead of 20°C, place 10°C per minute. The temperature for the thermogravimetric analysis adopted was 1000°C.

CHAPTER 04

4. RESULTS AND DISCUSSION

In this chapter the results of the analyses and tests are presented and discussed. The results of the experimental part of the dynamic modulus of elasticity, initial static modulus, compressive strength, apparent porosity and gas permeability of concrete are evaluated. In the analyses performed, scanning electron microscopy, x-ray diffraction and Raman spectroscopy will be addressed.

Correlations will also be made between the properties described above and the scenario found in the field in the pile cap foundation.

Before starting the discussion about the results of the lab tests performed it is important to highlight that the pathological manifestations observed in the pile cap block studied probably come from a variety of sources: structure design decisions, definition of materials to be used in the production of the concrete used and care in large volume concrete operations.

The objective of the research performed is not to define individual or collective responsibilities for the problems observed, but to highlight how the various factors have created conditions for pathological manifestations to occur so that practices can be adopted to minimize the possibility of even problems in the future.

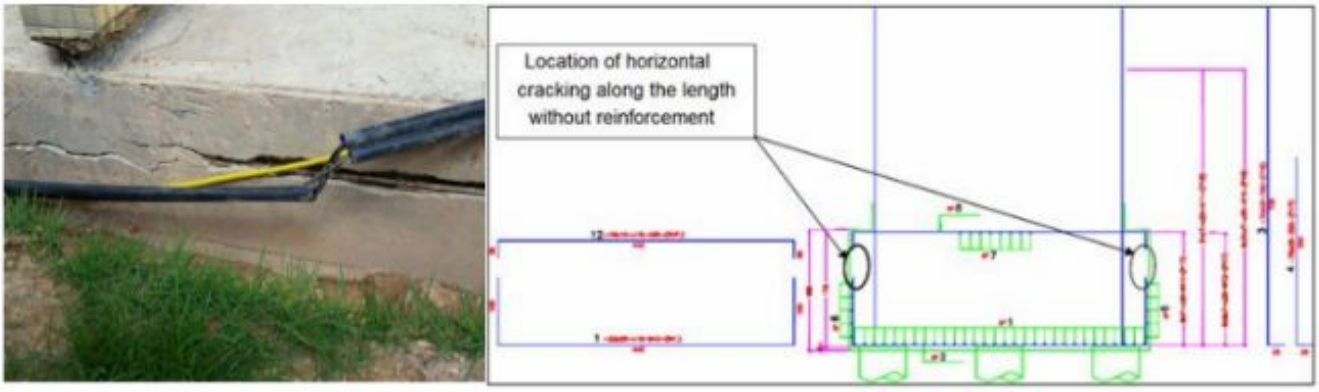

Figure 47. Detail of the reinforcement of this pile cap block [11].

Figure 47 shows the detail of the reinforcement of this block where the absence of connection between the top and the bottom steel bars is highlighted.

The pile cap block studied presents a detailing of the reinforcement that is very similar to other pile cap foundations of several constructions in the region (Figure 26) that presented the occurrence of a cracking process very close to that observed in the block under analysis (Andrade et al., 2006; Andrade, 2006; Figueirôa and Andrade, 2007; Silva, 2007; Gomes, 2008).

In the specific case of pile blocks the loss of tensile strength of concrete is especially damaging. In fact, as the struts fails though transverse cracking, and not by crushing, damage from chemical attack generates micro cracking in struts subject to high stresses. Micro cracking, thus, make easier the entry of moisture and the consequent transverse expansion. Therefore, even when compressed unidirectionally, the concrete can suffer considerable damage from chemical.

4.1 Results of the Tests Hired by the Building Owners

In the report previously performed in the pile cap blocks [11, 62] some tests and analyses were made to diagnose what problem there was in the pile cap foundation. Among them, a petrographic analysis was performed by ABCP (Brazilian Portland Cement Association), using stereoscopic and optical microscopy techniques for macroscopic analysis, macroscopically identifying the suspicious phases of concrete and characterizing petrographically the fine and large aggregates. Scanning electron microscopy of unpolished samples was also performed to detect the suspicious phases, using EDS to discover the elements present in these phases. The objective was to identify phases that would cause swelling reactions and lead the concrete to have the existing crack pattern.

According to the macroscopic analysis performed in [11, 62] the concrete presented normal aspects, from the point of view of densification, proportion between the constituents and adherence between paste/aggregate. It was also possible to observe the existence of frequent gel edges resulting from the alkali-aggregate reaction and pores partially or totally filled with ettringite. The aggregate analyzed was classified as potentially reactive against concrete alkalis, having as mineral deleterious the microgranular quartz, around 5 to 10% and recrystallized quartz (reactive minerals), confirmed through the report [11, 62]. It was classified as a milonite gneiss, a rock of metamorphic origin, gray in color, composed of biotite, amphibole, titanite, epidote and opaques. The types of coarse and fine aggregates used were crushed stone and natural sand, respectively.

From the physical-mechanical point of view, the aggregates used in the concrete were considered of good quality, with high tenacity and incipient alteration of its constituents. From the mineralogical point of view, a deformation was observed in the coarse aggregates that favors the

disenchantment of the alkali-silicate reaction coming from microgranular quartz and recrystallized quartz.

In the cement used there was availability of alkalis that together with the large aggregate and the humidity potentialized the necessary conditions for the alkali-aggregate reaction. The gel edges were frequently found around the coarse aggregates, and there was white material deposited on the mortar, as well as detachment of the coarse aggregate. The gel from the alkali-aggregate reaction was found mainly in pores and voids in the mortar, as well as in preferential disposal sites (such as interfacial transition zones).

In the images obtained with 10x magnification under stereoscopic microscope, the contact of the mortar (M) with the coarse aggregate (G), reaction edges and pores filled by the ettringite (Et) was observed (Figure 38).

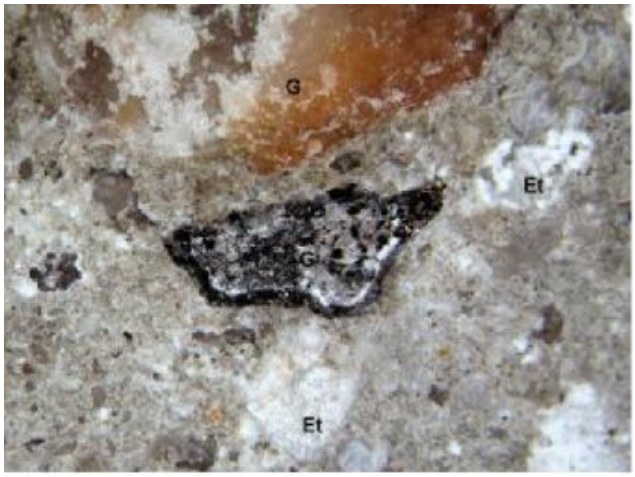

Figure 48. Characteristics observed visually in the sample of damaged concrete [11, 62].

According to information collected, pathological manifestations were observed in various pile cap blocks of the building and the results of a technical report hired by the owners presented the following results:

- Well-defined reaction edges;
- Presence of reaction gel filling pores and voids in the mortar;
- The reaction products were characterized as foliar or lancing crystals arranged at the interface aggregate paste and the alkali-silicate gel filling pores and voids;
- The concrete contained high porosity and a large amount of the pores and voids were filled with tufts of white acicular crystals of fibroradiating (etringita) habit;

- In the analysis performed with SEM and EDS, large quantities of alkali-aggregate reaction products were found, and even if pores filled with ettringite were found, it was not clearly evident that this mechanism caused swelling reactions in concrete.

Around 10 years of the construction of the building, the concrete of a similar pile cap foundation of the same building was analyzed, showing predominance of ettringite crystals.

During the execution of the foundation, some precautions such as temperature control and study of the cement to be used (with low hydration heat and admissible levels of aluminate and sulfate) are essential to avoid the appearance of pathological manifestations such as the delayed ettringite formation. What may have occurred in the studied block, which combined with the entrance of moisture by longitudinal cracking, triggered the process of formation of this reaction.

4.2 Results of the Tests Performed in The Research

4.2.1 Visual Inspection

Visual inspections were performed on the pile cap block itself as well as on the concrete samples extracted to identify naked eye signs of expansive reactions or chemical attacks to the concrete. From these inspections, it was possible to observe to see features of these expansion reactions already in place by observing the cracking in map forms on the external surface of the pile cap block. It is worth mentioning that at the time of the extraction a report had already been made to detect the causes of degradation, as well as several tests and analyses, and the pile cap block was in the process of recovery (Figure 49).

Figure 49. Map cracking on the surface of the pile cap block.

The samples were first visually examined in order to find clues of chemical attacks to concrete such as AAR and DEF. Macroscopically, gel edges from the alkali-silica reaction were observed in the aggregates. Cracks on the coarse aggregates, following to the cement paste, were observed as well as cracks on transition zone reaching the larger pores.

At some locations it was possible to observe detachment between the aggregate and the paste. Some aggregates contained a kind of whitish reaction product inside, very close to its extremities and and many dark edges or spots were found around the coarse aggregate.

Several micropores were fulled with ettringite and many pores were completely filled with white material. In some fragments a large amount of white material was found covering the concrete, like as leaching. It was also observed in some larger pores little deposition of white material, a fact also observed by Hasparyk in [48] in the visual inspection of concrete cores with alkali aggregate reaction.

In the preparation of some samples for some tests performed it was done polishing and after this process it was possible to find even smaller pores filled with whitish material as well as particles of aggregates with this same characteristic. The results from the visual inspection performed on the extracted specimens are summarized below:

- Alkali-silica gel edges in the aggregates;
- Pores with white material deposited at the bottom;
- White mass in several places in the concrete;
- Pores completely filled with ettringite;
- Cracking in coarse aggregates;
- Dark spots around the aggregate;
- White spots inside the aggregate;
- Leaching;
- White spot covering the concrete, mainly the mortar;
- Displacement between the aggregate and the paste;
- Cracking in the coarse aggregate following to the transition zone, with the presence of gel in these locations;

Figure 50 (a, b and c) and Figure 51 (a, b and c) show the main results of the visual inspection performed.

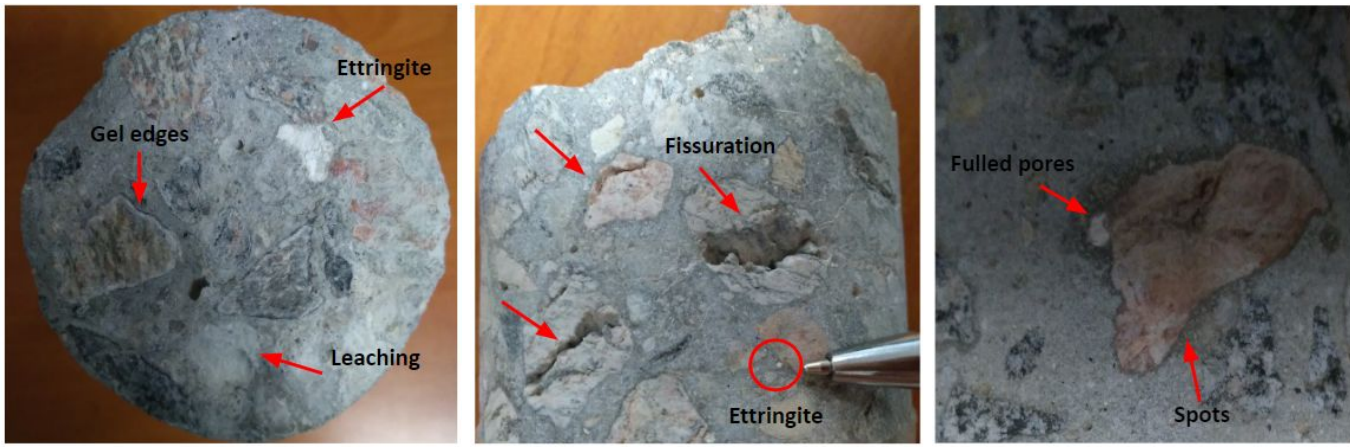

Figure 50. Symptoms of the expansion mechanisms found: a) Gel edges; b) Ettringite in the micropores and cracking; c) Spots in the aggregate.

Figure 51. Symptoms of the expansion mechanisms found: a) Pores fulled with ettringite; b) Spots in the aggregate; c) White material in the pores and Leaching.

The results of visual inspections performed on the concrete samples collected from the block are consistent with a scenario of occurence internal expansion reactions inside the element more compatible with DEF than with the ASR.

4.3 Mechanical Properties

4.3.1 Compressive Strength

Table 2 below presents the results of the compressive strength of the extracted samples. The results show that, despite the existence of cracks in the samples, the compressive strength values were high, even higher than the characteristic strength specified in the design - 35 MPa.

It was not necessary to apply a correction factor in the values of compressive strength because the relation between height and diameter of the samples has values very close to 2.

Table 2. Values of compressive strength of concrete.

Samples	Compressive Strength (MPa)	Mean Value (MPa)
AM - 1A	47,90	45,89
AM - 1B	46,76	
AM - 02	43,00	

Even with the existence of cracks in ITZ the compressive strength values are little affected, when we treat the AM-02 sample, being disregarded. Sanchez et al. explained in [41, 77, 78, 85, 86] that this occurs due to the crack being extremely localized and because there is a kind of stopping mechanism generated by the aggregates.

According to Table 3, the strength increase was 26% (in approximately 19 years after construction), with an order of magnitude similar to the value of the medium strength at infinity.

The strength values in Table 3 were calculated according to the recommendations of Brazilian Standard 6118:2014 [74] and describe the real and estimated values of this property in different ages.

Table 3. Values of medium compressive strength of concrete in different ages (real and estimated).

Age (years)	Fcm (MPa)	
	Estimated	Real
0,076 (28 days)	41,91	Not available
19	44,13	45,89
∞	44,94	

The values found are consistent with Standard 6118:2014 [74], because the estimated values are relatively lower than the real ones (if the execution processes are performed adequately), due to the weighting coefficient.

The results obtained in the study are consistent with other studies [41, 73, 77, 78] that reported that concrete deterioration mechanisms such as ASR and DEF do not significantly affect the compressive strength of concrete.

4.3.2 Static Modulus of Elasticity

The modulus of elasticity of the concrete is given by the slope of the stress-strain curve submitted to a uniaxial loading. The modulus of elasticity is an important property of concrete because its knowledge allows to understand the mechanisms of deformation that the material will present when subjected to loads.

From the strain graph a tangent line to the curve (σ-ε) at the origin was drawn to find the initial static tangent module of each concrete sample tested to compressive stress. Three values of the static module were obtained in GPa for samples AM-1A, AM-1B and AM-02.

The curve obtained from the concrete strength test is illustrated in Figure 52.

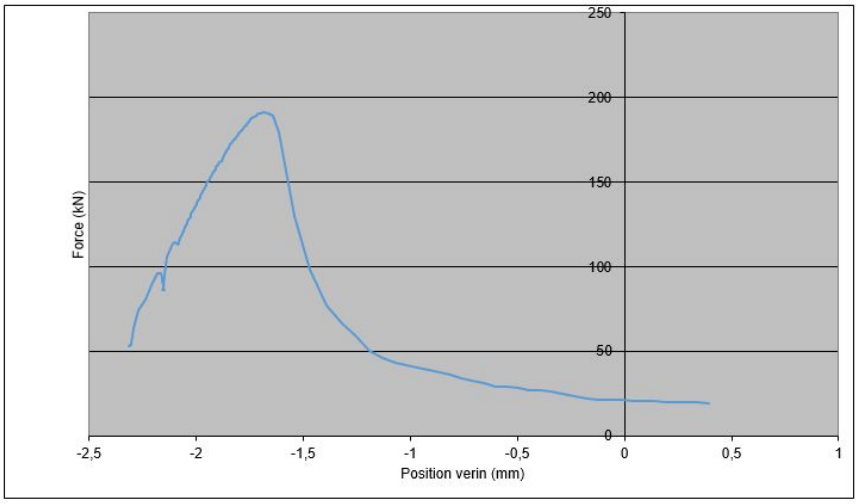

Figure 52. Curve Force (kN) x Position (mm).

Figure 53 shows the calculated trend line, showing one of the values found for the modulus.

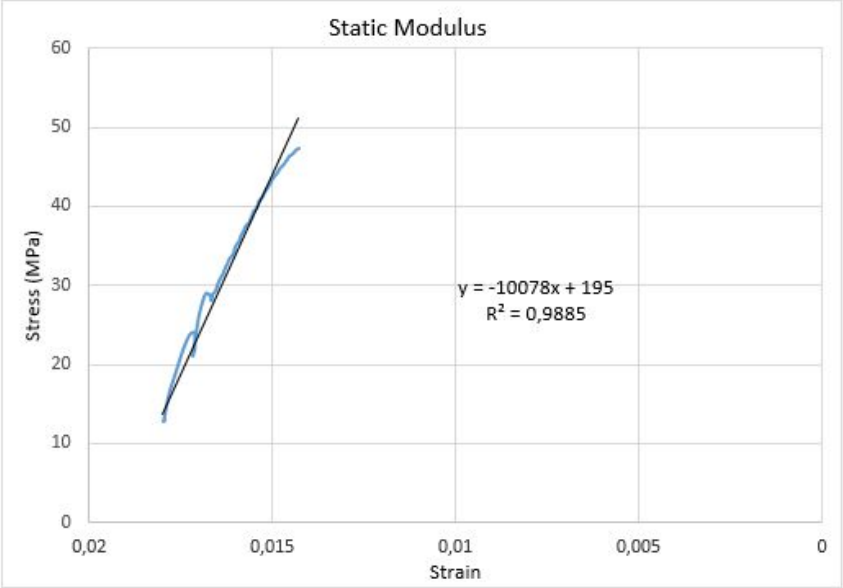

Figure 53. Slope of the stress-strain curve.

The values found in the modulus of elasticity test were organized in Table 4, and their mean value was presented. The modulus of elasticity values showed a large reduction when compared to the common concrete tested at 28 days. By extrapolation, according to Standard 6118:2014 [74], it was possible to arrive at the estimated modulus values at 28 days and in 19 years. The estimate of the static modulus at 19 years does not reflect reality. But based on a concrete Fck=35 MPa, we find 37.20 GPa for the 19 years.Table 5 presents these results.

Table 4. Values of static modulus of elasticity of concrete.

Samples	Static Modulus (GPa)	Mean Value (GPa)
AM - 1A	19,31	16,72
AM - 1B	12,44	
AM - 02	18,40	

Table 5. Values of static modulus of concrete (real and estimated).

Age (years)	Eci (GPa)	
	Estimated	Real
0,076 (28 days)	33,13	Not available
19	37,20	16,72

According to Sanchez et al. in [41, 77, 78], when the expansion increases to levels considered high (that is, up to 0.30%) new cracks appear in the system in small amounts within the reactive aggregates, and those that already exist increase in size. This causes the material to drop in stiffness, leading the modulus of elasticity to decrease to values of 60%.

Due to the action of DEF + ASR the reduction in stiffness of the concrete material studied was very high, corresponding to a loss of approximately 55% (Table 5). The value of the modulus found was 16,72 GPa, equivalent to 44,94% of the value expected after 19 years of building construction.

This value is consistent with the results found by Sanchez et al. in [41] for structures affected with DEF. When the degree of expansion is between 0,30% and 0,40%, the loss in stiffness can vary from 50 to 65%. At higher levels (expansion ≥ 0,50%) the decrease in this property can reach 85%.

This is compatible with the high degree of cracking found in the pile cap block, provided by the development of the ettringite crystals, expanding and later cracking the concrete in a very aggressive way.

4.3.3 Dynamic Modulus of Elasticity

The dynamic modulus of elasticity of concrete is a measure of the strength to elastic deformation of the material, according to [68]. The dynamic modulus is greater around 20, 30 or 40% than the static modulus of elasticity for concretes with high, medium and low strength [39]. This is because the instantaneous strain that occurs during the test is very small, not being able to produce either micro cracks or to develop creep.

Table 6 shows the values of modulus obtained through the test with the Grindosonic equipment. This decrease in the modulus values can explain the existing microcracks, because the dynamic modulus evaluates the existence or not of discontinuity of the concrete material. These damages cause the stiffness of the material to be reduced, a fact also observed by [66].

Table 6. Values of dynamic modulus of elasticity of concrete.

Samples	Dynamic Modulus (GPa)	Mean Value (GPa)
AM - 1A	26,19	20,87
AM - 1B	18,71	
AM - 02	17,70	

The static and dynamic modulus values are consistent with each other, as the dynamic modulus found is 19.88% higher than the static one.

A downward trend in dynamic modulus values was observed and reduction about 28% in the sample AM-1B, which has steel bars inside, when compared with sample AM-1A. A possibility of explanation for this behavior is that the transition zone between steel bar and concrete is fragile, causing the ultrasonic pulse to take longer to be transmitted. This way the modulus value is reduced, as shown in Figure 54.

Figure 54. Part of a steel bar in the concrete specimen (AM-1B) during the dynamic modulus test.

The value of the dynamic module is also influenced by the porosity of the material. As the concrete showed high apparent porosity (between 9,76 and 11,29%), this factor contributed significantly to the decrease of the module. This can be explained by the strong network of cracks in the cement paste that is generated through the DEF mechanism. In addition to ITZ cracks connecting to each other, increasing the density of cracks in the samples.

Mehta and Monteiro in [39] state that Ed is generally 30% larger than Eci in medium compressive strength concrete. The value corresponding to that statement, for this work, would be 48,36 GPa, but the module found in the test was 20,87 GPa. This value corresponds to a reduction of 56,84%, approximately. The large cracking network existing in concrete allowed the drop in the values obtained.

4.4.1 Transfer Properties

The transfer properties of both healthy and cracked concrete are very important for the study of its durability. One of the factors for the internal swelling reactions to occur is the moisture of the environment that can come into contact with certain concrete structures [83, 84]. However, for this interaction to be bad, the flow of liquid or gaseous agents through the porous or cracked medium must be evaluated. Some of the methods that can be used to characterize the pore structure are gas permeability, apparent porosimetry and mercury intrusion porosimetry. Porosity and permeability are indicators of concrete durability, because they depend on them for moisture input and other harmful agents inside the structure, such as salts, fluids and other deleterious agents.

4.4.1.1 Gas Permeability (K)

Figure 55 shows the graphs corresponding to the permeability test for samples P-01 and P-02. The intersection of the straight line with the Y axis corresponds to the intrinsic permeability coefficient of concrete.

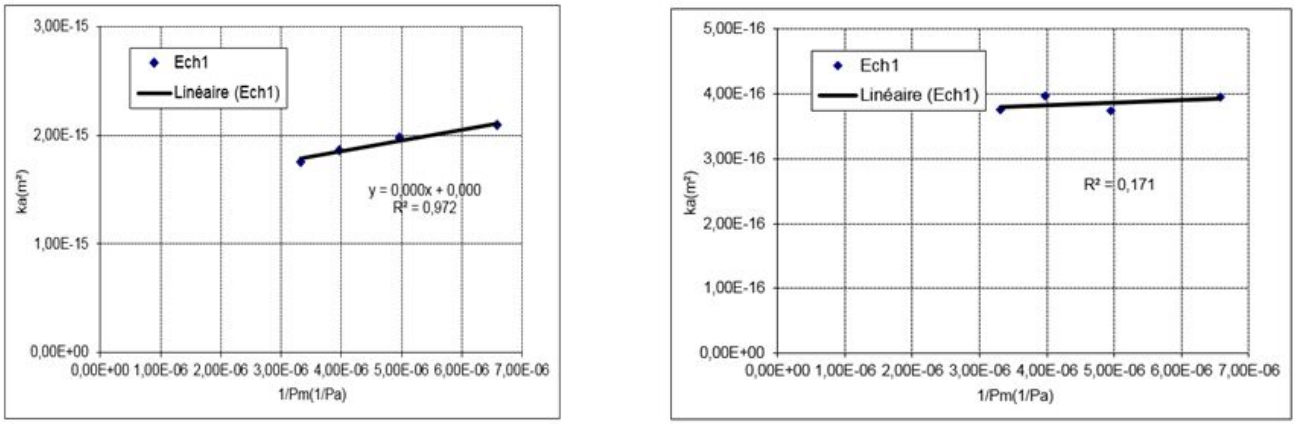

Figure 55. Permeability coefficients versus pressure for a) P-01 and b) P-02.

Table 7 summarizes the air permeability values for the two samples tested. The results found mean that the concrete samples have a high permeability. In fact, the usual values of this parameter for a concrete are in the range of 10^{-18}, 10^{-17} [6, 45].

Table 7. Values of gas permeability of concrete.

Sample	K (m²)
P-01	1,30E-15
P-02	3,90E-16

This high value of the permeability coefficient can explain the intense cracking process existing in the pile cap block investigated, which allowed the entry of moisture and development of the expansion mechanisms that deteriorated the concrete.

The permeability of the samples tested was proportional to the porosity, being higher for P-01. In this sample there was a greater predominance of microcracks. In P-02 there was a large pore, which makes these transport properties smaller.

According to [44, 81, 84] the microcracks resulting from the silica alkali reaction increase the permeability of concrete, a mechanism that may have contributed to the growth of the values of this property.

4.4.1.2 Apparent Porosity (ε)

Table 8 presents results of apparent porosity tests form samples P-01 and P-02.

Table 8. Values of apparent porosity of concrete.

Sample	ε (%)
P-01	11,29%
P-02	9,76%

The results obtained indicate a high porosity of concrete, a situation also confirmed by its high permeability. This explains the large amount of microcracking found in the field and consequently in the extracted samples. The pore structure of this concrete is then markedly compromised, an aspect that directly interferes with its durability and service life.

One aspect that deserves to be highlighted is that ettringite usually can cause greater expansions in small pores with low connectivity than in larger pores with wide connections [30]. This fact was observed in sample P-02 that presented a large amount of pore in its structure with porosity relatively lower than the P-01 sample, that presented a larger amount of microcracks.

It can also be confirmed that ettringite deposited in free pores does not contribute to expansion [28], because in sample P-02 it was found more pores filled with ettringite.

4.5.1 Physical-Chemical Analysis

4.5.1.1 Scanning Electron Microscopy (SEM)

The analysis performed through the scanning electron microstructure allowed the morphology of the samples to be evidenced by means of images. Energy Dispersive X-Ray Spectroscopy (EDX) enables microanalysis, providing chemical composition of the material, which can be used together scanning electron microscopy to get qualified information.

In the analyses performed with SEM, some specific parts that indicated the presence of delayed ettringite formation were chosen. The first point was 309, where the morphology indicated that it was an ettringite acycle. Figure 56 shows this part of the sample, with a magnitude of 1795x.

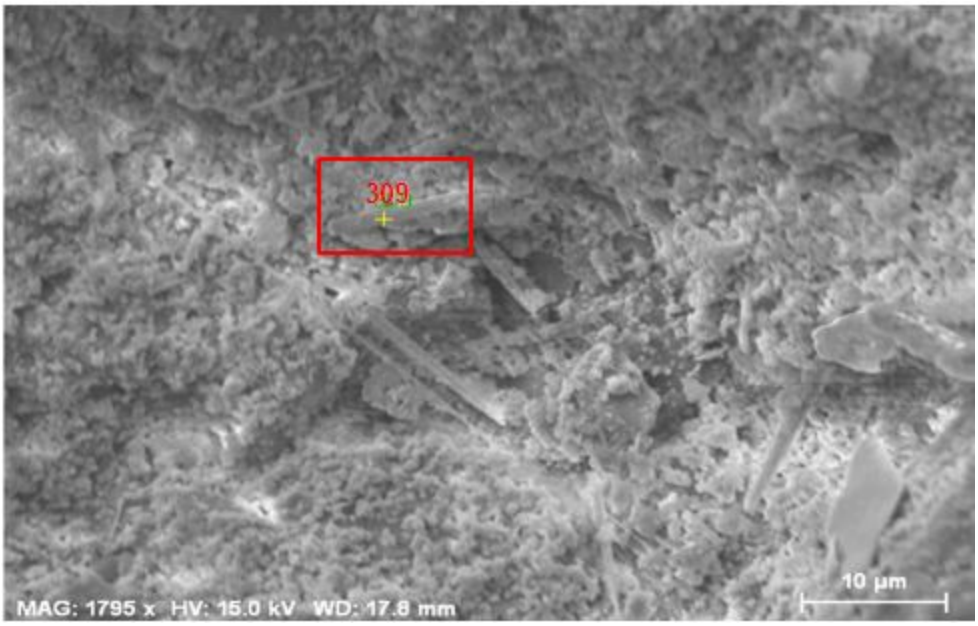

Figure 56. Acycular crystals of ettringite found in the mortar.

The chemical composition obtained by EDX is shown Figure 57, where the components such as Sulfur (S), Aluminum (Al) and Calcium (Ca) suggests the presence of delayed ettringite [3, 48].

Figure 58 illustrates ettringite crystals completely filling an existing pore in the concrete. The first magnitude is 23x, being increased to 340x.

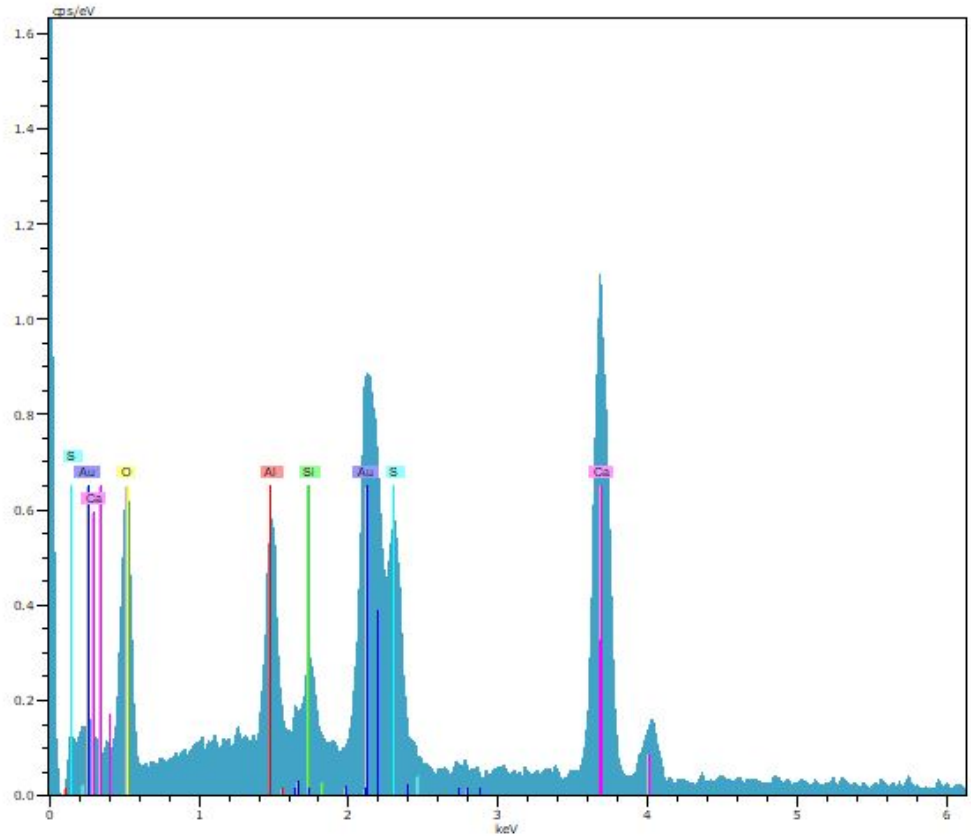

Figure 57. Components such as: Sulphur (S), Aluminum (Al) and Calcium (Ca) in the sample.

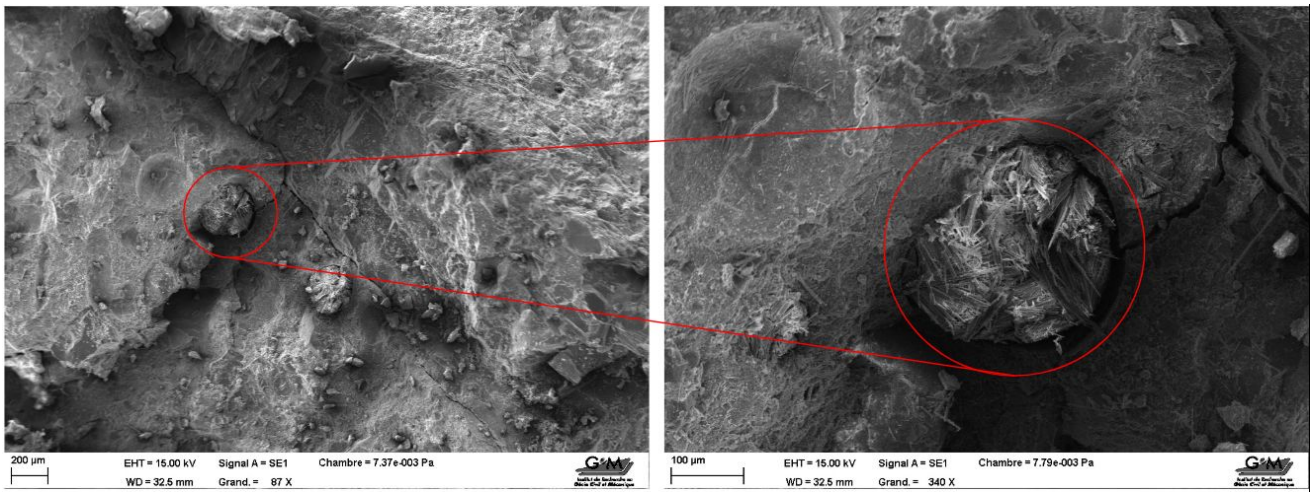

Figure 58. Ettringite crystals completely filling a pore (23x - 340x).

At point 308 (Figure 59) analyzed by SEM, it is possible to observe ettringite crystals developed and deposited in a pore and the corresponding chemical composition is presented in

Figure 60, with the presence of Sulfur (S), Aluminum (Al) and Calcium (Ca), aspect that confirms that it is delayed ettringite [48].

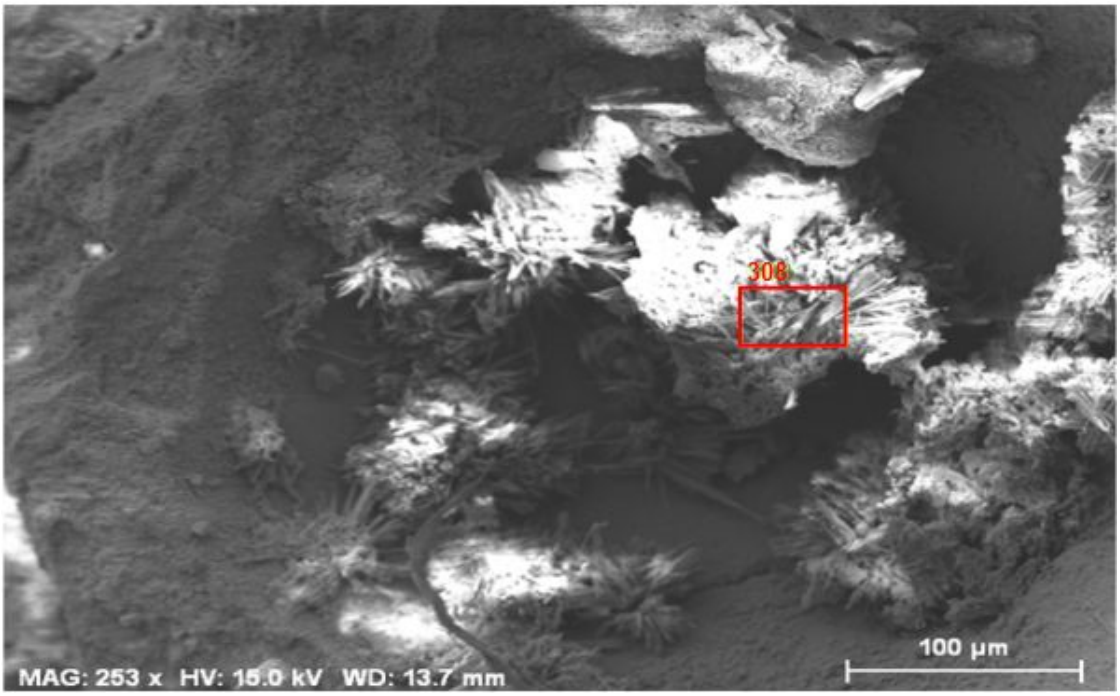

Figure 59. Ettringite crystals deposited in a pore.

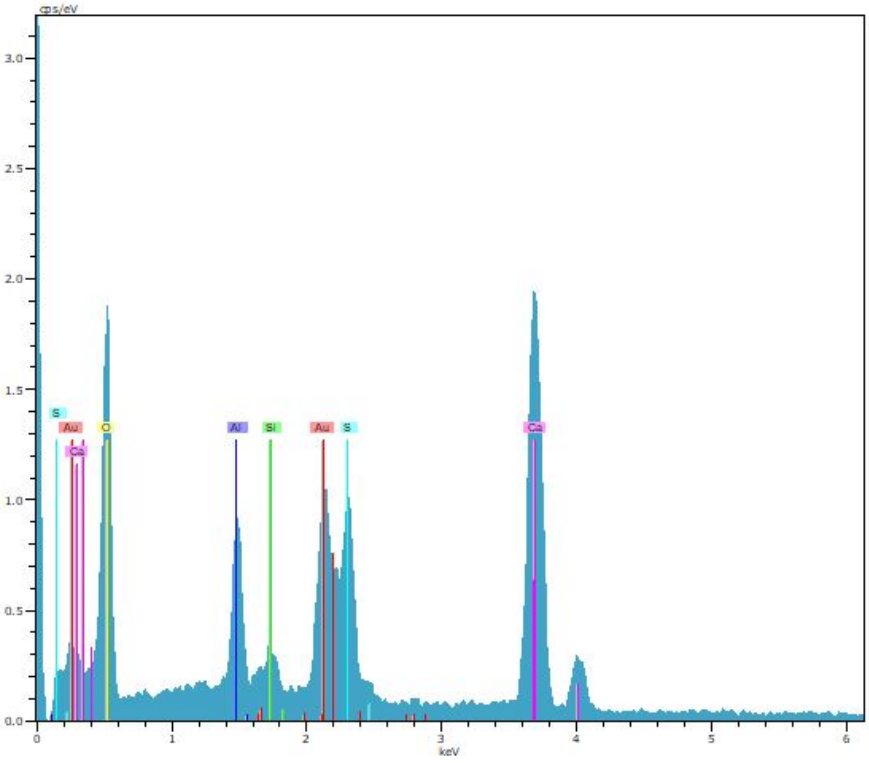

Figure 60. Chemical composition of the crystals.

This particle (point 304 - Figure 61) analyzed showed in its chemical composition Aluminum (Al), silicon (Si) and sodium (Na), indicating that there are components of delayed ettringite formation and crystalline products of alkaline reaction [48] acting together. Figure 62 illustrates the composition (Al, Si and Na) of this point analyzed.

Figure 61. Aggregate particle with crystalline products of the alkali-silica reaction.

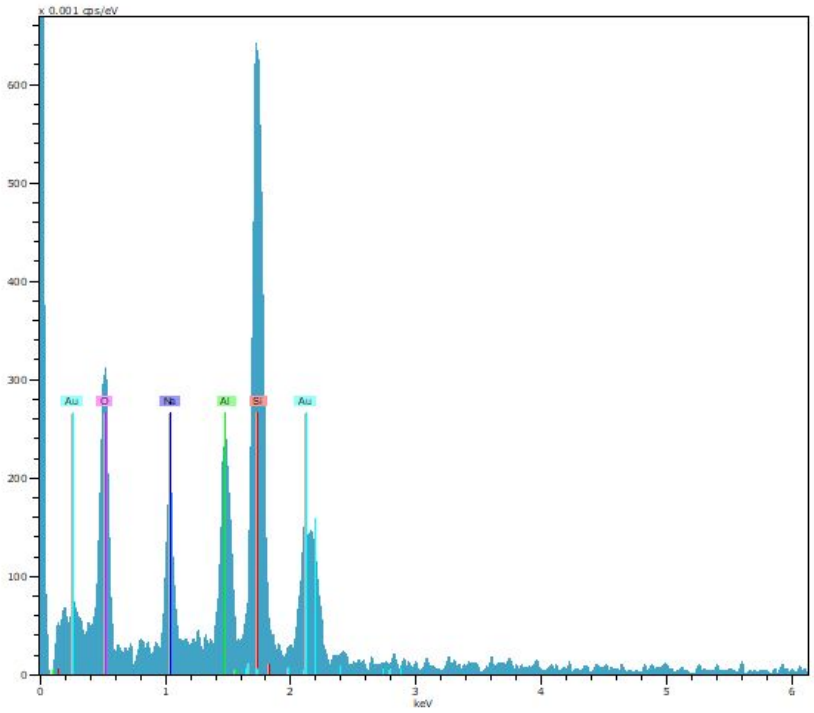

Figure 62. Crystalline product of alkaline silica reaction.

More images of the concrete microstructure, micro-cracks and pores filled with ettringite obtained through SEM analysis can be found in Appendice.

4.5.1.2 X-Ray Diffraction (XRD)

Through the X-ray diffraction it is possible to obtain the detailed information of the atomic and molecular structure of materials (mainly the crystalline ones).

In the analyses with EDX it was possible to observe a large amount of sulfur (S), aluminum (Al) and calcium (Ca), chemical elements predominantly found in crystals of ettringite [3]. The XRD analyses also proved the presence of ettringite and pyrite (sulphate) internally. These internal compounds associated with a high heat of hydration may have caused the formation of delayed ettringite. Figure 63 shows the patterns of concrete damaged by internal expansion reactions.

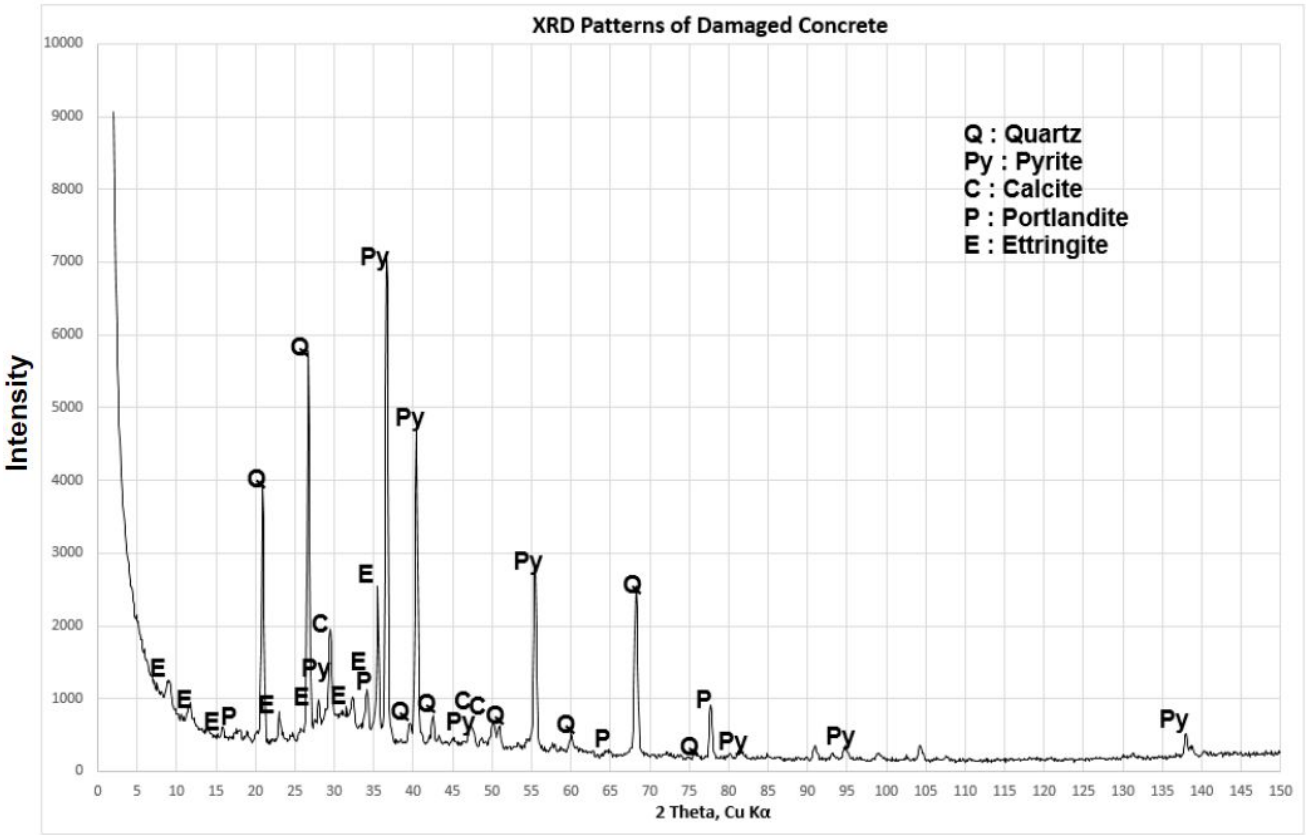

Figure 63. Presence of pyrite (sulphate), sodium hydroxide, calcium carbonate and silicon dioxide.

The highest peaks are from pyrite, followed by quartz and ettringite. They are similar to those found by [39, 48] in cases of dams affected by delayed ettringite and alkali-silica reaction, respectively.

The diffraction angles that showed strong reflection were: 2 theta of 37º, 2 theta of 41º and 2 theta of 55º, with high intensities, and refer to Pirita or Sulfate.

The ettringite with greater intensity is found in 2 theta of 36º, corresponding to the crystals present in all the concrete, predominantly of the pores and voids.

Another high intensity peak also recognized in the diffractometer was the mineral component quartz, corresponding to the crystalline products of the alkali-silica reaction. This mineral appeared more strongly in 2 theta of 21º, 2 theta of 27º and 2 theta of 68º, indicating crystalline phases of the material. These peaks are attributed to the contamination of the paste by the reactive aggregate.

4.5.1.3 Raman Spectroscopy

Figure 64 represents the coarse aggregate region of the RA-02 sample in expanded resolution. Four points (a, b, c and d) were chosen to be analyzed by Raman spectroscopy.

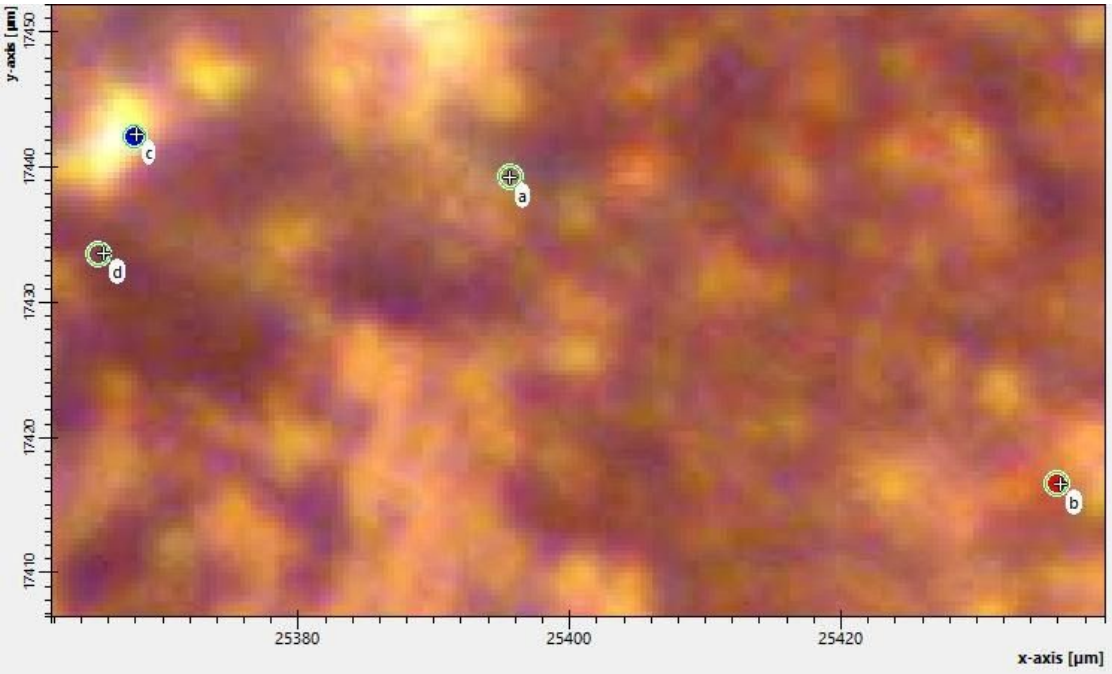

Figure 64. Points (a, b, c and d) where the Raman analysis was performed.

Figure 65 illustrates the Raman spectra of the crystalline products found in different locations of the same analyzed aggregate.

The Raman spectra were found between two wide bands, in the range of 100 and 600 cm-1 (low frequency region), indicating the amorphous nature of the gel.

The wave numbers identified (Figure 65) were similar to those found by the researchers for the aggregates that contained reactive mineral [3, 16].

When analyzing the edges of the aggregate, the bands of the crystalline product do not result in peaks, indicating only noises, a similar behavior found in [19].

The colour of the dots corresponds to the colour of the spectra, the corresponding sequence is: b, a, d and c.

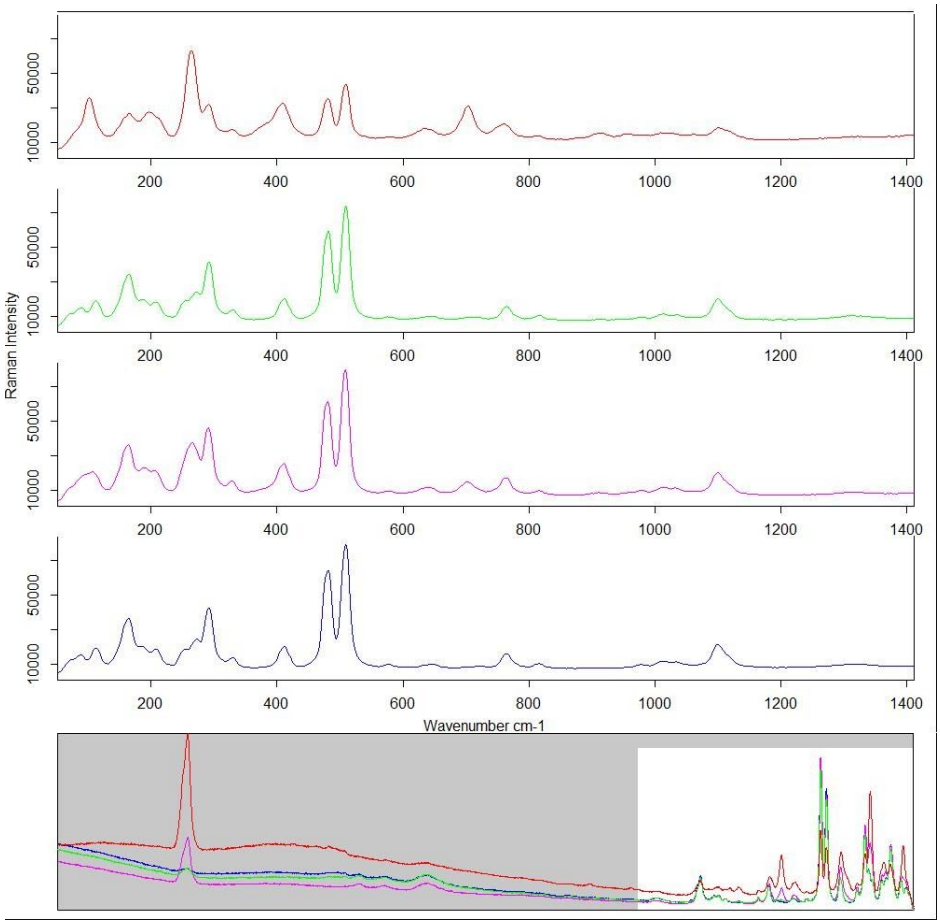

Figure 65. Raman spectra of the crystalline products at the four points analyzed in the RA-02 sample.

In the other samples analyzed, the spectra were not generated, even performing new polishing with silicon carbide (P120), because it showed an increase in noise, causing the signal of the products no longer recognized.

In a new analysis in the same sample, now in the blue and red points (Figure 66), different Raman intensities were found, but still in the same wavenumber range. The colour of the dots corresponds to the colour of the spectra.

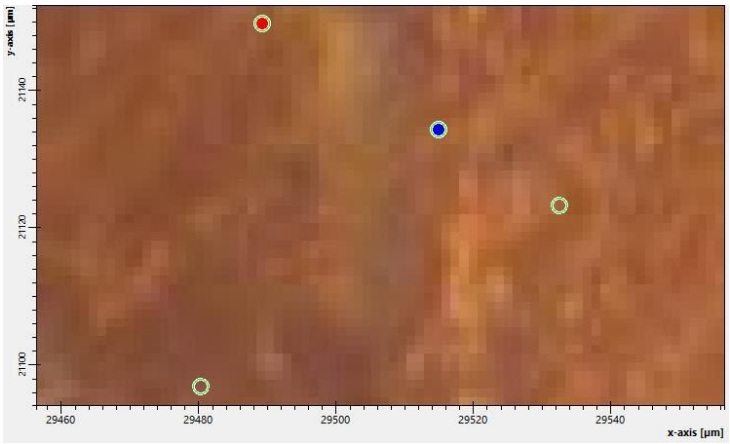

Figure 66. Points where the Raman analysis was performed (Sample RA-02).

In Figure 67 the crystalline product was found in the same range of wave numbers (from 100 to 600 cm-1), being different in peak intensity.

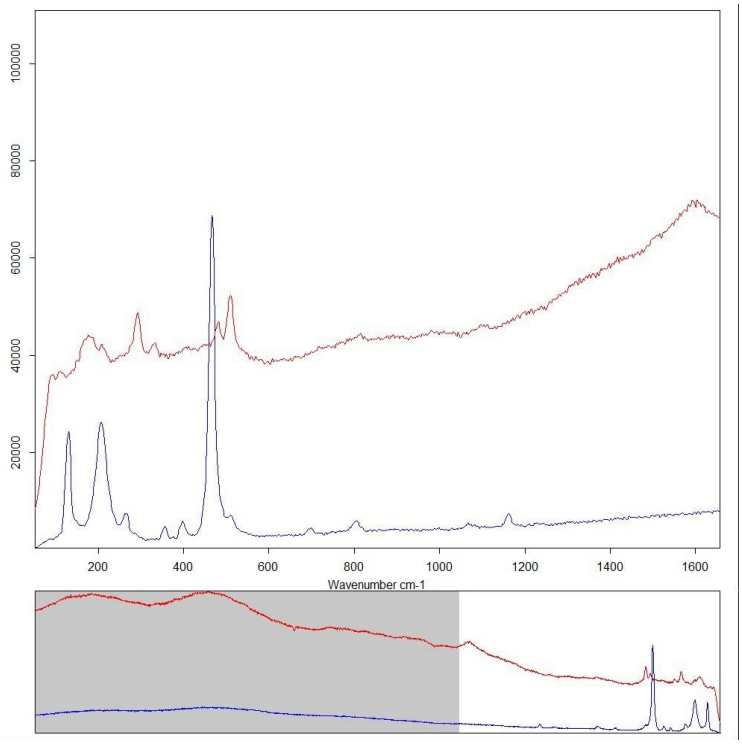

Figure 67. Range of 100 to 600 cm-1 analyzed.

Figure 68 shows the point from which this spectra was obtained and the Figure 69 shows the spectrum of the crystalline product located inside a pore in the RA-05 sample. There are different

peaks, the largest is in the range of 800 to 1000 cm-1. In the wavenumber 600 cm-1 there is a peak, similar to what was found by [3] as a peak of the alkali-silica reaction product.

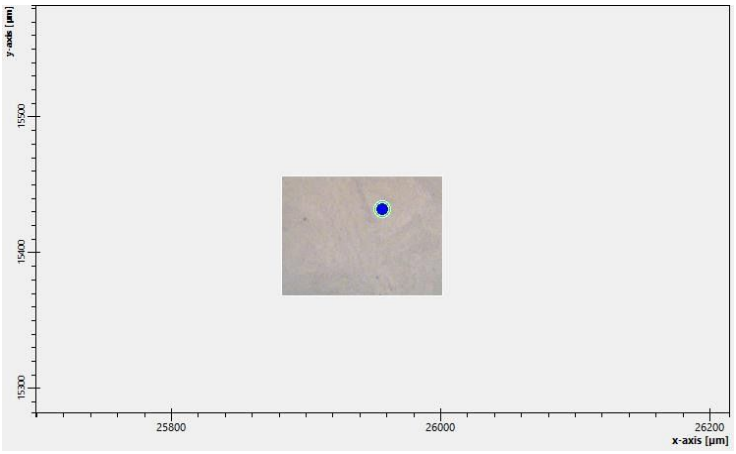

Figure 68. Crystalline product analyzed by Raman spectroscopy.

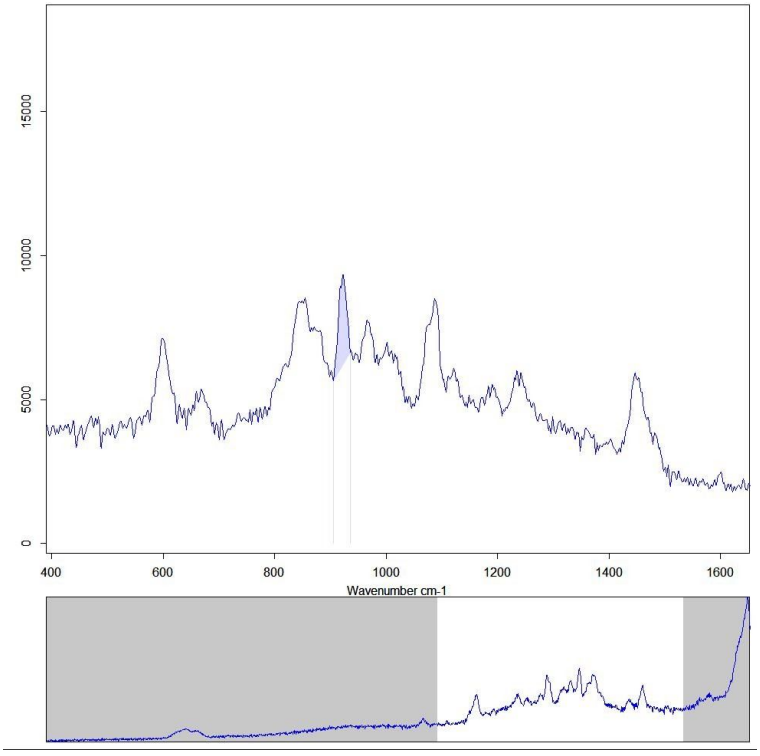

Figure 69. Raman spectra values found in the ASR products inside a pore.

The chemical analysis performed with the Raman spectroscopy indicated possible spectra corresponding to the crystalline products of the alkali-silica reaction, which confirmed the presence

of sodium in the previously obtained EDX spectra. The reactions (alkali-aggregate reaction and delayed ettringite formation) are acting concomitantly.

4.6 Summary of laboratory test results with a likely explanation of the origin of the problems found in the pile cap block from which the specimens were extracted

In this section a summary of the results of the laboratory tests performed as well as an indication of the probable cause of the degradation of the pile cap block observed during field inspections will be presented.

The main findings from the laboratory testing campaign of the extracted samples are presented below.

- The compressive strength tests performed indicated little change in the expected values and this fact allows us to conclude that the expansive reactions existing in the pile cap block studied did not affect the compressive strength of the concrete;

- The concrete deformation properties, evaluated from static and dynamic modulus of elasticity tests, showed important reductions in both modulus of deformation from the expected values. In fact, reductions of 55% and 57%, respectively, for the modulus of elasticity were observed;

- The high value of the permeability coefficient (10^{-15} and 10^{-16}) can explain the intense cracking process existing in the pile cap block investigated, which allowed the entry of moisture and development of the expansion mechanisms, like ASR, that deteriorated the concrete;

- In porosity, high values were found, between 9 and 11%, explained by the large amount of micro-cracks in the field and in the extracted samples;

- The pore structure was very compromised in this concrete, an aspect that directly interferes with its durability and service life.

In the analysis with SEM, the morphologies identified were those of ettringite acicular crystals in the mortar and also completely filling the pores, illustrated in Figure 70 (a, b and c). In the

dispersive energy spectroscopy the following components were obtained: sulfur, aluminum and calcium, characteristic minerals of the ettringite crystals. In the XRD standards these elements were also found, as well as the mineral pyrite (or sulfate) and the ettringite itself. Pyrite was the mineral with the highest peak intensity in the graph, confirming the high presence of DEF in the concrete.

Figure 70. Pores completely filled with ettringite crystals: a) and b) Concrete sample after compressive rupture; c) Concrete sample after extraction.

In the microstructure of the concrete there are pores and voids, and as [28] the ettringite crystals accumulate in the available free spaces, and often the ettringite that is deposited there does not contribute to the expansion. Thus, these products resulting from the reaction were deposited in the pores of the concrete and making a tamponade of existing voids. Through the process of pore-filling the pores [48], proven in visual inspections and SEM analyses, the compressive strength of the concrete showed high values. The cracking on a map of the block in its surface did not happen in the whole block, but in half of it. The AM-02 sample presented a lower strength value compared to the other two because it was extracted from a location of the block where there was little apparent cracking, and probably the products of the reactions had not filled the existing voids.

When analyzing pores filled with internal reaction products of expansion and interface aggregate paste in Raman spectroscopy, spectra with wave numbers and peaks similar to those of crystalline products from ASR studied in [3, 19] were found.

Regardless of the origin of the microcracks in the concrete, the permeability and porosity of this material increase [44]. Water is a factor that contributes to the migration of sulfate ions [44], generating expansion reactions in different locations of a concrete structure.

The mechanisms of ASR and DEF reactions depend on the flow of liquids or gases in the microstructure, so for these internal expansion reactions to develop it is necessary to have connectivity between the pores [66]. For the progress of these reactions it was necessary to have preferential paths for the moisture to enter and then trigger the expansion in the concrete, filling free pores and later cracking the structure of the pile cap foundation. It is possible that there is still residual expansion in the concrete, and new tests are necessary to evaluate this characteristic.

The samples adopted for the permeability and porosity tests (P-01 and P-02) were taken from the left side of the concrete block, differently from the samples used in the strength and modulus tests, which were on the right side, which explains the high values in the compressive strength test due to the filled pores, which would decrease the permeability, but at the same time showed high apparent porosity associated with the high gas permeability in the concrete, due to the non-uniformity of the behavior of these reactions.

According to the results of the analyses performed, the internal expansion reaction that generated the high degree of external cracking in the pile cap blocks of the building studied was predominantly delayed ettringite formation.

CHAPTER 05

5. CONCLUSIONS AND RECOMMENDATIONS FOR FUTURE WORKS

This chapter will present the main considerations and conclusions obtained from the results and analyses carried out in the experimental program, being valid for the materials and conditions that they were submitted.

5.1 Final Considerations

Based on the cracks observed in the field and taking as reference the results of the studies and laboratory analysis in the concrete cores presented in this work, it can be stated that the concrete structure presents chemical changes that have affected its integrity. The most relevant conclusions of these studies are as follows:

- The physical-chemical characterization performed indicated that the pile cap foundation from which the specimens were extracted was affected by internal swelling reactions in the concrete, notably ASR and DEF;

- Among the two reactions referred to DEF proved to be more predominant and is, in the author's opinion, the main reason for the observed cracking;

- DEF possibly originated in the high hydration heat that may have occurred in the concreting of the important concrete volume of the pile cap block;

- The detailing of the pile cap block reinforcement, without the adequate suspension of the lower reinforcement of the tie rods with the upper reinforcement, was an element that facilitated the large opening cracking existing in the pile cap block;

- As a consequence of the opening of the cracks, preferential paths were created for the ingress of moisture, water, and possible chemical agents that provided a favorable environment for the appearance of deleterious swelling reactions in the concrete;

- The alkali-silica reaction was found in concrete through dispersive X-ray spectroscopy, with the presence of mineral components, such as silicon and quartz and by means of Raman spectroscopy, with a wave number of about 600 cm-1, proving the presence of crystalline products of this reaction;

- The ettringite crystals that filled the pores were detected with the naked eye and by scanning electron microscopy and X-ray diffraction;

- The analysis with EDS obtained a predominance of sulfur, aluminum and calcium, being reaffirmed in the intensities of the XRD standards, where sulfate in the form of pyrite was found, as well as ettringite and calcite;

- The compressive strength of the concrete was not affected by the internal expansion reactions, possibly due to the filling of the pores by the reaction products;

- The microcracks also caused a decrease in the values of static and dynamic modulus of elasticity (55% and 57%, respectively);

- The permeability of the concrete showed high values (10^{-15} and 10^{-16}), allowing the entry of moisture and the development of expansion mechanisms that deteriorated the concrete;

- Porosity values between 9 and 10% were also high, in accordance with their permeability and with the extensive pore network existing in the concrete;

- Due to the non-uniformity of the behavior of the reactions in the concrete structure the permeability and porosity were not affected by the buffering of the pores, because the flow occurred through the microcracks in the material.

5.2 Future Works

The contribution of the results obtained in this study does not exhaust the vast field of research of the internal swelling reactions. For this reason, we highlight some aspects considered of greater relevance and that should be developed in the future:

- The physical characterization of concrete samples affected by internal expansion reactions, through the thermogravimetric analysis test, with the objective of identifying the degradation occurring in the material;

- The characterization of concrete transfer properties, such as porosity testing by mercury intrusion, in order to determine the pore structure of concrete at different scales;

- It is also important to perform a larger sample of the tests (apparent porosity and gas permeability) with samples taken from different points of the pile cap foundation in order to assess whether the transport properties are homogeneous throughout the pile cap block;

- Evaluating how the internal expansion reactions affect the tensile strength of concrete is of paramount importance for a better understanding of these mechanisms;

- Another study to be carried out is if the expansion is still occurring in the concrete damaged by the reactions, measuring the existence of residual expansion;

- The collection of a larger number of cores for a larger sample characterization is important for a better understanding of the impact they have on structures in order to develop new forms of construction aiming at the overall durability and safety of the building and the people who benefit from it.

REFERENCES

[1] A. Bourdot, V. Thiéry, D. Bulteel, and J.-G. Hammerschlag, “Effect of burnt oil shale on ASR expansions: A petrographic study of concretes based on reactive aggregates,” Construction and Building Materials, vol. 112, pp. 556–569, Jun. 2016.

[2] A. Leemann and P. Lura, “E-modulus of the alkali–silica-reaction product determined by micro-indentation,” Construction and Building Materials, vol. 44, pp. 221–227, Jul. 2013.

[3] A. Leemann, “Raman microscopy of alkali-silica reaction (ASR) products formed in concrete,” Cement and Concrete Research, vol. 102, pp. 41–47, Dec. 2017.

[4] A. Leemann, “The influence of lithium on the structure of ASR products in concrete,” in: H. Bernardes, N. P. Hasparyk (Eds.), Proceedings of the 15th ICAAR, São Paulo, Brazil, 2016.

[5] A. Leemann, G. Le Saout, F. Winnefeld, D. Rentsch, and B. Lothenbach, “Alkali-Silica Reaction: the influence of calcium on silica dissolution and the formation of reaction products,” Journal of the American Ceramic Society, vol. 94, no. 4, pp. 1243–1249, Apr. 2011.

[6] A. Leemann, L. Bernard, S. Alahrache, and F. Winnefeld, “ASR prevention - Effect of aluminum and lithium ions on the reaction products,” Cement and Concrete Research, vol. 76, pp. 192–201, Oct. 2015.

[7] A. Shayan and G. W. Quick, “Relative importance of deleterious reactions in concrete: formation of AAR products and secondary ettringite,” Advances in Cement Research, vol. 4, no. 16, pp. 149–157, Oct. 1992.

[8] A. Shayan and H. Morris, “Combined deterioration problems in a coastal bridge in NSW, Australia,” 12th International Conference on Alkali-Aggregate Reaction in Concrete. Beijing, China, International Academic Publishers, 2004.

[9] A. Shayan, R. Al-Mahaidi and A. Xu, “Durability and strength assessment of AAR-affected bridge deck planks,” 13th International Conference on Alkali-Aggregate Reaction in Concrete. Trondheim, Norway, BROEKMANS, M.A.T.A; WIGUM, B.J. (editors), 2008.

[10] ASTM C215-14, Standard Test Method for Fundamental Transverse, Longitudinal, and Torsional Resonant Frequencies of Concrete Specimens, ASTM International, West Conshohocken, PA, 2014, www.astm.org.

[11] B & C Engenheiros Consultores Ltda. Technical report: Damage to Pile Cap Blocks, 2016.

[12] B. Christaras, F. Auger and E. Mosse, “Determination of the moduli of elasticity of rocks. Comparison of the ultrasonic velocity and mechanical resonance frequency methods with direct static methods,” Materials and Structures. vol 27, pp. 222–228, 1994.

[13] B. Fournier and M. A. Bérubé, “Alkali-aggregate reaction in concrete: a review of basic concepts and engineering implications,” Canadian Journal of Civil Engineering, vol. 27, no. 2, pp. 167–191, Apr. 2000.

[14] British Cement Association, The Diagnosis of Alkali Silica Reaction - Report of a Working Party. England, (1992) (36p).

[15] BS EN 12504-4:2004 Testing concrete - Part 4: Determination of ultrasonic pulse velocity, British Standard, 2004.

[16] C. Balachandran, J. F. Muñoz, and T. Arnold, “Characterization of alkali silica reaction gels using Raman spectroscopy,” Cement and Concrete Research, vol. 92, pp. 66–74, Feb. 2017.

[17] C. Galle, “Effect of drying on cement-based materials pore structure as identified by mercury intrusion porosimetry A comparative study between oven-, vacuum-, and freeze-drying,” Cement and Concrete Research, p. 11, 2001.

[18] C. J. Benmore and P. J. M. Monteiro, “The structure of alkali silicate gel by total scattering methods,” Cement and Concrete Research, vol. 40, no. 6, pp. 892–897, Jun. 2010.

[19] C. Merz and A. Leemann, “Assessment of the residual expansion potential of concrete from structures damaged by AAR,” Cement and Concrete Research, vol. 52, pp. 182–189, Oct. 2013.

[20] C. Shon, A. Mukhopadhyay, D. Zollinger. Alkali silica reactivity potential of aggregate and concrete evaluated by dilatometer method performance-based approach. J Transport Res Board 2007:10–9.

[21] C. W. A. Pires Sobrinho, “Piles caps of building blocks affected by AAR - Case study,” 54° Brazilian Concrete Congress, Maceió, 2012 (in Portuguese).

[22] D. C. C. D. Molin, “Cracks in reinforced concrete structures - Analysis of typical manifestations and survey of cases occurred in the state of Rio Grande do Sul,” p. 238, 1988 (in Portuguese).

[23] D.W. Hobbs, Alkali–Silica Reaction in Concrete, Thomas Telford, London, 1988.

[24] Djerbi Tegguer, S. Bonnet, A. Khelidj, and V. Baroghel-Bouny, “Effect of uniaxial compressive loading on gas permeability and chloride diffusion coefficient of concrete and their relationship,” Cement and Concrete Research, vol. 52, pp. 131–139, Oct. 2013.

[25] E. A. O. Gomes, “Structural retrofitting works of pile caps blocks deteriorated by alkali aggregate reaction - Recife Experience,” Master Thesis, Catholic University of Pernambuco, 2008 (in Portuguese).

[26] F. Rajabipour, E. Giannini, C. Dunant, J. H. Ideker, and M. D. A. Thomas, “Alkali–silica reaction: Current understanding of the reaction mechanisms and the knowledge gaps,” Cement and Concrete Research, vol. 76, pp. 130–146, Oct. 2015.

[27] F. Leonhardt, E. Monning, “Concrete Constructions - Volume III: Basic Principles on the reinforcement of concrete structures, Ed. Interciência, 1978.

[28] F. P. Glasser, D. Damidot and M. Atkins, "Phase development in cement in relation to the secondary ettringite problem," Advanced Cement Research, 7 (26), pp. 57-68, 1995.

[29] G. A. Silva, “Retrofitting works of pile caps blocks affected by alkali aggregate reaction,” Master Thesis, Catholic University of Pernambuco, 2007 (in Portuguese).

[30] H. F. W. Taylor, C. Famy, and K. L. Scrivener, “Delayed ettringite formation,” Cement and Concrete Research, vol. 31, no. 5, pp. 683–693, May 2001.

[31] H. Carasek, N. P. Hasparyk, S. K. Melo, H. H. A. B. Silva and C. Martins, "Influence of hydration heat on the delayed ettringite formation (DEF) in pozzolanic Portland cement concrete," 53rd Brazilian Congress of Concrete, Florianópolis-SC, 2011.

[32] H. Ghanem, D. Zollinger, and R. Lytton, “Predicting ASR aggregate reactivity in terms of its activation energy,” Construction and Building Materials, vol. 24, no. 7, pp. 1101–1108, Jul. 2010.

[33] Hsu, T. C., ACI Monograph 6, p.100, 1971.

[34] I. F. Torres and T. Andrade, “Risk analysis of the delayed ettringite formation in pile caps foundation in the metropolitan region of Recife - PE - Brasil,” IBRACON Journal de Estruturas e Materiais, vol. 9, no. 3, pp. 357–394, Jun 2016.

[35] I. N. Serdyuk, N. R. Zaccai and J. Zaccai, “Raman scattering spectroscopy,” in Methods in Molecular Biophysics: Structure, Dynamics, Function, Cambridge: Cambridge University Press, 2007, pp. 573–600.

[36] J. Bensted, “Uses of Raman Spectroscopy in Cement Chemistry,” J American Ceramic Society, vol. 59, no. 3–4, pp. 140–143, Mar. 1976.

[37] J. P. Figueirôa, T. Andrade. “Alkali-aggregate reaction attack on concrete structures,” p. 228, 2007 (in Portuguese).

[38] J. V. Campos, I. R. Lavagnini, J. A. Ferreira, E. T. Montrazi, T. J. Bonagamba, and E. M. de J. A. Pallone, “Comparative analysis between different porosimetric tests on macroporous alumina,” Matéria (Rio J.), vol. 22, no. suppl 1, Jan. 2018 (in Portuguese).

[39] K. Mehta and P. Monteiro. “Concrete: Microstructure, properties and materials,” p.742, 2014.

[40] L. F. M. Sanchez, “Contribution to the study of test methods in the evaluation of alkali-aggregate reactions in concrete,” São Paulo, p. 170, 2008.

[41] L. F. M. Sanchez, T. Drimalas, B. Fournier, D. Mitchell, and J. Bastien, “Comprehensive damage assessment in concrete affected by different internal swelling reaction (ISR) mechanisms,” Cement and Concrete Research, vol. 107, pp. 284–303, May 2018.

[42] L. Sanchez, S. C. Kuperman, and P. Helene, “Using the accelerated Brazilian concrete prism test (ABCPT) to evaluate alkali aggregate reaction (AAR),” Revista IBRACON de Estruturas e Materiais, vol. 4, no. 4, pp. 575–581, Oct. 2011.

[43] M. Choinska, “Effects of temperature, mechanical state and their interactions on the permeability of structural concrete,” P.h.d. Thesis, Nantes University, 2006 (in french).

[44] M. Collepardi, “Damage by Delayed Ettringite Formation,” Concrete International, v. 21, n. 1, pp. 69-74, 1999.

[45] M. Tahlaiti, “Study of chloride penetration and corrosion initiation in saturated and tidal zones,” P.h.d. Thesis, La Rochelle University, 2010 (in French).

[46] M.D.A. Thomas, B. Fournier, K.J. Folliard, Y.A. Resendez, “Alkali-silica Reactivity Field Identification Handbook,” No. FHWA-HIF-12-022, 2011.

[47] MERL Report-09-23, “New Recommendations for ASR Mitigation in Reclamation Concrete Construction,” U.S. Bureau of Reclamation, Denver, Colorado, 2009.

[48] N. P. Hasparyk, “Investigation of concretes affected by the alkali-aggregate reaction and advanced characterization of exudate gel,” P.h.d. Thesis, Federal University of Rio Grande do Sul, p. 326, 2005 (in Portuguese).

[49] N. P. Hasparyk, S. C. Kuperman, and J. R. Torres, “Case study involving combined attack of AAR and DEF in building foundation concrete,” p. 16, 2012 (in Portuguese).

[50] N. Thaulow, U. H. Jakobsen, and B. Clark, “Composition of alkali silica gel and ettringite in concrete railroad ties: SEM-EDX and X-ray diffraction analyses,” Cement and Concrete Research, vol. 26, no. 2, pp. 309–318, Feb. 1996.

[51] Oberholster, B., Alkali-silica reaction, in B. Addis, & G. Owens (eds.). Fulton's Concrete Technology. Midrand: Cement & Concrete Institute, 8: pp. 163-185, 2001.

[52] P. Mounanga, A. Khelidj, A. Loukili, and V. Baroghel-Bouny, “Predicting Ca(OH)2 content and chemical shrinkage of hydrating cement pastes using analytical approach,” Cement and Concrete Research, vol. 34, no. 2, pp. 255–265, Feb. 2004.

[53] R. Dähn et al., “Application of micro X-ray diffraction to investigate the reaction products formed by the alkali–silica reaction in concrete structures,” Cement and Concrete Research, vol. 79, pp. 49–56, Jan. 2016.

[54] R. F. Blanks, H. L. Kennedy, “The Technology of Cement and Concrete,” vol. 1, Wiley, New York, 1955.

[55] R. N. Swamy, “The Alkali-Silica Reaction in Concrete,” p. 348, 1992.

[56] S. A. Marfil, P. J. Maiza, "Deteriorated pavements due to the alkali-silica reaction. A Petrographic study of three cases in Argentina," Cement and Concrete Research , v. 31, pp. 1017-1021, 2001.

[57] S. Diamond, “Mercury porosimetry An inappropriate method for the measurement of pore size distributions in cement-based materials,” Cement and Concrete Research, p. 9, 2000.

[58] T. Andrade, “History of recent AAR cases occurring in foundations of buildings in the metropolitan region of Recife,” 48° Brazilian Concrete Congress, 2006.

[59] T. Andrade, “RAA in foundations in the metropolitan region of Recife: 10 years of history,” IBRACON Journal Concrete and Buildings, vol. 76, pp. 113-120, 2014.

[60] T. Andrade, J. J. R. Silva, R. Almeida, J. P. Figueirôa, Y. Kihara and M. Pecchio, “Diagnosis of alkali-aggregate reaction in pile caps of a public building located in the city of Recife/PE,” 48° Brazilian Concrete Congress, 2006.

[61] T. E. Stanton, “Expansion of concrete through reaction between cement and aggregate,” Proceedings of American Society of Civil Engineers, vol. 66, n. 10. Dec. 1940, p. 1781–1811.

[62] TECOMAT and ABCP. “Technical report of diagnostic of pathological manifestation in reinforced concrete,” 2016.

[63] V. Baroghel-Bouny, “Microstructural and water characterization of pasta of cement and ordinary and very high concrete performances,” p. 554, P.h.d. Thesis, Paris University, 1994.

[64] V. Machoviè et al., “Raman micro-spectroscopy mapping and microstructural and micromechanical study of interfacial transition zone in concrete reinforced by poly (ethylene terephthalate) fibres,” p. 7, 2008.

[65] V. Picandet, “Influence of mechanical damage on the permeability and water diffusivity of concretes,” P.h.d. Thesis, Nantes University, 2001 (in french).

[66] V. Picandet, A. Khelidj and G. Bastian, “Effect of axial compressive damage on gas permeability of ordinary and high-performance concrete,” Cement and Concrete Research, vol. 31, no. 11, pp. 1525–1532, Nov. 2001.

[67] W. J. Malfait, V. P. Zakaznova-Herzog, and W. E. Halter, “Amorphous materials: Properties, structure, and durability: Quantitative Raman spectroscopy: Speciation of Na-silicate glasses and melts,” American Mineralogist, vol. 93, no. 10, pp. 1505–1518, Oct. 2008.

[68] W. P. Andrade and Team Furnas, “Concretes: Mass, Structural, Projected and Compacted with roll (Tests and Properties),” Vol. I, Ed. PINI, 1997.

[69] X. Hou, R. J. Kirkpatrick, L. J. Struble, and P. J. M. Monteiro, “Structural Investigations of Alkali Silicate Gels,” J American Ceramic Society, vol. 88, no. 4, pp. 943–949, Apr. 2005.

[70] LABORATOIRE CENTRAL DES PONTS ET CHAUSSÉES, Guide technique - Recommendations for preventing disorders due to Delayed Ettringite Formation, Paris, 2018 (French version published in 2017) .

[71] A. Azevêdo, “Interface influence on moisture transport in building components,” P.h.d. Thesis, Porto University, 2019.

[72] N. Mendes and P.C. Philippi, “A method for predicting heat and moisture transfer through multilayer walls based on temperature and moisture content gradients,” International Journal of Heat and Mass Transfer, vol. 48, pp. 37–51, 2005.

[73] Y. Kubo and M. Nakata, “Effect of reactive aggregate on mechanical properties of concrete affected by alkali-silica reaction,” 14th International Conference on Alkali-Aggregate Reaction (ICAAR). Texas, USA, 2012.

[74] ABNT - Brazilian Association of Technical Standards, “Design of concrete structures - Procedure,” Brazil, 2014.

[75] R. P. Martin, “Analysis on model structures of the mechanical effects of the internal sulfatic reaction of concrete," PhD thesis, Central Laboratory for Bridges and Pavements (LCPC), 2010.

[76] G. E. Blight and M. G. Alexander, “Alkali-Aggregate Reaction and Structural Damage to Concrete - Engineering Assessment, Repair and Management,” Book, published in 2011.

[77] A. Allard et al. “Expansive behavior of thick concrete slabs affected by alkali-silica reaction (ASR),” Construction and Building Materials, p. 236, 2018.

[78] Afshin Mohammadi, Ebrahim Ghiasvand and Mahmoud Nili. “Relation between mechanical properties of concrete and alkali-silica reaction (ASR); a review,” Construction and Building Materials, p. 258, 2020.

[79] Atsushi Teramoto, Masaki Watanabe, Ryota Murakami and Takaaki Ohkubo. “Visualization of internal crack growth due to alkali–silica reaction using digital image correlation,” Construction and Building Materials, p. 190, 2018.

[80] L. F. M. Sanchez, B. Fournier, D. Mitchell and J. Bastien, “Condition assessment of an ASR-affected overpass after nearly 50 years in service,” Construction and Building Materials, p. 236, 2020.

[81] M. Malbois et al., “On DEF expansion modelling in concrete structures under variable hydric conditions,” Construction and Building Materials, p. 207, 2019.

[82] R. B. Figueira et al., “Alkali-silica reaction in concrete: Mechanisms, mitigation and test methods,” Construction and Building Materials, p. 222, 2019.

[83] Renaud-Pierre Martin, Leandro Sanchez, Benoît Fournier and François Toutlemonde, “Evaluation of different techniques for the diagnosis & prognosis of Internal Swelling Reaction (ISR) mechanisms in concrete,” Construction and Building Materials, p.156. 2017.

[84] Renaud-Pierre Martin, Othman Omikrine Metalssi and François Toutlemonde, “Importance of considering the coupling between transfer properties, alkali leaching and expansion in the modelling of concrete beams affected by internal swelling reactions,” Construction and Building Materials, p. 49, 2013.

[85] Shagang Li et al., “Modeling of flexural strength degradation induced by alkali-silica Reaction,” Construction and Building Materials, p. 234, 2020.

[86] Simen Sørgaard Kongshaug et al., “Experimental investigation of ASR-affected concrete – The influence of uniaxial loading on the evolution of mechanical properties, expansion and damage indices,” Construction and Building Materials, p. 245, 2020.

APPENDICE (PHOTOS)

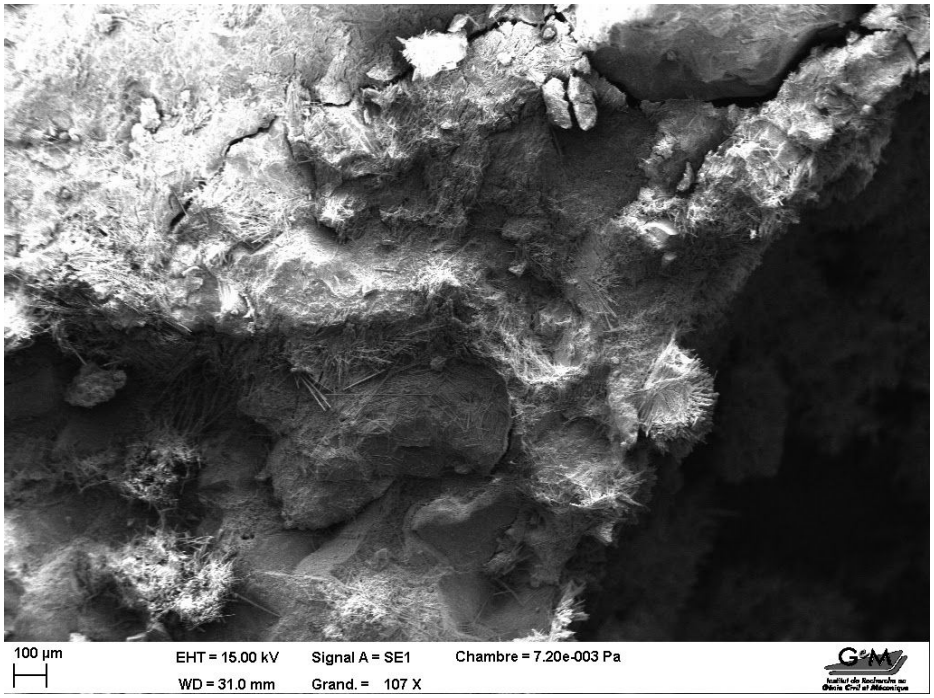

Figure 71. Crystals in acicular shape in the mortar and details of micro-cracks.

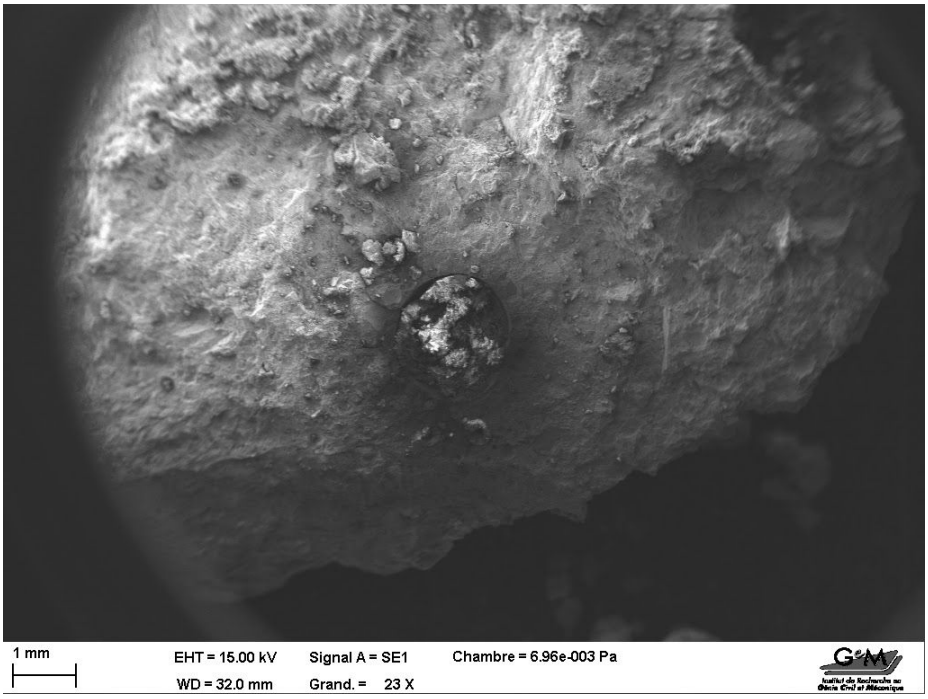

Figure 72. Pore image completely filled with delayed ettringite products.

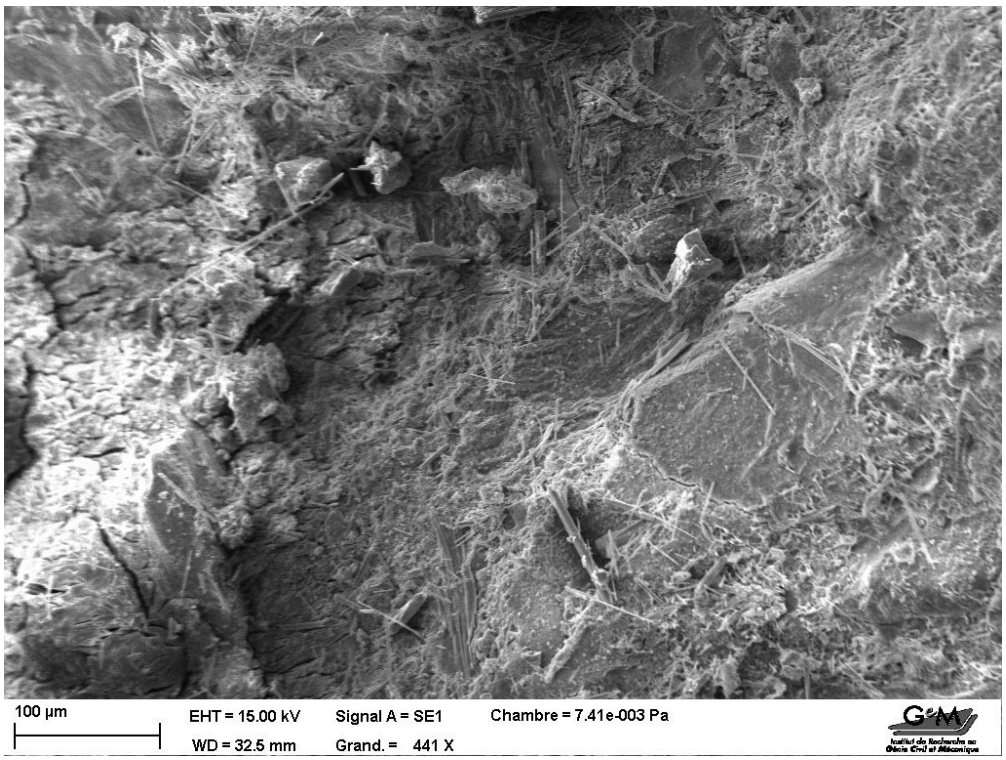

Figure 73. Detailing of the concrete microstructure and micro-cracks.

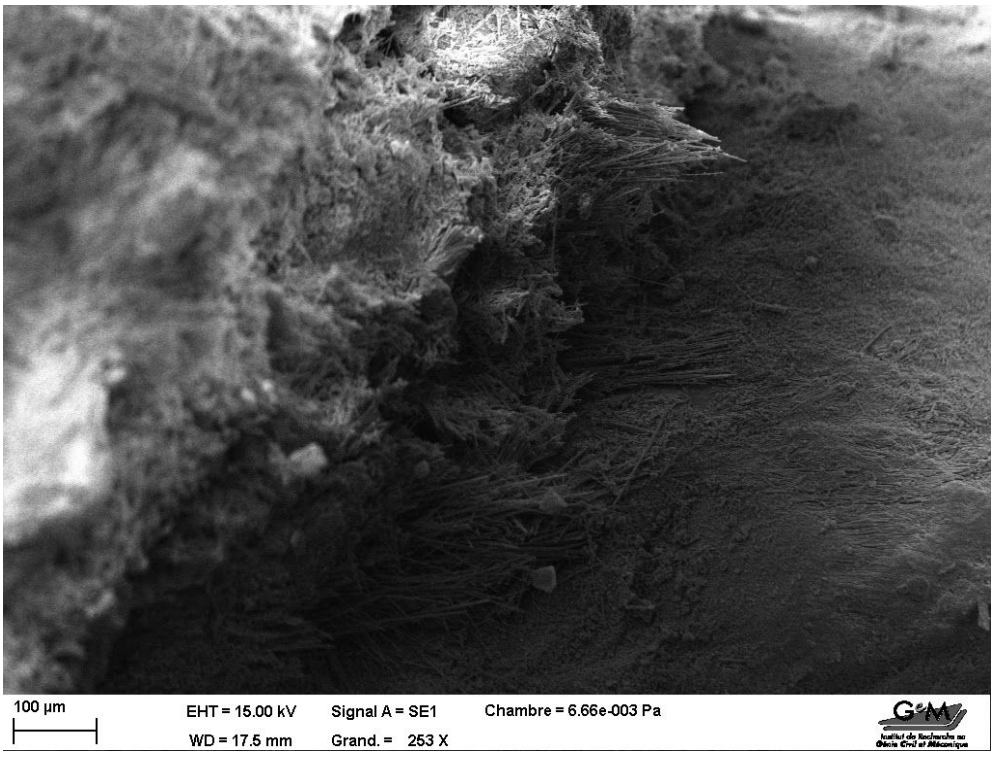

Figure 74. Ettringite molecules already formed and their direction in the microstructure.

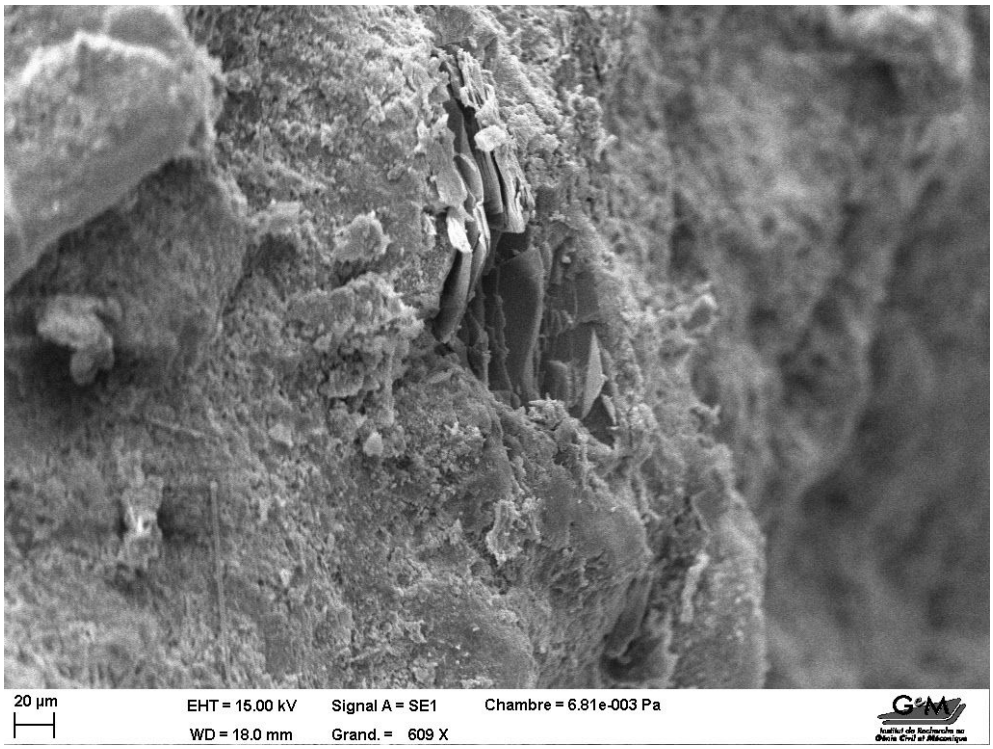

Figure 75. Detailing of the concrete microstructure.

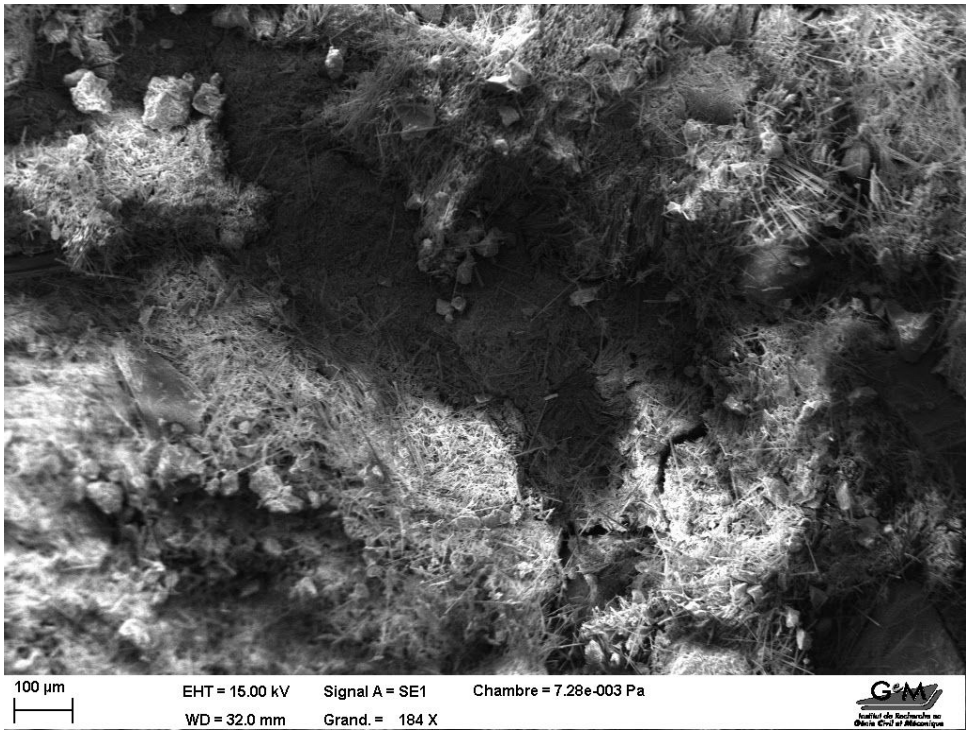

Figure 76. Acicular crystals and micro-cracks in the microstructure of the concrete.

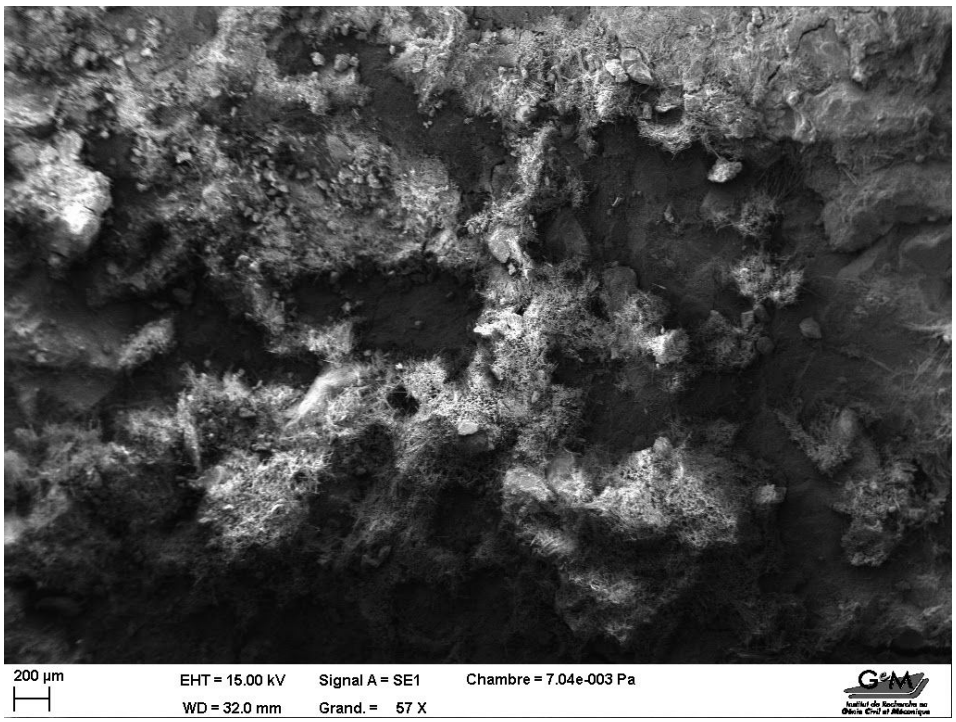

Figure 77. Etringita covering the cement paste phase.

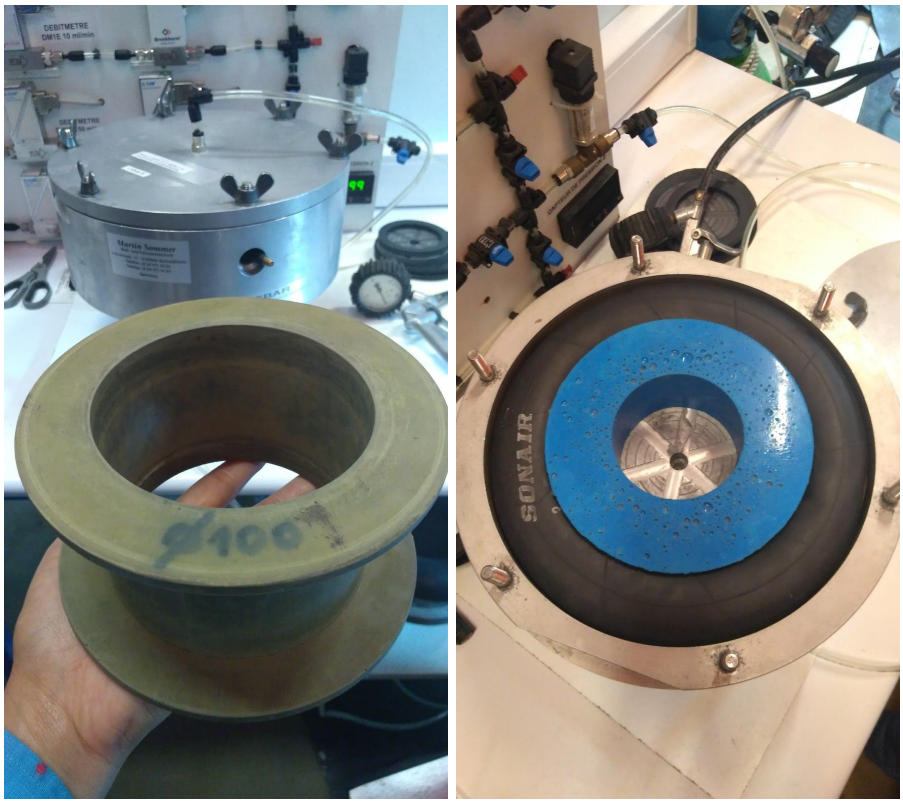

Figures 78 and 79. Shape for permeability test and cell where the sample is placed.

Figures 80 and 81. Details of the gas permeability equipment.

Figure 82. Sample already placed in the cell for the gas permeability test.

Figure 83. Desiccator where the sample was placed when it was removed from the greenhouse.

Figure 84. Vacuum pump on removal of all air from the system for apparent porosity test.